2009-09-04

Mechanisms of NOTCH1 Mediated Leukemogenesis: A Dissertation

Kathleen J. Cullion
University of Massachusetts Medical School

MECHANISMS OF NOTCH1 MEDIATED LEUKEMOGENESIS

A Dissertation Presented

By

Kathleen Jane Cullion

Submitted to the Faculty of the
University of Massachusetts Graduate School of Biological Sciences, Worcester
in partial fulfillment of the requirements of the degree of

DOCTOR OF PHILOSOPHY

SEPTEMBER 4, 2009

ii

MECHANISMS OF NOTCH1 MEDIATED LEUKEMOGENESIS

A Dissertation Presented
By

Kathleen Jane Cullion

The signatures of the Dissertation Defense Committee signifies completion and approval as to style and content of the Dissertation

Michelle Kelliher Ph.D., Thesis Advisor

Stephen Lyle M.D./Ph.D., Member of Committee

Nathan Lawson Ph.D., Member of Committee

Alan Rosnfarin M.D., Member of Committee

Jon Aster M.D./Ph.D., Member of Committee

The signature of the Chair of the Committee signifies that the written dissertation meets the requirements of the Dissertation Committee

Lucio Castilla Ph.D., Chair of Committee

The signature of the Dean of the Graduate School of Biomedical Sciences signifies that the student has met all graduation requirements of the school

Anthony Carruthers Ph.D.,
Dean of the Graduate School of Biomedical Sciences

September 4, 2009

Acknowledgments

I would to first like to thank my mentor, Michelle Kelliher, for her guidance and support during this part of my training. I would also like to thank members of my committee, Lucio Castilla, Nathan Lawson, Stephen Lyle, and Alan Rosmarin for their time, advice, and criticisms. I am also grateful to members of the Kelliher laboratory for their support and encouragement. I would especially like to thank Kyle Draheim who began the GSI efficacy studies (Figure 9A,C.D, 11, Table 1), Vishva Sharma for performing the chromatin immunoprecipitation assay (Figure 5) and contributions to Figure 8A, Jessica Tatarek for contributing to the clonality and mutational analyses (Figure 19), and Nicole Hermance and Sarah Morrissey for their help in many of the mouse studies.

I also appreciate the collaboration with Pradip Majumder from Merck Research Laboratories who provided compound, serum analysis, and performed the *in vivo* GSI and rapamycin analysis (Figure 17). I would also like to thank Dr. Thomas Look and Dr. Alejandro Gutierrez from Dana Farber Cancer Institute as well as Dr. Mark Levis from John's Hopkins Medical Center for providing the primary T-ALL samples used in the engraftment studies. Additionally, I would also like to thank Dr. Dale Greiner, Dr. Michael Brehm and Linda Paquin of University of Massachusetts Medical School for providing the NSG mice and for their expertise and assistance with these studies.

I would also especially like to thank my parents and my husband, Trevor, for their constant support and encouragement. I am certain I could have not done this without you.

Abstract

Gain of function *NOTCH1* mutations are common in both patients with T-ALL and in mouse models of the disease. Inhibiting the Notch pathway in T-ALL cell lines results in growth arrest and/or apoptosis *in vitro*, suggesting a requirement for Notch signaling in T-ALL. Therefore, we sought to examine the role of Notch1 signaling in both premalignancy and in the maintenance of leukemic growth. Using a murine model of T-ALL, in which expression of the *Tal1* and *Lmo2* oncogenes arrests thymocyte development, our preleukemic studies reveal that *Notch1* mutations are early events that contribute to the clonal expansion of DN3 and DN4 progenitors. We also demonstrate that progenitors are maintained within the tumor and are enriched in leukemia-initiating cell (L-IC) activity, suggesting Notch1 may contribute to L-IC self-renewal. By studying the effects of Notch signaling in murine T-ALL cell lines, we also demonstrate that Notch1 promotes the proliferation and survival of leukemic blasts through regulation of Lef1 and the Akt/mTOR pathways.

Given that T-ALL cell lines are dependent on Notch signaling *in vitro*, we investigated the effects of Notch inhibition *in vivo.* We provide evidence that Notch1 can be successfully targeted *in vivo* and that Notch inhibition, with γ-secretase inhibitors (GSIs), significantly extends the survival of leukemic mice. We also demonstrate that administration of GSIs in combination with rapamycin inhibits human T-ALL growth and extends survival in a mouse xenograft model. Given that NOTCH1 may be required to maintain both L-IC and bulk leukemic growth, targeting NOTCH1 may prove to be an efficacious targeted therapy for T-ALL patients with aberrant NOTCH1 activation.

Table of Contents

List of Tables

List of Figures

List of Abbreviations

4EBP-1	4E binding protein 1
ADAM	a disintigrin and metalloproteases
AML	Acute myelogenous leukemia
ANK	Ankryin repeats
bHLH	Basic helix loop helix
CSL	CBF1/RBP-J, Sh(H), Lag1
DAPT	*N*-[*N*-(3,5-difluorophenacetyl)-L-alanyl]-*S*-phenylglycine *t*-butyl ester
DN	Double negative
Dox	Doxycycline
DP	Double positive
EGF	Epidermal growth factor
ETP	Early thymic progenitor
GSI	γ secretase inhibitor
HD	Heterodimerization domain
HSC	Hematopoietic stem cell
ICN	Intracellular Notch
ISP	Immature single positive
Lef1	Lymphoid enhancing factor1
L-IC	Leukemic initiating cell
Lin	Lineage
Lmo2	LIM domain only 2
MAML	Mastermind-1 like
mTOR	mammalian target of rapamycin
NEC	Notch extracellular subunit
NOD/SCID	nonobese diabetic/ severe combined immunodeficient mice
NRR	Negative regulatory region
NTM	Notch transmembrane subunit
p70S6K	ribosomal protein S6 kinase
PEST	Pro-Glu-Ser-Thr
PI3K	Phosphatidylinositol 3-kinase
Pre-T α	pre T-cell antigen receptor alpha
Pre-TCR	Pre-T-cell receptor
PTEN	phosphatase and tensin homolog
Rag1/2	Recombinase activating genes 1 and 2
S6RP	ribosomal protein S6
SCF	Skp1-cullin-F-box
SP	Single positive
TACE	TNF-α converting enzyme
TAD	Transactivation domain
Tal1	T-cell acute lymphoblastic leukemia-1
T-ALL	T-cell acute lymphoblastic leukemia
TCR	T-cell receptor

CHAPTER I

INTRODUCTION

Acute lymphoblastic leukemia (ALL) is a malignancy that affects cells along the B or T-cell lineage. It is the most common form of leukemia in pediatric patients, as it accounts for 50% of all hematopoietic malignancies [1]. T-cell acute lymphoblastic leukemia (T-ALL) is a subtype of ALL that accounts for 15% and 25% of all pediatric and adult ALL cases, respectively [2-4]. Patients with T-ALL often exhibit high levels of circulating blasts in the peripheral blood, organ and central nervous system infiltration, and a thymic mass that can present as respiratory distress at diagnosis [5].

The development of T-ALL is a multi-step process involving a number of genetic events. Often, these events deregulate pathways that result in abnormal cellular proliferation, survival, differentiation and self-renewal. Chromosomal translocations contributing to T-ALL are rare, but often juxtapose genes to the T-cell receptor (TCR) locus, which is highly expressed in developing thymocytes. To date deregulation of genes including *HOX11*, *HOX11L2*, *HOXA*, *TAL1*, *LYL1*, *LMO1*, *LMO2*, *NOTCH1* and *c-MYB*, *PTEN*, *c-MYC*, *FBXW7*, and *WT1* have been documented to contribute to T-ALL [6-16].

Advancements in treatment regimens have increased survival rates dramatically for many types of leukemia, including B-cell acute lymphoblastic leukemia (B-ALL) [17,18]. However, patients with T-ALL, particularly those with TAL1 misexpression, have a poorer prognosis [5]. Greater than 50% of patients with TAL1 misexpression will relapse despite intensive chemotherapy and many eventually die from the disease [5]. For those patients who achieve remission following traditional chemotherapy, there can often be long-term side effects, including organ damage and/or failure, learning issues due to intrathecal prophylaxis, and the development of secondary malignancies such as acute

myelogenous leukemia (AML) [19]. However, some patients, including those with *NOTCH1* mutations, have a favorable prognosis [20,21]. In these patients, perhaps targeted therapy instead of intensive broad based chemotherapy should be considered. Therefore, there is an urgent need for understanding the pathogenesis of T-ALL and ultimately, for the rational design of targeted therapies that can exploit the molecular abnormalities driving this malignancy.

TAL1 is a basic helix-loop-helix protein required for normal hematopoiesis.

The T-cell acute lymphoblastic leukemia-1 gene (*TAL1*) (also known and *SCL* and *TCL5*) encodes a 42 kD class II basic helix loop helix (bHLH) protein [22] as well as a truncated 22kD form, which occurs as a result of translational initiation at an internal methionine [23,24]. Tal1 is expressed in mouse embryonic tissues at embryonic day 7.5 and in adult erythroid, mast, megakaryocytic, and myeloid cells [25]. Tal1 is also expressed in murine endothelial cells and in cells of the developing and adult brain [25-27]. Hematopoietic stem cells (HSCs) and committed multipotent progenitors (CMPs) express Tal1, however Tal1 expression is silenced during early thymocyte development (double negative stage 2, DN2) and is not expressed in mature T-cells [28-30].

Tal1 expression is required for a number of normal developmental processes including the development of blood lineages [31,32]. *Tal1 -/-* mice die at embryonic day 8.5-10 due to a specific lack of blood and yolk sac hematopoiesis [31,33]. Tal1 is also required for embryonic angiogenesis, erythroid and megakaryocytic differentiation and for HSC formation [31-36].

As a class II bHLH protein, Tal1 does not homodimerize but instead forms heterodimers with class I bHLH E2A proteins such as E2-2, E47, E12, and Heb, which can bind DNA as heterodimers [37-39]. During erythroid and megakaryocyte differentiation, Tal1 is part of multi-protein transcriptional complex containing E2A, Lmo2, Ldb1, Gata1/2 and Sp1 [40-42]. This multi-protein complex can bind E-box-Gata sites, and recruit co-activators (such as p300 [43] and p/CAF [44]) or co-repressors (such as mSin3A [45]) to regulate transcription.

TAL1 misexpression is observed in 60% of T-ALL patients.

The *TAL1* gene was first identified in a patient with T-ALL in which a rare translocation, t(1;14)(q33;11), juxtaposed *TAL1* on chromosome 1 to the *TCRδ* locus on chromosome 14 [22], and resulted in TAL1 overexpression. A t(1;7)(p32;q35) translocation has also been described, which juxtaposed *TAL1* to the *TCRβ* locus [46]. In an additional 20% of T-ALL patients, *TAL1* is overexpressed via a 90-kilobase deletion that places *TAL1* under control of the SCL-interrupting-locus (SIL) promoter, which is highly active in many tissues [47-50]. Together these genetic events account for the TAL1 overexpression that is seen in 25% of all T-ALL cases. However, recent studies reveal TAL1 overexpression accounts for as many as 60% of childhood and 45% of adult T-ALL cases [50]. This has led many to hypothesize that a currently unknown regulator of TAL1 may be commonly inactivated in T-ALL [50].

Mouse models of Tal1-mediated disease

Many strategies have been used to misexpress *Tal1* in developing thymocytes including the CD2 and SIL promoters. However, these mice fail to develop leukemia [51-54]. In transgenic mice, ectopic expression of *Tal1* using the proximal *Lck* promoter does result in a leukemic phenotype, with 27% of mice developing disease within 350 days [55]. Further analysis of these mice reveal the development a lymphoblastic disease, with evidence of a thymic mass, and infiltration of the central nervous system, kidney, liver, and spleen [55]. Collectively, these studies suggest that expression in a specific thymic progenitor and/or levels of Tal1 expression are critical for disease induction.

Lck-Tal1 preleukemic mice exhibit a thymocyte differentiation arrest at the double negative 3 (DN3) stage [56]. During this developmental stage, E47 heterodimerizes with Heb and regulates the expression of genes critical to normal development such as; recombinase activating genes 1 and 2 (*Rag1/2*), pre T-cell antigen receptor alpha (*Pre-Tα*), *TCR α/δ*, *CD4*, *CD3*, and *CD5* (reviewed in [57]). In human and mouse T-ALL cells TAL1/E47 and TAL1/HEB heterodimers are detected [38,56], suggesting Tal1 may interfere with E protein functions. To test this idea we mated our *Lck-Tal1* transgenic mice to *Heb* or *E2A* heterozygous mice to generate *Tal1/Heb+/-* and *Tal1/E2A+/-* cohorts. Consistent with the idea that Tal1 interferes with E protein function, *Tal1/Heb+/-* and *Tal1/E2A+/-* mice have a more severe perturbation in thymocyte development and disease acceleration compared to mice that only express *Tal1* [58]. *Tal1/E2A+/-* preleukemic thymocytes also exhibit significant reductions in the expression of E47/Heb regulated genes on a per cell basis compared to that observed in *Ta11* preleukemic thymocytes [58].

In T-ALL patients, TAL1 activation is often associated with secondary genetic events including p16/INK4A and p14/ARF loss, and c-MYC, LMO1 or LMO2, and NOTCH1 overexpression [28]. The long latency and incomplete penetrance seen with *Lck-Tal1* mice also suggests Tal1 alone is not sufficient to induce disease and that other acquired mutations must contribute to leukemogenesis [55]. Retroviral insertional mutagenesis studies using the Moloney Murine Leukemic Virus (MoMLV) have identified *Notch1*, *c-Myc* and a dominant negative form of *Ikaros* as collaborating oncogenes in murine *Tal1*-mediated leukemogenesis [59]. Misexpression of *Tal1* also collaborates with either a *p16Ink4a* or *p19Arf* deletion or the overexpression of LIM domain only 1 and 2 (*Lmo1* and *Lmo2*), to induce disease in mice [60-62]. Lmo proteins normally interact with Tal1 as part of a multi-protein complex in erythroid cells and are not typically expressed in developing thymocytes [41,60,63]. However, LMO proteins are also targets of chromosomal rearrangement in patients with T-ALL and have been demonstrated to interact with TAL1 in leukemic extracts [41,63-66]. In patients, the two proteins are often co-expressed [28] and 2 of the 3 children who developed T-ALL due to retroviral insertions in the LMO2 locus, as part of the X-linked severe combined immunodeficiency (SCID) gene therapy trial, exhibit TAL1 activation [67,68].

Thymocyte development

Mature T-cells, like all cells in the hematopoietic system develop from HSCs that reside in the bone marrow. HSCs can be divided into two populations [69], a long-term subset (LT-HSC), which is capable of extensive and indefinite self-renewal, and a short-

term population (ST-HSC) that has limited self-renewal capability [70]. ST-HSCs give rise to the transient multipotent progenitor population (MPP) that can generate common myeloid progenitors (CMPs) and common lymphoid progenitors (CLPs) [71]. CLPs have the potential to mature along either a T or B-cell developmental program [72]. Once committed to the T-cell lineage, cells within the thymus undergo a tightly controlled developmental process that is determined by expression of the CD4 and CD8 co-receptors (reviewed in [73]). Based on expression of CD4 and CD8, developing thymocytes can be divided into 4 major subpopulations; CD4 and 8 double negative (DN), CD4 and 8 double positive (DP), and CD4 or CD8 single positive (SP) (Figure 1).

The DN population, the most immature committed thymic progenitors, is made up of 4 subpopulations; DN1-4 [74]. The exact cell type that seeds the thymus is unknown, but early thymic progenitors (ETPs) are the earliest known committed T-cell progenitor in the thymus [75]. ETPs are lineage (lin) and CD25 negative, express CD44, cKit, and Sca1, and comprise 80% of the DN1 committed progenitor population [75]. The DN1 population is heterogeneous and is also comprised of the more mature Lin-, CD44+, CD25-, $cKit^{lo}$ cells [76,77]. Upon appropriate environmental signals the next stage of development involves the acquisition of the CD25 co-receptor, which is coincident with maturation to the DN2 stage. DN2 progenitors can give rise to two different T lineages; αβ and γδ (reviewed in [76]). This lineage choice depends on which TCR becomes successfully recombined. Using Rag1 and 2, cells rearrange the *TCRδ*, *TCRγ*, or *TCRβ* genes. If progenitors fail to generate an in-frame *TCRδ*, *γ*, or *β* coding sequence, they undergo apoptosis. Cells that successfully generate TCRγ and TCRδ proteins, develop

into mature γδ T-cells. Cells that generate a successful TCRβ rearrangement continue to develop along the αβ lineage.

During the DN3 stage, cells lose CD44 expression and rearrange the *TCRβ* chain [78]. The β selection checkpoint ensures that only cells with an appropriate TCRβ rearrangement will differentiate further [79]. Here, developing thymocytes pair the TCRβ chain with Pre-Tα and CD3 proteins to generate a pre-T-cell receptor (pre-TCR) [80,81].

Pre-TCR signaling activates the RAS–mitogen-activated protein kinase (MAPK) pathway as well as phospholipase C, which results in activation of several transcription factors including Ets-1, Id3, NFAT and NFκB [82-86]. Proper pre-TCR signaling arrests *TCRβ* gene rearrangement, provides essential survival signals, and permits further differentiation [73,87-89]. Cells then lose CD25 expression and progress to the DN4 and transient immature single positive (ISP) [90] developmental stages, both of which are characterized by extensive proliferation [73]. This is followed by the upregulation of CD4 and CD8 co-receptors and progression to the CD4 and CD8 DP stage.

DP thymocytes rearrange the *TCRα* chain and pair it with a β chain on the cell surface forming an αβ TCR. These cells then undergo both positive and negative selection [91,92]. As many as 95% of thymocytes will not make it through this selection process and will die in the thymus [93]. Surviving thymocytes then mature to either CD4 or CD8 SP cells and enter the periphery.

Notch signaling is critical for thymocyte development.

T-cell lineage commitment and proper development requires many environmental and cell intrinsic signals, including those generated by the Notch family of receptors (reviewed in [94]). Notch receptors transmit extracellular messages, following ligand activation, by translocating to the nucleus and forming a transcriptionally active complex. Of the four known Notch receptors, Notch1 is critical for early T-cell development. Conditional deletion of *Notch1* in the thymus results in reduced thymic cellularity, alterations in thymocyte development, and ectopic B-cell development [95,96]. Conditional deletion of *CSL*, a Notch binding partner required for transcriptional regulation, also results in thymocyte development arrest and B-cell development in the thymus [95,97]. Consistently, pharmacological inhibition of Notch in fetal thymic organ cultures (FTOC) results in B-cell maturation at the expense of T-cell development [98,99]. Collectively, these studies suggest that Notch1 is essential for T-cell development and these effects are likely Notch1/CSL dependent.

Conversely, gain of function studies demonstrate that expression of constitutively active intracellular Notch1 stimulates DP T-cell development and blocks B-cell development in the bone marrow [100]. Moreover, transducing bone marrow stromal cells with Notch ligands drives T-cell development and inhibits B-cell development in *in vitro* culture assays [101,102]. While constitutively active Notch1 causes T-cell proliferation in the bone marrow, overexpression of known Notch1 target genes *Hes1 and Hes5* fail to induce ectopic T-cell expansion in the bone marrow or perturb T-cell maturation in the thymus. *Hes1* or *Hes5* expression does result in a partial disruption of B-cell development

[103], suggesting that additional Notch1 regulated genes are required to specify T-cell development.

Normally, Notch ligands, Jagged 1 and Jagged 2 (Jag1, Jag2) and Delta-like 1,3,4 (Dll1,3,4) are highly expressed in the murine thymus and in the murine bone marrow stroma [104-106]. Notch receptors are expressed in hematopoietic progenitor cells in the bone marrow and on double negative thymic progenitors [105-109]. ETPs are the earliest known progenitor within the thymus with active Notch signaling. ETPs are DN1 thymocytes but also express high levels of Sca1 and c-Kit and resemble more primitive progenitors [77,110,111]. Notch signaling is essential for ETP generation and differentiation [112,113], suggesting the critical lineage specification signals that promote T-cell commitment may be received upon thymic entry.

Notch1 is not only required for lineage commitment, but is also essential for DN thymocyte differentiation. During early thymocyte development, *Notch1* expression is highest in early DN thymocytes and increases as cells progress to the DN3 stage of development. Following progression to the DN4 and DP stage of development *Notch1* expression is downregulated [105,114], suggesting precise regulation of *Notch1* expression during the DN3 – DN4 progression is critical. Consistently, conditional deletion of *Notch1* in developing thymocytes results in a partial DN3 differentiation block. This developmental arrest is in part due to impaired β chain rearrangement [115-117]. Notch1 is also required for proper pre-TCR signaling, which is essential for the proliferative burst and subsequent maturation of thymocytes [118]. Some studies suggest that Notch1 also directs αβ T-cell fate at the expense of γδ development [117,119,120] and CD4 versus CD8 SP

cell fate, however those subjects remains highly controversial [97,116,121-123]. Lastly, Notch signaling is also involved in both T helper 1 and 2 (Th1 and Th2) cell differentiation. Notch1 is required for Th2 differentiation and this is mediated by IL-4 signaling and Gata-3 upregulation [124,125]. While gain of function studies suggest Notch signaling also drives Th1 development [126], it remains unknown if Notch signaling is essential for the Th1 response [124,127].

Other Notch receptors may also function during early thymocyte development. Notch3 and to a lesser extent Notch2 are also expressed in early DN thymocytes [105]. Notch3 over-expression in early thymocyte development leads to phenotypes similar to that seen when Notch1 is overexpressed [128]. However, further studies reveal that unlike Notch1-deficient mice, Notch2- or Notch3- deficient mice do not display defects in early T-cell development [129,130]. These data suggest that Notch1 is a critical regulator at this developmental stage.

The Notch signaling pathway

Notch was first identified in 1917 through a loss of function phenotype that resulted in notched wings in *Drosophila melanogaster* [131]. Since that discovery, further examination of Notch signaling in *Caenorhabditis elegans* (*C. elegans*), vertebrates, and mammals has proven the pathway to be more complex. There are four members of the mammalian Notch family (Notch1-4), each are single pass transmembrane receptors with highly conserved protein domains [132,133]. In addition, there are 5 mammalian Notch ligands; Jag1,2 and Dll1,3,4. Notch ligands are structurally very similar, however Jag

ligands contain a greater number of epidermal growth factor (EGF) repeats and a cysteine-rich region close to the membrane that are not found in Dll ligands [134]. It is through the four receptors and 5 ligands that mammalian Notch signaling regulates cell fate, differentiation, proliferation and survival in a diverse array of biological processes from angiogenesis to hematopoiesis.

Unlike the two Notch homologs in *C. elegans* (Lin-12 and GLP-1), which are functionally redundant [135], mammalian Notch proteins have both overlapping and unique roles in normal development and disease. Structurally, however, Notch proteins are similar and contain two major subunits; the extracellular subunit (NEC) and the transmembrane subunit [34 136]. The NEC domain contains 29-36 EGF repeats, which bind Notch ligands [137], and a negative regulatory region (NRR). The NRR consists of three LIN12/Notch repeats and a heterodimerization domain (HD), which prevents ligand independent signaling. The NTM subunit contains a RAM domain and ankyrin (ANK) repeats, which are essential for protein interactions [138-141]. A full transactivation domain (TAD) is found in the NTM subunit of Notch1 and 2 proteins, however, Notch3 and 4 proteins contain significantly shorter TAD regions [138,142]. The NTM subunit also contains a C-terminal Pro-Glu-Ser-Thr (PEST) domain that is ubiquitinated to regulate Notch protein stability [143].

Generation of the mature Notch receptor requires three proteolytic cleavage events (Figure 2). The first is by a furin-like protease in the Golgi, which results in the cleavage of the NTM and the NEC [136]. These two domains then become noncovalently associated and the receptor is shuttled to the membrane. Once at the membrane the

second and third cleavage events are initiated by binding to membrane-bound ligands; Jag or Dll [144-146]. Cleavage by a TNF-α converting enzyme (TACE), a member of the a-disintegrin and metalloprotease (ADAM) family, occurs first and cleaves Notch close to the transmembrane domain [147]. This cleavage creates a short-lived transmembrane associated protein that is then cleaved at valine 1744 by a γ-secretase protein complex [148]. The γ-secretase complex is a multiprotein complex containing Presenilin, Nicastrin, Presenilin enhancer 2 (Pen-2), and Anterior pharynx defective 1 (Aph-1) [148-152].

The result of these cleavages is the release of the intracellular form of Notch (ICN) from the membrane. ICN then translocates to the nucleus where it binds to the helix-loop-helix transcription factor CSL (CBF1/RBP-J in mammals Suppressor of Hairless in *Drosophila* and Lag1 in *C.elegans*) and recruits coactivators; Mastermind-like 1 (MAML) and CBP/p300 [141,153,154]. In the absence of ICN binding, CSL binds the corepressor complex containing; KyoT2, CIR, N-CoR/SMRT, SKIP, Sin3A, SAP18, SAP30, RbAp46/48 and HDAC and inhibits transcription [155-160]. However, ICN binding to CSL replaces corepressors and recruits coactivators, which facilitates transcription [161].

The ICN, CSL, MAML, p300 complex then binds to CSL consensus sites (TGGGAA) within the promoter region of target genes. Targets including, *Notch1*, *Hes1*, *Deltex1*, *Notch3*, *Nrarp*, *Pre-Tα*, *Cyclin D1*, *p21*, *c-Myc*, *CDK4/6*, *CD25* are directly regulated by Notch1 [59,162-164].

The regulation of the Notch signaling pathway.

Precise Notch signaling is critical for a number of biological processes including apoptosis, proliferation, differentiation, and self-renewal. Therefore Notch signaling is tightly regulated by a variety of mechanisms. One mechanism is by the Fringe family of glycosyltransferases. There are three Fringe family members in mammals; Lunatic fringe, Manic fringe, and Radical fringe [165,166]. Fringe family members contribute to Notch pathway regulation by modifying the EGF repeats on the extracellular domain of the Notch receptor [165]. Although the role of EGF modification is not entirely understood, one function includes controlling Notch ligand/receptor binding specificity. For example, modification of Notch1 by Lunatic fringe specifically promotes Notch1/Dll interactions and inhibits Jag1 mediated signaling [167].

Notch protein stability is also regulated though ubiquitin modification by Itch, Numb, and Fbxw7. Itch, a HECT-domain E3 ubiquitin ligase, interacts with membrane-bound Notch1 both *in vitro* and *in vivo* [168] and targets Notch1 for a lysosome-degradation pathway [169]. Numb, a membrane-associated protein, interacts with ITCH to promote ubiquitination of membrane-bound Notch1 and also mediates degradation of the intracellular domain following ligand dependent cleavage [170].

Fbxw7 (also known as Sel-10, hCdc4), an F-box containing protein, is one of the four subunits of ubiquitin protein ligase complex called SKP1-cullin-F-box (SCFs) [171]. Fbxw7 interacts with substrates via its WD40 repeats following phosphorylation of the substrate within the Cdc phosphodegrons (CPDs) [172,173]. Following phosphorylation of Notch within the PEST domain by CycC:CDK8, Fbxw7 specifically binds and recruits

the ubiquitin ligase SCF complex to PEST domain [174]. The addition of ubiquitin subsequently targets the protein for degradation by the proteosome [175-179]. Fbxw7 is a haploinsufficient tumor suppressor that has a number of cellular targets besides Notch receptors, including Cyclin E, Myc, c-Jun, and mTOR [180-182].

Notch signaling is also regulated by ligand and receptor availability (reviewed in [183]). Both Notch ligands and receptors have distinct patterns of expression that limit Notch activation. Notch1 is widely expressed throughout a number of tissues including; the brain, liver, heart, lung, kidneys, stomach, intestine, bone marrow, skeletal muscle, spinal cord, eye, and thymus. Notch2 expression is also broad, as it is found in brain, liver, kidney, and stomach. Notch3 and Notch4 expression however, are more restricted. Notch3 is found expressed in vascular smooth muscle, the central nervous system, and hematopoietic cells, while Notch4 expression is limited to vascular endothelial cells. As mentioned previously, some structural variability is observed among Notch receptors, in that Notch1 and Notch2 included a full-length TAD, while Notch3 and Notch4 have truncated or the absence of the TAD entirely [138,142]. Presence or absence of a TAD may affect Notch signal strength and lead to activation of specific target genes. Therefore, the distinct pattern of expression of each of the 4 Notch receptors could also be a mechanism to regulate the effects of Notch signaling.

The role of Notch signaling in development.

Notch signaling is critical for a number of cellular functions both embryonically and postnatally. During embryogenesis, Notch receptors and ligands are essential and

have non-redundant roles. Targeted deletion of *Notch1* and *Notch2* results in embryonic lethality at day 11.5 due to severe defects in somitogenesis and vasculogenesis [184,185]. Consistently, deletion of Notch ligands *Dll1*, *Dll4*, or *Jag1* also result in embryonic lethality during E9.5–E12.5 [186,187]. While, *Notch3* null and *Notch4* null mice survive, severe defects in vascular development are also observed [188]. In humans, the requirement for proper Notch signaling is demonstrated in Alagille syndrome, an autosomal-dominant disorder, characterized by *JAG1* deletions and severe abnormalities of liver, heart, eye, skeleton, and kidneys [189]. Cerebral autosomal dominant arteriopathy with subcortical infarcts and leukoencephalopathy (CADASIL), a hereditary stroke disorder resulting from blood vessel degeneration, is associated with *NOTCH3* mutations [190,191]. These syndromes highlight the importance of Notch signaling throughout mammalian development.

Studies in *Drosophila* and *C. elegans* demonstrate that one function of Notch is the regulation of lineage choice. Notch promotes lineage specification via lateral induction or lateral inhibition (reviewed in [132]). Lateral induction implies that some cells express Notch ligands (potential for higher Notch signaling) and other cells express Notch receptors (potential for lower Notch signaling). Through cell-to-cell interactions, some cells generate more Notch signaling activity, which induces a certain cell fate. The other proposed mechanism, lateral inhibition, suggests that groups of precursors express both Notch ligands and receptors. However, by a mechanism that is currently unknown, some cells within the group acquire higher Notch signaling than the others. This effect can be amplified, as Notch signaling has the potential to feedback and inhibit ligand

expression. Eventually distinct groups of cells with differing levels of Notch signaling are formed, dictating different lineage choices.

Notch signaling is important for lineage choice decisions in a variety of cellular contexts (reviewed in [132]). In the skin, Notch1 is essential for hair follicle development from precursor cells [192,193]. Targeted deletion of *CSL* in the skin results in hair loss and epidermal hyperkeratinization [194], suggesting Notch/CSL promote hair formation and block epidermal differentiation. In vascular development, Notch signaling specifies arterial versus venous endothelial cell fate decisions. It is hypothesized that the default pathway of the endothelial precursor cell is a venous cell fate. However, Dll4/Notch signaling directs endothelial cells to an arterial fate [195,196]. Consistently, expression of Notch receptors and ligands are found restricted to arteries [90,197]. Studies using *CSL* null mice and evaluation of patients with *NOTCH3* mutations demonstrate that loss of Notch/CSL signaling results in severe arterio-venous-malformations [198].

In the intestine, Notch signaling also promotes cell lineage specification. The intestinal epithelium is comprised of enterocytes, endocrine, paneth, and goblet cells that are all derived from multipotent stem cells located in the intestinal crypts. Enterocytes, which comprise the majority of the intestinal epithelium, have an absorptive function and can differentiate from crypt stem cells following signals from Notch target gene, *Hes1* [199]. Notch signaling also inhibits the differentiation of mucous secreting goblet cells from crypt stem cells by repressing *Klf4* [200]. Consistent with these data, pharmacological inhibition of Notch signaling can result in a differentiation shift of crypt stem cells from the enterocyte fate to the goblet cell fate [201].

The Notch signaling pathway also regulates functions commonly co-opted in malignancy, such as proliferation and self-renewal. Self-renewal is defined as the capacity of cells to produce daughter cells indefinitely, while retaining the ability to produce more differentiated progeny, through asymmetric division (reviewed in [202]). To date a number of pathways, including the Notch pathway, have been implicated in regulating stem cell self-renewal. Specifically, roles for Notch1 in self-renewal have been described in epithelial, neuronal, intestinal, and mammary stem cells [201,203-206]. In neuronal stem cells (NSC), Notch1 signaling is required for stem cell maintenance, as *CSL* or *Notch1* deficient mice have a significant reduction in NSCs[204,205]. Similarly, in the intestinal epithelium, *CSL* deficient mice have a decrease in stem cell number and conversely, constitutive expression of *Notch1* results in intestinal stem cell hyperplasia [203].

A role for Notch signaling in HSCs has also been proposed. While it is clear that Notch1 is essential for the generation of hematopoietic stem cells in the embryo [207-209], the role of Notch1 in HSC maintenance remains controversial. Expression of Notch ligands or intracellular Notch1, increases self-renewal and blocks differentiation of HSCs [210]. Constitutive Notch1 expression in murine HSCs resulted in a cytokine dependent HSC cell line that retains both myeloid and lymphoid pluripotency [211]. However, blocking Notch signaling in HSCs via overexpression of a dominant negative form of the Notch coactivator Mastermind-like 1 (DnMAML), or using *CSL* deficient HSCs showed no defect in HSC self-renewal capabilities [212]. Consistent with this finding, *Notch1*/*Jag1* double knockout mice appear to have normal HSC function [213]. One possible explanation

for these conflicting results is that Notch receptors have functionally redundant roles in promoting HSC self-renewal or regulate self-renewal of HSCs via a CSL independent pathway. It is also possible that high levels of Notch1 signaling achieved in gain of function studies may alter HSC function. Thus, deregulated Notch1 signaling may confer self-renewal capabilities on stem cells or progenitors and thereby contribute to malignancy.

***NOTCH1* is the most frequently mutated gene in T-ALL.**

NOTCH1 was first implicated in T-ALL through a rare chromosomal translocation t(7:9)(q34:q34.3) originally described in 1991 [214]. In less than 1% of patients with T-ALL, the 3' region of *NOTCH1* (chromosome 9) is translocated to the *TCRβ* locus (chromosome 7). This translocation results in a truncated, constitutively active form of NOTCH1 capable of ligand independent signaling. Expression of this constitutively active protein transforms cells *in vitro* [215] and mice reconstituted with intracellular NOTCH1 expressing bone marrow develop a T-ALL-like disease [216]. Additional experiments demonstrate that expression of activated NOTCH1 in the murine thymus also results in T-cell neoplasms [217]. Mutational analyses demonstrated that the ankyrin domain (ANK), nuclear localization sequences (NLS), and transcriptional activation domain (TAD) of NOTCH1 are each required for leukemic transformation [218]. Taken together these studies confirmed that constitutively active NOTCH1 is oncogenic and contributes to leukemic transformation.

Since the discovery of the t(7:9)(q34:q34.3) translocation, gain of function

mutations affecting NOTCH1 have been detected in approximately 70% of T-ALL patients [219-224]. *NOTCH1* mutations in the HD and/or PEST domains are the most common and occur in 50% of T-ALL patients [224]. HD mutations cause an amino acid sequence change that results in ligand independent cleavage by the TNF-α converting enzyme [225]. C-terminal PEST domain mutations appear less frequently and are generally deletions or insertions that truncate the protein [224]. As ubiquitination of the C-terminal PEST domain targets NOTCH1 for degradation by the proteasome, deletion of the PEST domain results in increased NOTCH1 stability [176]. Interestingly, 18% of T-ALL patients harbor HD mutations and PEST mutations in the same *NOTCH1* allele, which results in a 10-fold increase in reporter activity compared to *NOTCH1* alleles containing only HD or PEST mutations [224]. Recently, internal tandem duplications within the juxtamembrane domain (JME) of *NOTCH1* were observed in an additional 3% of T-ALL patients [223]. These mutations facilitate metalloprotease cleavage and result in ligand independent activation of NOTCH1 [223]. Inactivating mutations in the NOTCH1 E3 ligase, *FBXW7*, are also found in 8.6% of primary T-ALL samples. These heterozygous missense mutations occur within the substrate-binding domain of *FBXW7* and reduce substrate recognition, resulting in increased levels of intracellular NOTCH1.

Unlike intracellular NOTCH1, the *NOTCH1* alleles with either HD or PEST mutations only, do not generate sufficient levels of NOTCH1 expression to initiate leukemia in bone marrow transplantation assays [226]. However, these alleles can accelerate K-Ras induced T-ALL development [226]. These data suggest that many of the gain of function *NOTCH1* mutations commonly seen in T-ALL are most likely secondary or

cooperative events in leukemia.

Other Notch family members have been implicated in leukemogenesis, but to a lesser extent than NOTCH1. While no mutations or translocations affecting *NOTCH2* or *NOTCH3* have been described as of yet, intracellular NOTCH2 is capable of transforming rat kidney cells that had been previously immortalized by E1A (RKE cells) *in vitro*, albeit less efficiently than NOTCH1 [215]. A transgenic mouse model that expresses constitutively active *Notch3* in thymocytes also develops T-cell leukemia [128]. NOTCH3 overexpression has also been described in relapsed human T-ALL samples [227]. In contrast, no association with NOTCH4 has been demonstrated in T-ALL.

Notch1 mutations are frequent in mouse T-ALL models.

In a number of mouse T-ALL models, *Notch1* mutations are common cooperating events [228-231]. In the *Lck-Tal1* T-ALL model, spontaneous *Notch1* mutations are detected in 74% of the resultant tumors [230]. Mutations predominantly occur in the PEST regulatory region, resulting in a truncated, stable form of Notch1 (91.5%), and HD mutations are rare (8.5%) [230]. The reason for the difference in the type of *NOTCH1* mutations detected among murine and human T-ALL samples is unclear, but might indicate that murine T-cell leukemic blasts still rely on ligand activation, or harbor an as yet unknown mutation that promotes ligand independent signaling. Murine *Tal1* tumors were also analyzed for the presence of mutations in *Notch2*, *3*, and *4*. However when these regions were sequenced in 28 tumors, no mutations were found. These data suggest that like human T-ALL, there is preferential activation of Notch1 in *Tal1* induced leukemogenesis [230].

NOTCH1 mediates leukemic growth by directly regulating c-MYC expression

The prevalence of *NOTCH1* mutations in T-ALL suggests that aberrant Notch signaling may be required for leukemic growth and/or survival. To test a requirement of NOTCH1 for leukemic growth, T-ALL cell lines were cultured with γ-secretase inhibitors (GSIs), and cell proliferation and viability were measured. GSIs inhibit Notch cleavage by the γ-secretase complex, and therefore prevent the generation of intracellular Notch. GSI treatment caused a G1 cell cycle arrest and/or apoptosis in both murine and human T-ALL cell lines [224,230,232,233]. In addition, GSI treatment decreased intracellular NOTCH1 expression and reduced NOTCH1 target gene expression [224,230,233]. Although the γ-secretase complex has a number of substrates, including Notch ligands, ErbB4, CD44, Growth hormone receptor, N- and E-cadherins, and Amyloid precursor protein [234-237], the G1 arrest/ apoptosis observed in human and mouse T-ALL cell lines can be rescued by retroviral expression of intracellular Notch1 (ICN1) prior to GSI treatment [59,224]. Additionally, similar effects on leukemic growth are also observed when Notch signaling is inhibited via overexpression of a dominant negative form of the Notch coactivator Mastermind-like 1 (DnMAML) [233]. Collectively, these data demonstrate that Notch1 is required for leukemic growth and suggest GSIs inhibit leukemic growth via Notch1 inhibition.

Although Notch1 has clearly been shown to be required for leukemic growth *in vitro*, how Notch1 mediates transformation is unknown. Retroviral expression of many Notch1 regulated genes, such as Hes1, Hes5, and Cyclin D3, fail to rescue leukemic cells

from the effects of Notch inhibition, indicating that these target genes are not sufficient for leukemic growth [233]. Gene expression profiling has identified c-MYC as a novel direct transcriptional target of NOTCH1 in both murine and human T-ALL cells [59,163,238]. Importantly, c-MYC, like ICN1, is sufficient to fully rescue many murine and human T-ALL cell lines from the effects of Notch1 inhibition *in vitro* [59,163]. *c-Myc* deletion in mouse T-ALL cells also inhibited leukemic growth, suggesting that c-Myc may be required for Notch1 leukemic growth *in vivo* [239].

However, unlike ICN1, c-MYC is unable to rescue 2 of 10 murine and 2 of 5 human T-ALL cells lines from the effects of Notch1 inhibition[59,163], suggesting other Notch1 target genes contribute to leukemogenesis. Additional studies have identified a number of cell cycle mediators including *p27*, *CYCLIN D3*, *CDK4*, and *CDK6* as genes regulated by NOTCH1 in T-ALL cells [164,240]. While these genes likely contribute to leukemic growth, overexpression of these targets provides only a partial rescue from GSI induced G1 arrest in human T-ALL cell lines [164]. One goal of this thesis research is to identify additional Notch1 regulated genes in T-ALL and to evaluate their role in leukemic growth and survival. Data presented in Chapters 2 and 3 of thesis establish that Notch1 positively regulates Lef1 and the AKT/mTOR pathway, both of which are important for murine leukemic growth.

Notch1 directly regulates Lymphoid enhancing factor 1 (*Lef1*) expression in murine T-ALL cells.

Lymphoid enhancing factor 1 (*Lef1*) is a member of the T-cell factors (Tcf)

family of DNA binding transcription factors [241,242]. The four family members (*Lef1*, *Tcf1*, *Tcf3*, *Tcf4*) are highly homologous and contain four critical protein domains; β catenin, cysteine-rich domain (CRD), high mobility group binding (HMB) domains, and alternatively spliced C-terminal tails (reviewed in [243]). The most N-terminal domain is the β catenin binding domain, which shares 60% homology between all Tcf family members. The CRD domain is the most diverse among family members, sharing 15-20% homology, and is critical for recruitment of the corepressor, Groucho. The HMG domain is highly conserved among family members (95-99% homologous) and is essential for DNA binding. The functions of the C-terminal tails is not well understood but are thought to contribute to specific regulation of target genes. Two LEF1 isoforms have been described, a full-length 54kDa nuclear protein and a truncated protein that lacks the HMB binding domain [244].

Lef1 is a integral component of the highly conserved WNT/β catenin signaling pathway (reviewed in [245]). WNT proteins are secreted glycoproteins that facilitate cell-to-cell interactions by binding to membrane bound receptor complexes. In the absence of WNT signaling, β catenin is phosphorylated and restricted to the cytoplasm. In this case, Lef1 functions as a transcriptional repressor through interactions with Groucho[246,247]. Upon WNT pathway activation, β catenin is dephosphorylated and translocates to the nucleus where it binds Lef1 or other Tcf family members, and activates transcription [248]. Lef1 also contributes to transcriptional regulation by bending DNA and providing essential contacts between transcription factors [249]. Transcriptional target genes of Lef1 include, *Cyclin D1*, *Survivin*, *c-Myc*, Myc Binding Protein (*Mycbp*) and the *Dll1* [250-253].

Tcf family members are critical for a number of diverse, context dependent processes including embryogenesis, intestinal and skin stem cell maintenance, granulopoiesis, hair follicle formation, B-cell progenitor proliferation, and thymocyte development [254-256]. In murine thymocyte development, Lef1 and Tcf1 are highly expressed and appear to have partially redundant roles. While *Lef1* deficient mice have normal T-cell development, and *Tcf1* deficient mice have an incomplete DN1, DN2, and ISP block, *Lef1/Tcf1* double knockout mice have a complete block at the ISP stage of early thymocyte development [257]. This developmental stage is a period of thymocyte progenitor expansion, suggesting Lef1 may contribute to thymocyte expansion possibly through enhancing c-Myc levels.

In addition to normal lymphopoiesis, Lef1 has been implicated in leukemogenesis. Mice reconstituted with Lef1 expressing bone marrow developed alterations in myeloid and lymphoid development [258]. These mice also develop B-ALL or AML, revealing that Lef1 misexpression contributes to leukemogenesis. Consistently, in primary human acute leukemia samples, *LEF1* expression is often higher than normal bone marrow or lymphocyte controls [259]. While Lef1 has been implicated in B-ALL and AML, whether Lef1 is important in T-ALL remains unknown. In Chapter 2 of this thesis, we demonstrate that Lef1 is a direct target of Notch1 in murine T-ALL and examine its role in leukemic growth.

Notch1 activates the PI3k/Akt/mTOR pathway in normal thymocyte development and in murine T-ALL.

Phosphatidylinositol 3-kinase (PI3K) phosphorylates phosphoinositide lipids to promote a number of critical cellular functions including proliferation, survival and cellular movement. There are four classes of PI3Ks (1A,1B, II, III), which are classified based on complex subunits [260]. Class I PI3Ks, the most studied, are activated by extracellular signals and oncogenes, such as Ras [261] (Figure 3). Once activated PI3K phosphorylates phosphoinositides and generates phosphatidylinositol-3,4-bisphosphate ($PI(3,4)P_2$) and phosphatidylinositol-3,4,5-triphosphate ($PI(3,4,5,)P_3$). $PI(3,4,5,)P_3$ is the major mediator of downstream PI3K signaling and is regulated by phosphatases including, phosphatase and tensin homolog (Pten) and inositol polyphosphate-5-phosphatase D (Ship1/2)[262,263]. Once $PI(3,4,5,)P_3$ is generated, it promotes the translocation of Akt to the cellular membrane, which facilitates its activation by kinases including phosphoinositide-dependent kinase 1 (Pdk1), the mTORC2 complex, and Akt itself [264-268]. Once activated, Akt promotes survival and cell growth through the phosphorylation of a number of downstream targets, including, Bad, Glycogen synthase kinase-3β (Gskβ), Forkhead transcription factors (Foxo), and the mammalian target of rapamycin (mTOR) [269-273].

mTOR is a protein kinase that is highly conserved from yeast to human. TOR was first identified through a mutational study in yeast that resulted in resistance to the macrolide antibiotic; rapamycin [274]. The mammalian form, mTOR, was later identified based on its binding capability to rapamycin [275-278]. mTOR is a member of two functional

protein complexes; mTORC1 and mTORC2 (Figure 3)(reviewed in [279]). mTORC1, the rapamycin sensitive complex, is involved in protein translational initiation through phosphorylation of downstream targets such as; eukaryotic translation initiation factor 4E binding protein 1 (4EBP-1), ribosomal protein S6 (S6RP), and ribosomal protein S6 kinase (p70 S6 K) [280,281]. The mTORC2 complex is relatively nutrient and rapamycin insensitive and can activate the Akt signaling pathway through phosphorylation [282,283].

mTOR signaling is critical for a number of diverse cell functions including protein translation, autophagy, cellular growth, and metabolism (reviewed in [284]). mTOR signaling responds to environmental signals and are generally regulated by growth factors and amino acid availability or by mitogens through the Ras/MEK/ERK pathway [279]. Stimulation of the PI3K/Akt pathway also activates mTOR signaling by directly phosphorylating and inhibiting Tsc1/2 protein complex, which is a negative regulator of mTORC1 (reviewed in [284]).

When activated, one of the functions of the mTORC1 complex is protein translation initiation through the phosphorylation and inhibition of 4EBP-1 [285]. Protein translation is initiated when the eukaryotic translation initiation factor (eIF4F) complex, composed of eIFAE, eIF4G, eIF4A, is assembled and recruited to the 5' cap structure of mRNA (reviewed in [286]). Assembly of this complex is tightly controlled. Under conditions that require reduced protein translation, 4EBP-1 binds to eIF4E and prevents its association with eIF4G and eIF4A. However, upon mTORC1 activation, 4EBP-1 is phosphorylated and inhibited [285]. This allows the formation of the eIF4F complex and cap dependent translation. mTOR also regulates translation through phosphorylation and

activation of target p70 S6 K [287]. P70 S6 K activation then phosphorylates a number of downstream targets including S6RP. Activation of S6RP promotes the translation of mRNAs that primarily encode ribosomal proteins and members of the translational machinery.

Since the mTOR signaling pathway is a key regulator of protein translation, cell growth, and metabolism, it is often misregulated in cancer (reviewed in [288]). Often, the upstream regulators of mTOR signaling are deregulated by growth factor receptor upregulation, gain of function mutations affecting PI3K/Akt directly, or through deregulation of Pten. Interestingly, many mouse models of tumorigenesis driven by *Pten* deletion or constitutively Akt activation, are sensitive to mTOR inhibition by rapamycin [289,290]. These studies suggest that mTOR is a critical factor in PI3K-mediated tumorigenesis.

In addition to classical regulation by growth factors or pathways such as Ras, there is growing evidence that, Notch1 may also regulate the PI3K/Akt/mTOR pathway. During the DN3 to DN4 transition in thymocyte development, Notch1 provides critical proliferative and survival signals following the generation of a productive pre-TCR. Constitutively activated Akt can rescue early double negative thymocytes from apoptosis associated with Notch inhibition and can restore the ability of cells to undergo β selection in the absence of Notch signaling [118]. These findings suggest Notch1 promotes double negative thymocyte survival through activation of the PI3K/Akt pathway. These data have major implications for T-ALL and suggest Notch1 may mediate leukemic survival by activating the Akt pathway. The work presented in Chapter 3 of this thesis

demonstrates that the AKT/mTOR pathway is aberrantly activated in murine T-ALL and its activation is in part mediated by Notch1 signaling. We also demonstrate that the mTOR pathway mediates essential survival signals in murine T-ALL cell lines. Moreover, we demonstrate that Notch and mTOR pathway inhibition reduces human T-ALL growth *in vivo*.

Analysis of leukemic initiating cell population in T-ALL

50% of TAL1+ T-ALL patients relapse following chemotherapy [28]. Relapse may occur because genomic instability and diversity among the malignant cells contributes to drug resistance and disease relapse. Relapse may also occur because malignancies harbor a subset of tumor cells, leukemia-initiating cells (L-ICs), that are inherently resistant to conventional treatment. In many hematopoietic malignancies, including AML and chronic myelogenous leukemia (CML), there is evidence of a L-IC population. Although the genes and pathways involved in L-IC biology are relatively unknown, evidence suggests that pathways critical to the maintenance of normal stem cells, such as the Notch pathway [201,203-206], maybe required for L-IC maintenance.

L-ICs were first identified in AML [291,292] and are described as a subpopulation of cancer cells that have the unique ability to initiate disease. Like normal stem cells, L-ICs can self-renew and give rise to more L-ICs (daughter cells) that retain increased proliferative capacity (reviewed in [202]). L-ICs also have the potential to divide and differentiate into progenitor cells with finite proliferative capacity. These progenitor cells often comprise the bulk of the tumor cells and are thought to have diminished initiating

potential. Importantly, L-ICs, like normal HSCs, have been shown to be resistant to apoptotic stimuli, and may also express increased levels of ATP-associated transporters which renders cells relatively resistant to conventional chemotherapy [293,294].

For most AML subtypes, human leukemic cells enriched in the capacity to initiate disease in nonobese diabetic/ severe combined immunodeficient (NOD/SCID) mice express CD34 and lack CD38 expression, which is immunophenotypically similar to primitive hematopoietic stem cells [291,292]. This suggests that AML is organized in a hierarchical manner, like normal hematopoiesis, and that L-ICs arise due to mutations within HSCs. The finding that hematopoietic or adult stem cells are enriched in L-IC activity is probable because of the inherently long lifespan of stem cells that could permit the acquisition of numerous mutations required for transformation. In addition, stem cells are already capable of both self-renewal and differentiation, which are critical for tumor initiation.

However, recent studies using mouse models of leukemia suggest that committed progenitors may also be the targets of transformation and harbor L-ICs. While committed progenitors may have the ability to proliferate and differentiate, they do not have the ability to self-renew. Therefore, committed progenitors must acquire the ability to self-renew through transformation events. In CML, Gsk3β missplicing leads to enhanced β catenin activity that results in aberrant self-renewal of granulocyte-macrophage progenitors (GMPs) [295,296]. Inhibition of β catenin through *Axin* overexpression inhibits the ability for GMPs to initiate leukemia in recipient mice [295]. Similarly, in mouse models of AML, numerous studies have demonstrated that fusion proteins such as MLL-ELL,

MLL-GAS7, MLL-AF9, MOZ-TIF2, and Cbfβ-SMMHC can transform restricted myeloid progenitors that lack self-renewal capacity [297-301]. Hence these studies demonstrate that L-ICs may arise from transformation events occurring in either the HSC or in the committed progenitor compartments.

While the presence of L-ICs has been well documented in AML and CML, there is less evidence implicating L-ICs in ALL. A L-IC population has recently been identified in pediatric T-ALL patients [302,303] and GSI treatment of a few T-ALL patients reduced engraftment in NOD/SCID mice [302]. Data presented in Chapter 4 of this thesis demonstrate that clonal mouse T-ALL tumors are phenotypically heterogeneous, containing immature DN3-like and DN4-like thymic progenitors and differentiated DP and/or SP leukemic blasts. Importantly, the DN3/DN4 progenitors are Notch active and are enriched in disease initiating potential, whereas mice injected with DP leukemic blasts failed to develop leukemia. These data suggest T-ALL, like AML and CML, harbors a leukemic stem cell population.

Targeting the Notch pathway in T-ALL

The dependence of T-ALL cell lines on Notch signaling [224,230,232,233], and the emerging role of the Notch pathway in the maintenance of L-ICs [302], make this pathway a potential therapeutic target. To date there are a number of proposed mechanisms to inhibit Notch signaling. One is to block cleavage events required for Notch receptor processing through the use of GSIs, as mentioned previously, or inhibitors that affect the enzymatic activity of the ADAM metalloproteases [304,305]. Another approach is to interfere

with Notch receptor and ligand binding using monoclonal antibodies (reviewed in [306]). Notch signaling could be inhibited in the nucleus, using small molecules that mimic dominant negative Mastermind-like 1 (DnMAML) or by using siRNAs to specifically disrupt the protein-protein interactions that are required for Notch-dependent transactivation [307,308].

To date GSIs and monoclonal antibodies to the Notch receptor are being tested clinically [306,309] however systemic inhibition of Notch has been associated with several toxicities, including secretory diarrhea due to goblet cell metaplasia of the small intestine, reversible thymic suppression, and hair pigmentation and loss [200,310]. A phase 1 clinical trial opened to test the effects of GSIs on 8 relapsed leukemia and lymphoma patients [309]. The patients were administered GSI continuously and because of associated toxicities, the trial closed prematurely before the clinical efficacy of GSIs could be evaluated. The work presented in Chapter 3 of this thesis tests whether *in vivo* GSI administration has anti-leukemic activity in preclinical mouse models. We developed an intermittent dosing regimen to minimize toxicities and demonstrated that Notch1 inhibition limits mouse and human leukemic growth *in vivo*. The work presented in this thesis also explores the possibility of using GSIs in combination with other anti-cancer drugs as a possible treatment regimen for T-ALL.

In summary, the work presented in this thesis aims to determine the mechanisms of Notch1 mediated leukemogenesis in the mouse. Data presented in Chapter 2 and 3 of this thesis identify that in murine T-ALL, Notch1 regulates Lef1 and the Akt/mTOR pathway. Data presented in Chapter 3 of this thesis also examine the possibility of GSIs

as monotherapies or as a combination therapy for extended periods *in vivo*. Lastly, the work in Chapter 4 of this thesis provides evidence that T-ALL is driven by L-IC population and identifies that this population is enriched within committed thymic progenitors.

Figure 1. Scheme of T-cell development. Thymocyte development proceeds via discrete stages with DN progenitors giving rise to DP (CD4+ and CD8+) thymocytes that differentiate into CD4 or CD8 SP thymocytes. The DN progenitors can be distinguished by CD25 and CD44 staining pattern with DN1 stage consisting of (CD44+, CD25-), DN2 (CD44+, CD25+), DN3 (CD44-, CD25+), and DN4 (CD44-, CD25-) cells. Fluorescence intensity, as measured by flow cytometry on an arbitrary scale, is indicated for each marker. (Figure adapted from Ceredig and Rolink, *Nat. Rev. Immunol.* 2002).

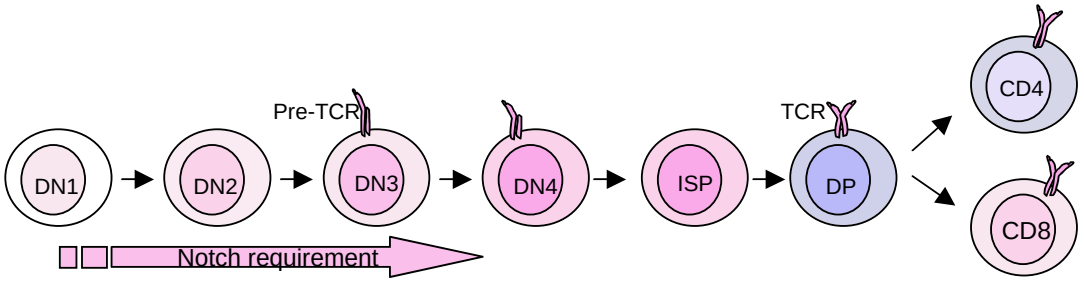

Pro-T1	**Pro-T2**	**Pre-T1**	**Pre-T2**	**ISP**	**DP**	**SP**
c-kit +++	c-kit +++	c-kit +	c-kit ^{low}	c-kit -	c-kit -	c-kit -
CD44+++	CD44+++	CD44+	CD44^{low}	CD44-	CD44-	CD44-
CD25-	CD25++	CD25++	CD25-	CD25-	CD25-	CD25-
IL-7Rα-	IL-7Rα+	IL-7Rα^{low}	IL-7Rα-	IL-7Rα-	IL-7Rα-	IL-7Rα-
CD3-	CD3-	CD3^{low}	CD3^{low}	CD3^{low}	CD3+	CD3++

Figure 2. Scheme of the Notch signaling pathway. There are 4 mammalian Notch receptors (Notch 1-4) and five ligands (Jag 1,2 and Dll1,3,4). Notch signaling is triggered upon ligand and receptor interaction, which induces two proteolytic cleavages; the first is by metalloproteases and the second is by the γ-secretase complex. Cleavage by the γ-secretase complex results in the release of the intracellular domain of Notch that translocates into the nucleus and associates with CSL. The association of intracellular Notch and CSL leads to the recruitment of coactivators (MAML, p300) and forms a transcriptionally active complex. Release of ICN can be inhibited with γ-secretase inhibitors (GSIs). (Figure was adapted from Nam et al. *Current Opinion in Chemical Biology* 2002).

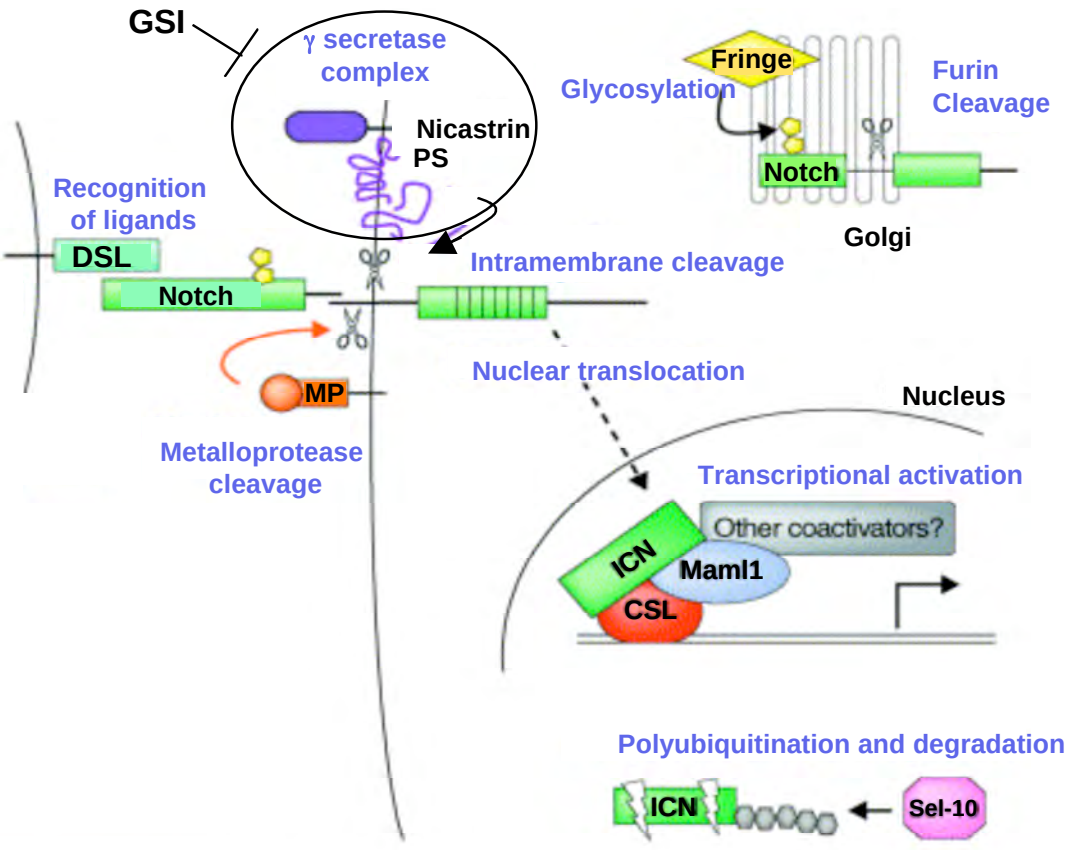

Figure 3. Model of the PI3K/Akt/mTOR signaling pathway. Extracellular signals and RAS regulate PI3K, which promotes phosphorylation of Akt through PDK1 or through mTORC2. Once activated, Akt regulates FOXOs, GSK3β, Mdm2, and also inhibits TSC1/2, which causes the activation of Rheb and mTORC1. mTORC1 regulates mRNA translation and ribosome biogenesis via inhibition of 4EBP1 and activation of p70 S6 K. Genes designated in green have been demonstrated to harbor gain of function mutations or be upregulated in T-ALL. Genes in orange are commonly deleted in T-ALL. (Figure adapted from Sabatini et al. *Nature Reviews Cancer* 2006).

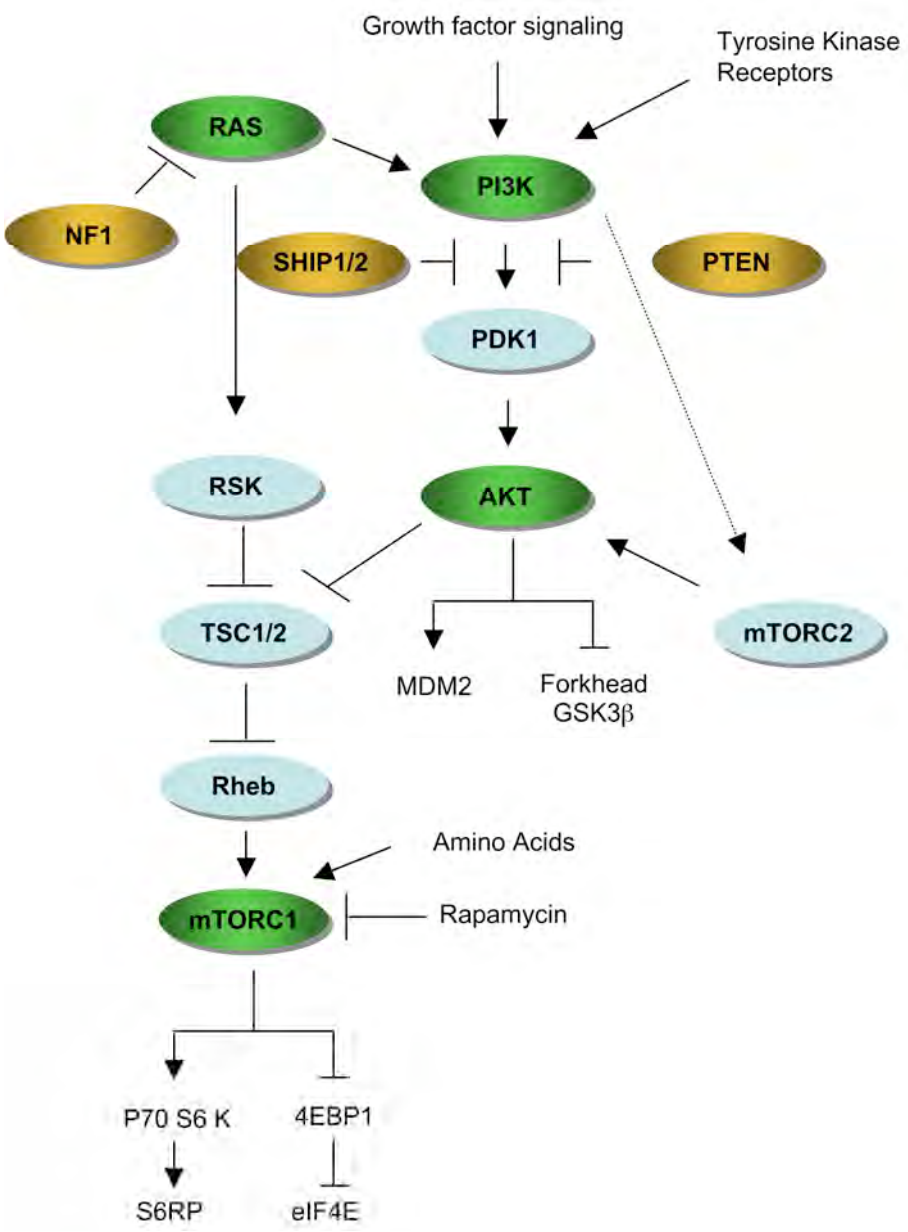

CHAPTER II

Differential Regulation of LEF1 in Murine and Human T-ALL cell lines

Figure Contribution:

Kathleen Cullion performed experiments in Figures 4A-D, Figure 6 A,B, Figure 7 A-E.

Introduction

Activating mutations in the NOTCH1 receptor have been detected in greater than 50% of T-ALL patients and are often found as secondary mutations in murine models of the disease [224,228-230]. Recent studies have highlighted the requirement of the Notch signaling pathway in T-ALL by using γ-secretase inhibitors (GSIs) to interfere with Notch signaling [224,230,233,311]. In mouse models of T-ALL and in human T-ALL cell lines treatment with gamma secretase inhibitors results in G1 arrest and/or apoptosis that can be rescued via retroviral expression of intracellular Notch1 (ICN1) [224,230,233,311]. In both human and mouse T-ALL cell lines, Notch1 driven leukemogenesis is mediated at least in part through direct transcriptional regulation of c-*MYC* [59,163,238]. While certainly a critical target, *in vitro* studies indicate that, unlike ICN1, *c-MYC* in unable to rescue the effects of Notch withdrawal in all murine and human T-ALL cell lines, suggesting that other as yet unknown Notch1-regulated genes contribute to leukemogenesis [59,163,312].

To identify genes dependent on Notch1 signaling we developed a mouse T-ALL cell line that expresses a doxycycline-regulated form of ICN1 [59]. To identify the Notch1 transcriptional signature in mouse T-ALL we performed gene expression profiling of these cells in the presence and absence of doxycycline. *c-Myc,* Lymphoid enhancing factor 1 (*Lef1*), Early growth response factor 1 (*Egr1*) as well as known Notch1 targets; *Hes1*, *Deltex1*, *Notch3*, *Nrarp*, *Ifi202b*, were identified in this initial screen [59].

Lef1, a member of the WNT/β catenin pathway, was an attractive target because several reports suggest that the Notch1 and WNT pathways may be coordinately regulated in development and potentially misregulated in cancer [210,313-320]. Here we

validate that *Lef1* is a direct Notch1 target in our *Tal1* mouse T-ALL mode1. Importantly, we demonstrate that while *Lef1* is Notch1 regulated in murine T-ALL cell lines, *LEF1* does not appear Notch1 regulated in human T-ALL cell lines. Moreover, positioning of CSL sites is not conserved among the mouse and human *LEF1* genes and unlike intracellular Notch1 and c-Myc, retroviral driven expression of Lef1 fails to rescue T-ALL cell lines from the effects of Notch inhibition.

Results

Lef1 is a Notch1 dependent gene in murine T-ALL.

To identify Notch1-regulated genes in T-ALL, a microarray analysis was performed using a leukemic cell line expressing a doxycycline-regulatable intracellular Notch1 (ICN1) construct [59], in which the addition of doxycycline inhibits the expression of ICN1. Lef1 mRNA levels changed 3.5 fold in the initial microarray screen. To validate the array finding, *Lef1* expression was evaluated in several mouse T-ALL cells by quantitative PCR. The doxycycline-regulatable ICN1 cell line, 3404, was treated with 2μg/ml of doxycycline *in vitro*. Decreases in Lef1 mRNA and protein levels were observed in the doxycycline treated cells compared to control (Figure 4A,B). Multiple mouse leukemic cell lines with detectable *Notch1* mutations generated from *Tal1* murine T-ALL model were then analyzed. These lines were treated with 1μM DAPT for 48 hours and Lef1 mRNA and protein levels were examined. We observed decreases in both Lef1 mRNA and protein expression in all GSI-treated mouse leukemic cell lines examined (Figure 4C,D). These data suggest that in mouse T-ALL cell lines, Lef1 expression is Notch1-dependent.

Lef1 is a direct Notch1 target in murine T-ALL.

The decrease in *Lef1* mRNA expression in response to GSI or doxycycline treatment suggests that *Lef1*, like *c-Myc*, may be a gene transcriptionally regulated by Notch1. Consistent with this idea, two consensus CSL binding sites, TGGGAA, are present in the murine *Lef1* promoter approximately 130 and 1200 base pairs upstream of

the transcriptional start site (Figure 5A). To determine if Notch1 directly regulates *Lef1* expression, we performed a chromatin immunoprecipitation assay using the doxycycline-regulated ICN1 leukemic cell line [59]. Using this system, we previously demonstrated a doxycycline-dependent recruitment of intracellular Notch1 to the promoters of known Notch1 targets *Hes1* and *c-Myc* [59]. Similarly, we observe a doxycycline-dependent recruitment intracellular Notch1 and its coactivator, Mastermind-like 1 (MAML) to the murine *Lef1* promoter at the -130-135 site (Figure 5B). Consistent with direct transcriptional activation of the locus, ChIP analysis revealed the recruitment of RNA polymerase II, Cyclin dependent kinase 9 (CDK9) as well as increases in H3 and H4 acetylation at the murine *Lef1* promoter in Notch1 active leukemic cells (Figure 5B). Upon the addition of doxycycline and the inhibition of intracellular Notch1 expression, we observed decreased binding of ICN1, MAML, RNA polymerase II and CDK9. These findings indicate that Notch1 regulates *Lef1* expression in mouse leukemic cells.

Lef1 expression fails to rescue leukemic cell lines from the effects of Notch inhibition.

Not all murine T-ALL cell lines can be rescued by retroviral expression of c-Myc prior to Notch inhibition, suggesting other Notch1 targets remain to be identified. Lef1 may provide critical proliferation and/or survival signals by regulating targets such as *Cyclin D1*, *c-Myc*, Myc binding Protein (*Mycbp*), and *Survivin* [250-253]. To test this, we infected two mouse leukemic cell lines; one previously shown to be rescued by c-Myc (720) and one unable to be rescued by exogenous-Myc (5046) with the MSCV retrovirus,

or a retrovirus expressing intracellular Notch1 (ICN1), or Lef1, or c-Myc. Following 5 days of GSI treatment, we observed a reduction in the number of viable, GFP+, MSCV- or Lef1- infected cells, compared to those infected with ICN1 (Figure 6A,B). As expected, retroviral expression of ICN1 or c-Myc prevented GSI-induced cell death in cell line 720 (Figure 6A). While expression of ICN1 protected 5046-cells from GSI-induced cell death, expression of neither c-Myc nor Lef1 was capable of rescuing this cell line from the effects of Notch1 inhibition (Figure 6B). These results suggest Lef1 expression alone is not sufficient to mediate leukemic growth by Notch1.

LEF1 does not appear NOTCH1 regulated in human T-ALL cell lines or primary T-ALL samples.

While our group and others have shown *Lef1* is a direct Notch1 target in murine T-ALL cell lines [321], whether *LEF1* is NOTCH1 regulated in human T-ALL cell lines and hence a relevant therapeutic target gene remained an unanswered question. To determine if NOTCH1 regulates *LEF1* expression in human T-ALL cell lines we treated human T-ALL cell lines, DND-41 and KOPT-K1, with 1μM Compound E or DMSO and examined *LEF1* expression using quantitative PCR. Both cell lines have *NOTCH1* mutations, express TAL1, and have previously been demonstrated to be GSI sensitive [233]. Unlike *c-MYC*, there was little change in *LEF1* expression following 4 or 7 days of GSI treatment in either DND-41 or KOPT-K1 (Figure 7A,B). These data suggest that at least in these two human T-ALL cell lines, *LEF1* does not appear NOTCH1 responsive. To rule out the possibility that LEF1 may no longer be NOTCH1 regulated in human T-ALL cell lines,

we extended our studies to primary T-ALL samples. We identified two patients, 05-386 and 202-67-64, which express TAL1 and have detectable intracellular NOTCH1 protein expression (Figure 7C). These patient cells were treated *in vitro* with GSI for 48 hours and *LEF1* and *c-MYC* gene expression was examined. In contrast to *c-MYC*, we found *LEF1* expression unaffected by GSI treatment (Figure 7D,E).

Discussion

When expressed by a retrovirus, c-Myc is unable to rescue some human and murine leukemic cell lines from the effects of Notch inhibition [59,163,312], which suggests that other novel Notch1 target genes may contribute to leukemogenesis. Using a murine cell line in which transcription of intracellular Notch1 is doxycycline inducible [59], *Lef1* was identified as Notch1 responsive. Further examination revealed Lef1 to be aberrantly expressed in cell lines derived from primary *Tal1* murine tumors. Using chromatin immunoprecipitation we also demonstrated doxycycline-dependent recruitment of intracellular Notch1 and co-factor, Mastermind-like 1, to the murine *Lef1* promoter. These data suggest not only is *Lef1* Notch1 regulated in murine T-ALL, but also is a direct Notch1 target gene. Since this study, *Lef1* was also identified as a direct transcriptional target of Notch1 in a *E2A-/-* model of T-ALL [321]. These complimentary studies strengthen the finding that Notch1 directly regulates Lef1 in murine leukemogenesis.

To assess whether Lef1 signaling is sufficient to maintain leukemic growth in the absence of Notch1 signaling, murine T-ALL cell lines were infected with Lef1 and subsequently treated with a GSI. However, retroviral expression of Lef1 in murine leukemic cell lines failed to rescue from GSI induced apoptosis. Although not sufficient to sustain leukemic growth, a recent study finds a decrease in the proportion of cells in the S phase of the cell cycle upon reduction of Lef1 mRNA expression [321]. These data suggest that although not sufficient, Lef1 expression is essential for leukemic expansion. Lef1 contributes to thymocyte expansion during early thymocyte development [322],

however, Lef1 expression is not Notch1 dependent in normal T-cell progenitors [321]. The reason for direct regulation of *Lef1* in murine leukemia and not in normal thymocytes is unknown, but could be due to increased intracellular Notch1 expression in leukemic cells. This possibility would suggest that the association of Notch1 to the *Lef1* promoter is of low affinity and only occurs when there are excessive levels of intracellular Notch1.

Surprisingly, *LEF1* expression does not appear positively regulated by NOTCH1 in the human T-ALL cell lines or human primary samples tested. The reason for the differential regulation of LEF1 in murine versus human T-ALL cell lines is unclear and unexpected. Examination of the human *LEF1* promoter revealed two potential CSL binding sites at positions -500 and -680. However, the site proximal to the transcriptional start site is not a conserved CSL consensus site (TGGGGA compared to TGGGAA) (data not shown). Perhaps this subtle alteration in the consensus site reduces CSL binding affinity to the human *LEF1* promoter. The true consensus site in the human *LEF1* promoter is located -680 basepairs upstream of the transcriptional start site. The sequences flanking this site do not maintain sequence homology to either of the sites found in the mouse promoter. Therefore, it remains possible that transcriptional regulation of *LEF1* by NOTCH1 is not achieved in human T-ALL because of an inability to recruit essential coactivators to this site.

These data do not rule out the importance of LEF1 in human T-ALL pathogenesis, but does imply that in human T-ALL, LEF1 cannot be the molecular link, if any, between Notch1 and WNT signaling. Interestingly, increased expression of TCF1 is also reported in T-cell malignancies [323], but whether TCF1 contains conserved CSL

binding sites and is a direct NOTCH1 target has not been tested. It is also possible that in human T-ALL, another direct NOTCH1 target contributes to Notch1/WNT cross talk. For example, in endothelial cells, Nrarp acts as a molecular link between Notch and WNT signaling [319], however, whether NRARP is misexpressed in human T-ALL and retains these functions in this model system remains unknown.

Materials and Methods

Mouse and Human T-ALL Cell Lines

Murine leukemic cell lines were cultured in RPMI with 10% FBS, 1% glutamine, Penicillin/ Streptomycin, 50μM β mercaptoethanol at 37 C under 5% CO_2. Human T-ALL cell lines and primary human leukemic cells were cultured in RPMI with 10% FBS, 1% glutamine, Penicillin/ Streptomycin at 37 C under 5% CO_2. To inhibit Notch1 signaling, cells were plated at $1x10^6$ in a 10cm dish in the presence of either MRK-003 (Merck Research Laboratories, Boston, MA) at 1μM or compound E (Axxora, San Diego, CA) at 1μM. Mock treated cells were cultured with DMSO at a final concentration of 0.01%.

Western Blot Analysis

Murine leukemic cells lines were lysed in 20mM Tris buffer pH 7.4 containing 0.14 M NaCl, 1% NP-40, 10% glycerol, 1mM sodium orthovanadate and protease inhibitors and protein concentrations determined using the Bradford assay (Bio-Rad, Hercules, CA). Protein was resolved on a 10% SDS-PAGE gel, transferred to a nitrocellulose membrane. The following antibodies were used for immunoblotting: ICN Val1744 (#2421 Cell Signaling Technology, Beverly, MA) and Lef1 antibodies (Clone 2D12 Upstate, Lake Placid, NY). Blots were stripped and reprobed with β-Actin (#A5441, Sigma, St. Louis, MO) to ensure equal loading.

RNA Analysis

RNA was extracted from murine T-ALL cell lines using Trizol. cDNA was synthesized using Superscript First - Strand Synthesis System (Invitrogen, Carlsbad, CA). Primers

were designed using Primer Express software (Applied Biosystems, Foster City, CA). The primer sequences are as follows; murine *Lef1* forward, 5'-TCCTCTCAGGAGCCCTACCA-3'; murine *Lef1* reverse, 5'-GGCCTCCGTCTGGATGCT-3'; human *LEF1* forward, 5'-TACCACGACAAGGCCAGAGAA-3'; human *LEF1* reverse, 5'-TGGCATCATTATGTACCCGGA-3'. Human *C-MYC* expression was measured using: human *C-MYC* forward, 5'-GCAGCTGCTTAGACGCTGGATTTT-3'; human *C-MYC* reverse, 5'-GCAGCAGCTCGAATTTCTTCCAGA-3'. The copy number obtained for the gene of interest was normalized to the copy number for ß-Actin, using primers previously described [59]. Relative quantities of mRNA expression were analyzed using QRT-PCR in the presence of SYBR green (Applied Biosystems ABI prism 7300 Sequence Detection System, Applied Biosystems, Foster City, CA).

ChIP Assay

Chromatin immunoprecipitation was performed as described previously [59]. The following primer set was used to amplify the region of the murine *Lef1* promoter forward: GAAGCGACGCAAGTGAATAGCTT; murine *Lef1* promoter reverse: AATGTCCGAATGCCAGGGCCCACGA.

Figure 4. Notch1 regulates mouse Lef1 expression. (A) Expression of *Lef1* was examined by quantitative PCR following 48 hours of treatment with doxycycline or DMSO control using the doxycycline-regulated ICN1 T-ALL cell line, 3404. β-Actin was used an internal control. **(B)** Cells left untreated or treated with 2μg/ml doxycycline for the time periods indicated. Cell lysates were separated by 10% SDS-PAGE gel and then probed with anti-Lef1 and anti-β Actin antibodies. **(C)** Mouse T-ALL cell lines, 720 and 5046, were treated with DMSO or 1μM GSI (DAPT) for 48 hours and *Lef1* expression was examined using quantitative PCR. **(D)** Cell lysates were separated by 10% SDS-PAGE gel and then probed with anti-Lef1 and anti- β Actin antibodies.

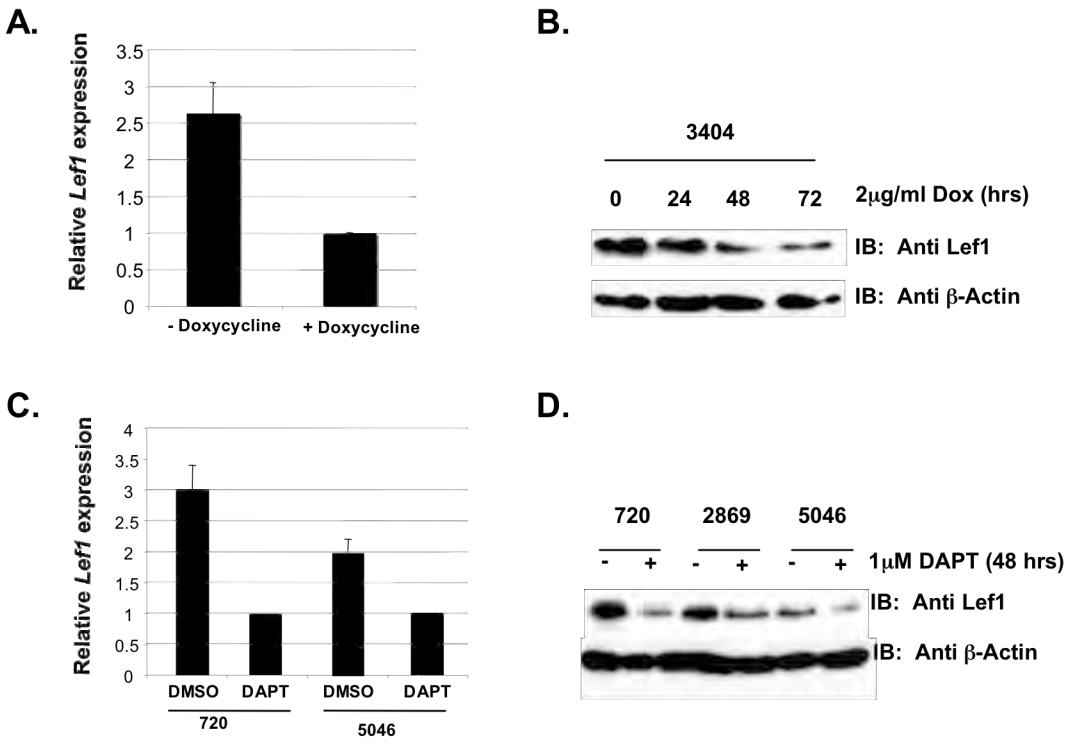

Figure 5. Dox-dependent recruitment of ICN1 and Mastermind-like 1 (MAML) to the *Lef1* promoter. (A) Schematic representation of the murine *Lef1* promoter. Canonical CSL binding sites and their positions relative to the transcriptional start site are highlighted. **(B)** Chromatin immunoprecipitation assay (ChIP) for CSL, Notch1, MAML, RNA polymerase II, and CDK9 at the murine -130-135 site. The dox-dependent 3404 leukemic line was treated with doxycycline (2μg/ml) for 48 hours or left untreated. Immunoprecipitations (IPs) were carried out using respective monoclonal or polyclonal antibodies or without antibody (No-Ab) as control. Immunoprecipitated and input DNA were amplified by PCR using primers specific for the *Lef1* promoter. PCR amplified products were analyzed on a 2% agarose gel.

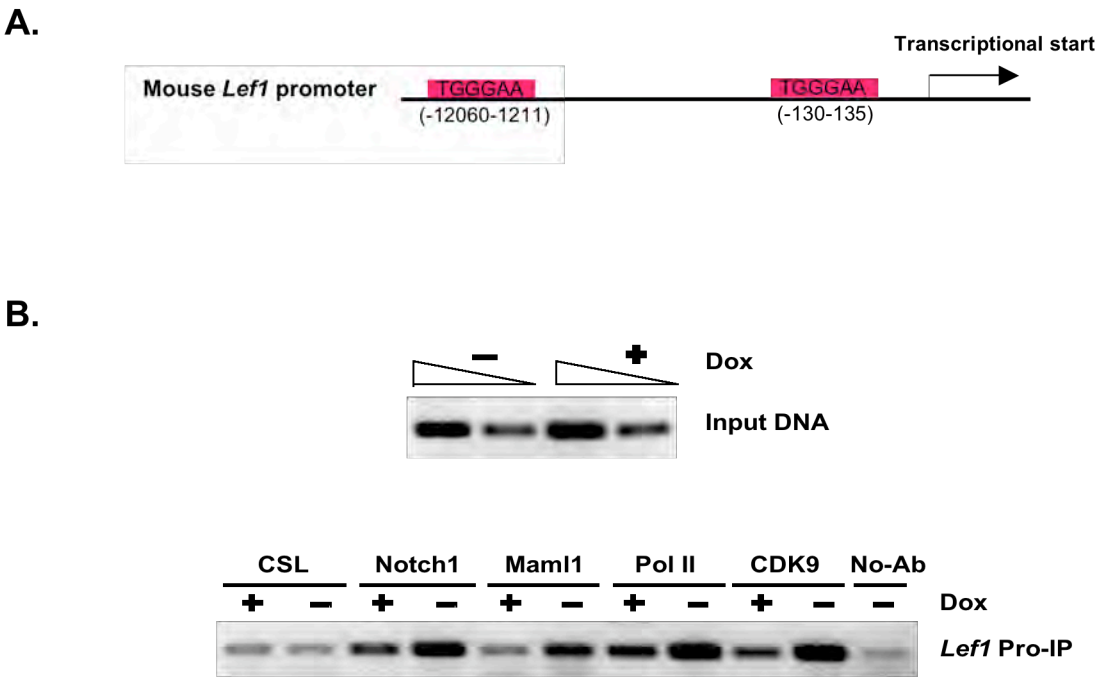

Figure 6. Lef1 does not rescue leukemic cells from the withdrawal of Notch signaling. Two murine leukemic cell lines, 720 **(A)** and 5046 **(B)** were left uninfected or were infected with MSCV retroviral vectors expressing Lef1, c-Myc or ICN. GFP+ cells were then treated with DMSO or with 1μM GSI (DAPT) for 6 days, and viability was determined by trypan blue staining.

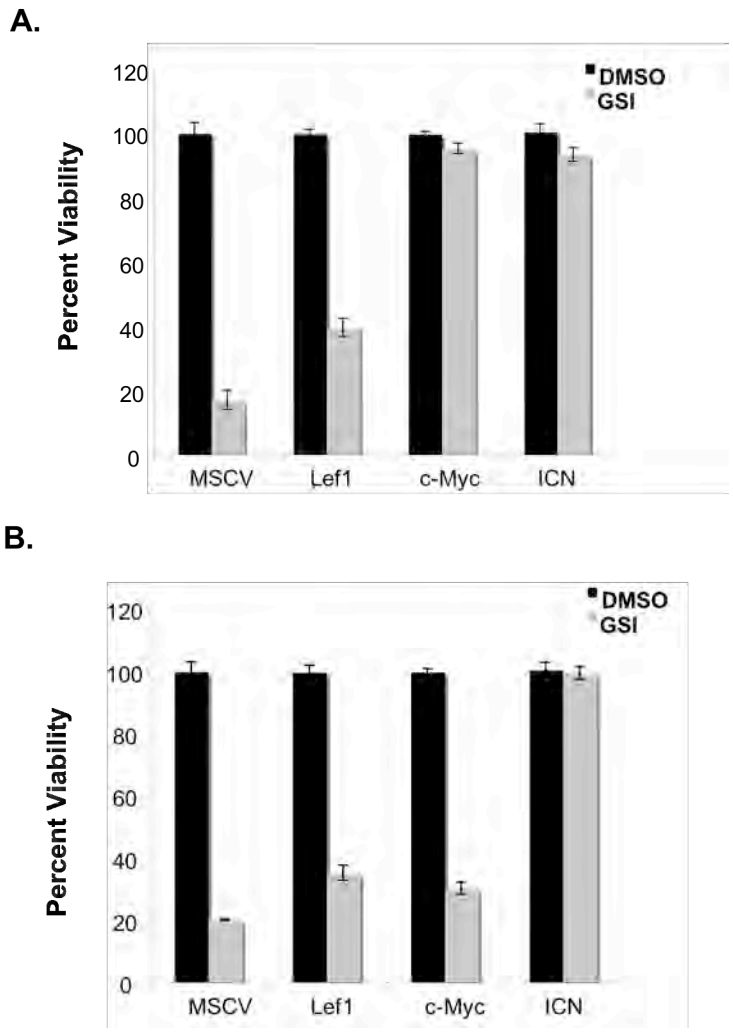

Figure 7. *LEF1* does not appear NOTCH1 regulated in human T-ALL cell lines or primary samples tested. Human leukemic cell lines DND-41 **(A)** and KOPT-K1 **(B)** were left untreated or were treated with Compound E (1μM) for the time points indicated. *LEF1* and *c-MYC* expression was examined by quantitative PCR. β-Actin was used an internal control. Primary patient samples were examined for intracellular Notch1 and human TAL1 expression by immunoblotting with intracellular Notch1 (anti-Notch^{IC} Val11744) and human TAL1 antibodies **(C)**. Cells from patient 05-386 **(D)** and 202-67-64 **(E)** were left untreated or were treated with Compound E (1μM) for 48 hours. *LEF1* and *c-MYC* expression was examined by quantitative PCR. β-Actin was used an internal control.

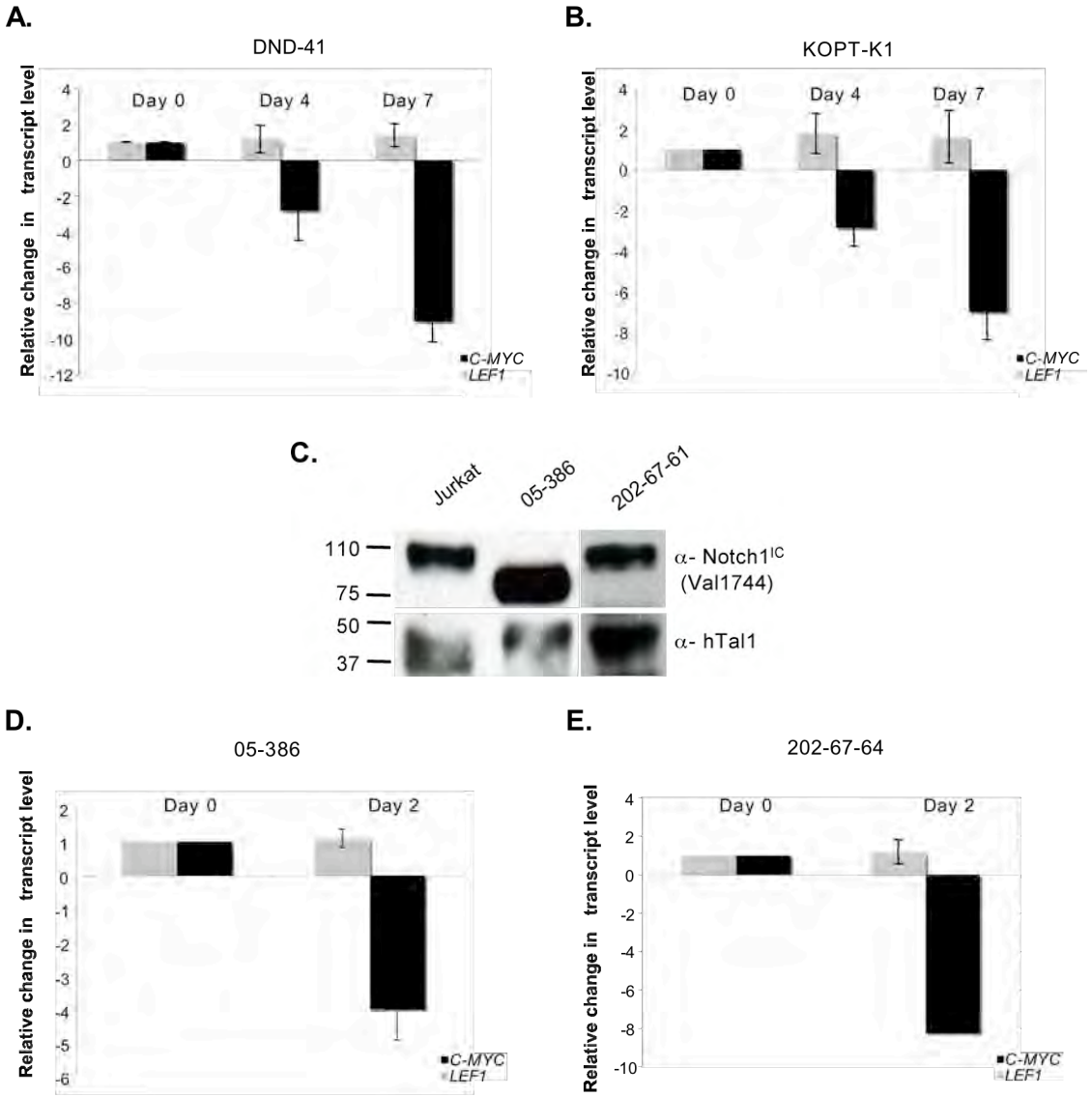

Chapter III

Targeting the Notch1 and mTOR pathways in a Mouse T-ALL Model

Data presented in this chapter has been published as:

Targeting the Notch1 and mTOR pathways in a mouse T-ALL model

Cullion K, Draheim KM, Hermance N, Tammam J, Sharma VM, Ware C, Nikov G, Krishnamoorthy V, Majumder PK, Kelliher MA.
Blood. 2009 Jun 11;113(24):6172-81.
PMID: 19246562

Figure Contribution:

Kathleen Cullion provided the data in Figure 8B, 9B, 10, as well as Figures 12- 16 and Table 2.

Introduction

Treatment of mouse *Tal1* leukemic cell lines *in vitro* with γ-secretase inhibitors (GSIs) results in cell cycle arrest and apoptosis, revealing that Notch1 signaling is required for leukemic growth/survival [230]. Although the majority of mouse *Tal1* leukemic cell lines undergo apoptosis upon GSI treatment *in vitro,* it remains to be tested whether Notch1 can be inhibited for extended periods of time *in vivo*. An additional concern regarding targeting the Notch pathway in T-ALL is that in contrast to mouse, many human T-ALL lines appear relatively GSI resistant *in vitro* [224,232,238], raising the possibility that GSIs alone may not prove effective in the treatment of T-ALL patients. Moreover, whether GSIs can be administered *in vivo* for extended periods of time at lower doses without associated toxicities remains uncertain.

In this study, we examined the effects of GSI treatment in our mouse T-ALL model. To examine GSI efficacy, we treated near end stage leukemic mice and found that GSI treatment extends the survival of leukemic mice, but is not sufficient to eliminate disease. In addition, we find that mouse *Tal1* leukemic cell lines isolated from GSI treated mice exhibit mTOR pathway activation, suggesting that mTOR inhibitors may synergize with GSI to limit leukemic growth/survival. Treatment of mouse T-ALL cell lines with GSI or rapamycin reduces mTOR activity, however combined GSI and rapamycin treatment further ablates mTOR kinase activity, resulting in increased apoptosis. GSI and rapamycin treatment reduced human leukemic growth *in vivo* and significantly increased overall survival. Collectively, this work supports the idea of targeting NOTCH1 in the treatment of T-ALL.

Results

MRK-003 represses Notch1 target gene expression and induces apoptosis of mouse T-ALL cell lines and primary *Tal1/Ink4a/Arf*+/- tumors.

The prevalence of mutations that result in activated NOTCH1 in patients with T-ALL raises the possibility that GSIs used to inhibit Notch1 and other GS-dependent substrates *in vitro* may have anti-leukemic activity in the clinic. To evaluate the ability of the GSI, MRK-003, to inhibit Notch1, multiple mouse T-ALL cell lines were treated with 1μM or 10μM of MRK-003 and Notch1 target gene expression examined. Decreased levels of *Hes1* and *Deltex1* expression were observed in the MRK-003 treated cultures following treatment for 24 hours (Figure 8A). We then compared the relative effectiveness of MRK-003 with *N*-[*N*-(3,5-difluorophenacetyl)-L-alanyl]-*S*-phenylglycine *t*-butyl ester (DAPT), another GSI known to inhibit mouse leukemic growth [230]. Multiple mouse T-ALL cell lines were treated with 1μM MRK-003 or with 1μM DAPT for three days and cell cycle analysis performed. In all three of the cell lines tested, increases in the percentage of apoptotic cells were observed in MRK-003 treated cultures compared to treatment with either DMSO (vehicle) or DAPT (Figure 8B). These *in vitro* data suggest that MRK-003 may be effective at inhibiting Notch1-mediated leukemic growth *in vivo*. To test this, thymic tumor explants (masses) isolated directly from *Tal1/Ink4a/Arf* +/- mice were treated with DMSO (vehicle) only, with 1μM DAPT or 1 μM MRK-003 for three days. The percentage of apoptotic cells was then determined by Annexin V/PI staining followed by flow cytometry. We found MRK-003 treated cultures contained

significantly more apoptotic cells than were observed in either the DMSO or DAPT treated cultures (Figure 8C; p=0.0273 by Kruskal-Wallis test [324]).

GSI treatment prolongs survival in a mouse T-ALL model.

These *ex vivo* studies indicated that MRK-003 administration to leukemic mice might induce apoptosis *in vivo*, decrease tumor burden, and increase overall survival. To test this possibility, we treated mice daily with 50mg/kg, 200mg/kg or 1000 mg/kg of MRK-003 and determined plasma concentrations of the compound. We found that effective plasma MRK-003 concentrations (1-10μM) were achieved in mice treated with all three doses (Figure 9A). However, when the MRK-003 compound was given daily at 150mg/kg, the mice began to develop diarrhea and lose weight (Figure 9C: R1 compared to V1). Chronic GSI administration is known to result in gastrointestinal (GI) toxicity due to Notch inhibition in the intestinal epithelium, resulting in gut metaplasia [201,203,310,325]. To assess GSI efficacy on mouse leukemic growth, we adopted an intermittent GSI dosing regimen that achieved effective concentrations of the drug without associated toxicities. Specifically, mice treated with 150mg/kg MRK-003 for three days followed by a four day rest period, had effective plasma compound levels (Figure 9B), did not exhibit evidence of body weight loss (Figure 9C: R2 compared to V1), and exhibited limited gut metaplasia (Figure 10). MRK-003 plasma levels peak following administration and effective drug concentrations are detected at 24 hours post treatment. Between 3-4 days post MRK-003 administration, compound levels decrease to below detectable levels and by 96 hours, decreases in goblet cells can be observed in the colons of the treated mice

(Figure 10). These data indicate that the gut epithelium recovers during the 4 day "off" period. GSI plasma concentrations were also measured each week following three full cycles of the intermittent dosing regimen to determine if the compound accumulates upon successive treatment. We found no significant change in plasma concentration following three cycles of intermittent dosing (data not shown). Additionally, in a pre-clinical mouse model, this intermittent dosing schedule was well tolerated, as no evidence of intestinal effects were detected following a 35 day treatment period (Tammam et al. Manuscript in preparation).

In an attempt to accurately reflect the clinical experience, near end stage leukemic *Tal1/Ink4a/Arf+/-* mice were treated with either vehicle or 150mg/kg MRK-003 for three days followed by a four day recovery period. Following the three days of GSI treatment, plasma compound levels were determined and an EC_{50} of 5-10μM of MRK-003 was achieved. Leukemic mice were treated with vehicle or MRK-003 following the three days on, four days off treatment regimen throughout the duration of the study. We found that GSI treatment resulted in a statistically significant increase in overall survival of leukemic mice when compared to vehicle treated mice (Figure 9D; $p< 0.005$). The median survival period for GSI treated mice was 18 days compared to 3 days for the vehicle treated group. In most cases, responses were evident in the MRK-003 treated mice immediately following the three day treatment period, as measured by an increase in physical activity and improved rates of respiration. Importantly, body weights are maintained in MRK-003 treated animals following successive cycles of intermittent GSI dosing (Table 1). This pilot study supports the idea that GSI-associated toxicities may be

overcome with intermittent dosing and provides evidence that Notch1 inhibition improves mouse leukemic survival *in vivo*.

GSI treatment induces apoptosis of leukemic cells *in vivo*.

To determine whether GSI treatment induced apoptosis *in vivo*, we performed TUNEL staining on thymomas isolated from vehicle or GSI treated mice. We detected increases in the percentage of apoptotic tumor cells in mice treated with MRK-003, compared to tumors exposed to vehicle only (Figure 11A and B; p=0.0339 by Wilcoxon's rank sum test [324]). However, similar to our *in vitro* data (Figure 8B), the *in vivo* response to GSI was variable. Three of the four GSI treated mice examined exhibited an increase in apoptosis of leukemic cells, ranging from 2-10-fold increases in TUNEL positive tumor cells (Figure 11B). An increase in TUNEL positive cells was not observed in one of four tumors from the GSI treated group (mouse 6448). However, we were unable to detect a Notch1 mutation in this tumor. The reasons for the variable GSI responses both *in vitro* and *in vivo* are unclear. One possibility for the variable *in vivo* responses may be that some tumors require longer treatment periods. For these studies, leukemic mice were treated with vehicle or with GSI for 3 days and then the mice were sacrificed and tumor sections analyzed for the presence of apoptotic cells. It is conceivable that more consistent responses may be observed in leukemic mice treated with multiple GSI doses. Nonetheless, GSI treatment clearly induced apoptosis and extended the survival of leukemic mice.

Transient GSI responses do not reflect development of GSI resistance.

Another potential reason for variable responses may be that the GSI treated mice develop GSI resistance. To exclude this possibility, T-ALL cell lines were generated from the GSI and vehicle treated mice and their response to GSI quantified *in vitro*. As expected, truncated Notch1 proteins were detected in the vehicle treated tumor 6856 and the GSI treated tumors 6838 and 6904. In contrast, a full length Notch1 protein appears expressed in tumor 6837, although increased intracellular Notch1 protein levels are observed, suggesting that this tumor may harbor mutations in other regulators of Notch1 protein stability. In all tumors, GSI treatment *in vitro* significantly reduced Notch1 protein levels, as assessed by immunoblotting with the anti-Notch1 V1744 antibody, which is specific for cleaved Notch1 (Figure 12A). Leukemic cell lines also clearly remained dependent on Notch1 for growth, as G1 arrest and apoptosis was observed upon GSI treatment (Figure 12B). These findings indicate that transient responses to GSI *in vivo* do not reflect the development of GSI resistance.

Repression of Notch1 target gene expression in GSI treated mice.

To further understand why GSI treatment prolonged survival but failed to eliminate disease, we examined Notch1 target gene expression (*Deltex1, c-Myc, Hes1* and *Pre-Tα*) in the vehicle and GSI treated leukemic cohorts using real time PCR (Figure 13A-D). We found *c-Myc* and *Deltex1* expression was reduced in MRK-003 treated leukemic mice compared to mice treated with vehicle only (Figure 13A,C). The difference in *c-Myc* and *Deltex1* expression in the GSI versus vehicle treated leukemic

mice was statistically significant (p=0.015 and p=0.027, respectively by Wilcoxon's rank sum test [324]). Moreover, the *c-Myc* and *Deltex1* mRNA levels observed *in vivo* approximate expression levels observed when the mouse T-ALL cell line 720 was treated with GSI *in vitro*. In contrast, differences in *Hes1* and *Pre-Tα* expression did not reach statistical significance (Figure 13B,D), suggesting that these genes may also be regulated by other transcription factors in mouse T-ALL cells. This study also raises the possibility that *C-MYC* and/or *DELTEX1* expression levels may serve as reliable biomarkers of NOTCH1 activity in T-ALL patients.

mTOR pathway is active in mouse T-ALL tumors and cell lines.

Published work by Chan et al reveal mTOR activation in human T-ALL cell lines and their *in vitro* studies suggest that GSI and the mTOR inhibitor rapamycin may act synergistically to arrest human leukemic growth *in vitro* [326]. To assess mTOR activity in murine T-ALL, we examined primary mouse T-ALL tumor cells and murine T-ALL cell lines for evidence of Akt/mTOR activation. By staining thymomas with antibodies specific to phospho-Akt and phospho-S6 ribosomal protein, we identified a subset of primary murine T-ALL tumor cells as Akt/mTOR active (Figure 14A). Similarly, staining of primary murine T-ALL tumor cells prior to conversion to culture revealed evidence of mTOR activation, as measured by staining phospho-S6 ribosomal protein, intracellularly (Figure 14B). Phosphorylation of S6 ribosomal protein is reduced upon rapamycin treatment, suggesting activation is mTOR dependent.

In addition, all of the mouse T-ALL cell lines we examined exhibited mTOR

activation as assayed by phospho-p70 S6 kinase and phospho-S6 ribosomal levels (Table 2, n=10). Activation of the Akt pathway, as assayed by phospho-Akt, was not observed in all of the cell lines examined. Cell lines in which phospho-Akt was not detected, did have increased expression of Pten. Expression of Pten and suppression of the Akt pathway was not correlated with Notch1 mutational status or GSI sensitivity as suggested by recent studies (Table 2, n=10) [327]. Irrespective of the Pten status, all mouse leukemic lines exhibited increased amounts of phosphorylated mTOR substrates, which suggest at least in Pten-positive cell lines, the activation of the mTOR pathway is occurring in an Akt independent manner.

GSI treatment reduces mTOR pathway activity

To asses whether active Notch signaling contributes to mTOR activation in murine T-ALL, three mouse T-ALL lines (720, 5046 and 5151) were treated with GSIs and mTOR pathway activation was assayed by measuring phospho-p70 S6 kinase and phospho-S6 ribosomal protein levels. In each of the three lines, GSI treatment resulted in reduced phospho-p70 S6 kinase and phospho-S6 ribosomal protein levels (Figure 15A). However, GSI treatment was not sufficient to abolish mTOR activity in any of the mouse T-ALL cell lines examined. Notch1 has been thought to mediate thymocyte survival by direct activation of Akt [118], and based on these findings we examined the phosphorylation of Akt using an anti-phospho-Akt Ser 473 antibody. In mouse leukemic cells where Pten is not expressed, GSI treatment reduced the phosphorylation of Akt (Figure 15B), however, Akt phosphorylation could not be measured in leukemic cell lines where Pten

was expressed. Collectively, these data indicate that at least in Pten-negative mouse leukemic cells, Notch1 signaling stimulates Akt activity. Additionally, GSI treatment reduces but does not eliminate mTOR activity, indicating that GSIs and the mTOR inhibitor rapamycin may be required to completely inactivate mTOR in leukemic cells.

GSI and rapamycin treatment ablates mTOR kinase activity and induces apoptosis.

These signaling data suggested that rapamycin treatment may inhibit leukemic growth and that GSI and rapamycin treatment may prove more effective at inducing leukemic cell death. We tested this possibility by treating our mouse leukemic cell lines with vehicle, 1μM MRK-003, 10nM rapamycin or with 1μM MRK-003 and 10 nM rapamycin and quantified the apoptotic leukemic cells by PI staining followed by flow cytometry. In all cases, treatment with GSI and rapamycin induced more cell death than treatment with GSI or rapamycin alone (Figure 16A). At the concentrations tested, the effects of MRK-003 and rapamycin treatment on leukemic apoptosis appeared at a minimum, additive.

To obtain a molecular readout of the combination treatment, we measured mTOR targets; phospho-p70 and p-85 S6 kinase levels in leukemic cell lines treated with vehicle, GSI or rapamycin alone or with both GSI and rapamycin. We found that treatment with either GSI or rapamycin reduced phospho-p70 S6 kinase activity, but treatment with either single agent failed to ablate mTOR activation (Figure 16B). In contrast, p70 S6 kinase activity and the hyperphosphorylated p85 S6 kinase were undetectable when leukemic cell lines were treated with both GSI and rapamycin (Figure

16B). These findings indicate that the suppression of the mTOR and Notch1 pathways result in extensive apoptosis of mouse leukemic cells, thereby supporting the idea that GSI and rapamycin may be efficacious in the clinic.

Moreover, our *in vitro* studies and work done by Chan et al [326] support the idea that MRK-003 and rapamycin may have synergistic effects on mouse leukemic growth. To test this possibility, mouse leukemic cells were cultured with 1nM rapamycin and increasing concentrations of MRK-003 (10^{-5} – 10^{1} μM) for 72 hours and leukemic growth was assayed using MTT assay. Treatment with 1nM of rapamycin resulted in modest growth inhibition and as expected, MRK-003 caused extensive cell death between the 1 and 10μM concentrations (Figure 16C). Treatment of both drugs, specifically at low pharmacologic doses, appeared to have synergistic effects, resulting in a greater than additive amount of growth inhibition detected. These results support the idea that reduced concentration of GSIs may be used when administered in combination with rapamycin to increase the therapeutic window.

GSI and rapamycin treatment inhibits human T-ALL growth and prolongs survival.

One potential limitation of these studies is that mouse leukemic cell lines appear more sensitive to GSI treatment than established human T-ALL cell lines [224,232,233,238]. GSI treatment of mouse leukemic cell lines induces apoptosis by 48-72 hours (Figure 16A and Figure 8B), whereas human T-ALL cell lines require six or more days of GSI treatment to induce, at best, a modest G1 arrest. The reasons for the differential response

to GSI remain unclear and may reflect activation of additional anti-apoptotic pathways in the human T-ALL. Alternatively, mouse leukemic cell line sensitivity to GSIs may reflect inherent differences between the species. To test the effects of GSI and rapamycin treatment on human leukemic growth and survival, human T-ALL cell lines were treated *in vitro* with increasing concentrations of MRK-003 in the presence of 1nM or 100nM rapamycin and ATP activity was measured using a Vialight assay kit. As expected, increasing amounts of GSI reduced human leukemic growth, however the addition of rapamycin enhanced the effects of GSI treatment, resulting in greater inhibition of growth (Figure 17A). Thus, reduced concentrations of GSI may be used *in vivo* in combination with rapamycin to minimize on target GSI-associated toxicities and to maximize efficacy.

We then tested whether GSI and rapamycin in combination could have additional efficacy against human leukemic growth *in vivo*. To perform this study, approximately 5 $x10^6$ human T-ALL cells from the cell line T-ALL1 were implanted subcutaneously into nude mice and once the tumors reached $200mm^3$, mice were randomized into four treatment groups of eight mice each. Mice were then treated with vehicle, a non-efficacious dose of GSI (MRK-003 150mg/kg/once per week), rapamycin (Rapamune 20mg/kg daily) or GSI and rapamycin and time to disease progression determined. Mice treated with GSI or rapamycin exhibited inhibition of tumor progression, as measured by percent test normalized to control tumor volume (Figure 17B), however, overall survival was not affected (Figure 17C). In contrast, mice treated with GSI and rapamycin survived on average longer than vehicle treated mice or mice treated with either single agent (GSI or rapamycin alone) (Figure 17C). The administration of GSI and rapamycin

resulted in an increase in the percentage of mice surviving (60 versus 25%) as well as an increase in the mean survival period of more than 50 days ($p<0.058$ by logrank test). Mice treated with either GSI or rapamycin succumbed to disease rapidly with an average latency of approximately 40 days. Collectively, these *in vivo* studies suggest that GSI in combination with the mTOR inhibitor rapamycin may have added efficacy in the treatment of T-ALL patients that exhibit NOTCH1 activation.

Discussion

The prevalence of NOTCH1 and FBXW7 [219-224] mutations in human T-ALL and in mouse T-ALL models [228-231] prompted several laboratories to ask whether leukemic growth remained NOTCH1-dependent. GSI treatment of mouse and human T-ALL cell lines and primary mouse tumors expressing mutated Notch1 proteins revealed that sustained Notch1 signals appear required for continued growth and survival *in vitro* [224,230,232,233,238]. These findings raise the exciting possibility that Notch1 inhibition may prove effective in treating T-ALL patients and led to the opening of a phase 1 clinical trial involving 8 relapsed leukemia and lymphoma patients. Most of the patients were dosed with a continuous GSI dosing schedule, which was poorly tolerated, and the trial closed prior to being able to demonstrate clinical activity of GSIs in T-ALL [309]. A well-tolerated intermittent GSI dosing regimen for patients has since been identified thereby facilitating future clinical evaluations of GSIs in T-ALL and potentially other cancers.

Here we examined the effect of GSI treatment in our mouse T-ALL model where the effects of Notch1 inhibition could be addressed on primary tumors opposed to patients with relapsed or refractory disease. Seventy four percent of *Tal1/Ink4a/Arf+/-* transgenic mice develop a T-ALL like disease due to mutations that result in premature truncation of the Notch1 receptor [230]. To investigate whether Notch1 could be targeted *in vivo*, we developed an intermittent GSI dosing regimen (150mg/kg three days on and four days off) that had minimal toxicity and then tested whether this regimen had any effect on the survival of leukemic *Tal1/Ink4a/Arf+/-* mice. We found that GSI treated mice survived on average 15 days longer than leukemic mice treated with vehicle only. The

expression of Notch1 target gene expression *Deltex1* and c-*Myc* was repressed and increased numbers of apoptotic cells were detected in the thymic masses of diseased mice treated with GSI. These data support the idea that Notch can be successfully targeted *in vivo* and that treatment with GSI as a single agent has efficacy and extended the survival of leukemic mice.

Despite the expression of other T-ALL associated oncogenes such as *Tal1* and *Lmo1/2* and the loss of tumor suppressors (*Ink4a/Arf, Pten*), mouse T-cell leukemic growth appears preferentially 'addicted' to the Notch1 proliferative signal(s). Although GSI treatment significantly increased the overall survival period, it was not sufficient to cure the mice and 100% of the GSI treated mice eventually succumbed to disease. The transient GSI response was not due to the development of GSI resistance, as all mouse tumors tested remained GSI responsive when re-examined *in vitro*. One possibility is that the transient response to GSI may reflect the intermittent dosing regimen and long term suppression of Notch1 activity may require more frequent GSI administration or combination therapies. Alternatively, chronic GSI treatment may promote reliance on other growth and survival pathways. For example, Gleevec administration to mice with CML-like disease shifts the reliance from activated ABL towards a greater dependence on the IL-7 signaling pathway [328].

As in human T-ALL [327], PTEN loss of expression is frequently observed in our mouse T-ALL model (Table 2). In human T-ALL cell lines and primary samples, loss of *PTEN* has been associated with resistance to *NOTCH1* inhibition [327]. Interestingly, 2 of 6 mouse T-ALL cell lines examined harbor *Notch1* mutations and express Pten, whereas

the remaining 4 mutant Notch1 mouse T-ALL cell lines do not express Pten. Yet, all 6 mouse T-ALL cell lines remain GSI responsive, irrespective of their Pten status. Unlike the reported role of PTEN in GSI resistance in human T-ALL cell lines [327], we observe no correlation between Pten status and GSI responsiveness. However, it is important to note that GSI resistant mouse T-ALL cell lines are relatively rare and thus far, we have isolated only 2 GSI resistant mouse T-ALL cell lines; one of them retains Pten, whereas the other does not. Nonetheless, it is clear in our mouse T-ALL model, Pten loss does not result in GSI resistance and these mouse T-ALL cell lines remain dependent on Notch1 for their growth and survival.

Although the results from this mouse GSI study are promising, many human T-ALL cell lines are far less responsive to GSI treatment *in vitro* [224,232,233,238]. Even at increased concentrations and extended incubation periods, only modest amounts of cell death are observed when human T-ALL cell lines or primary leukemic samples are treated with GSIs. These findings cast doubt as to whether GSI or other Notch1 inhibitors will be effective in T-ALL patients. Collectively, these data suggest that combination therapies may be needed to successfully treat T-ALL patients. We provide evidence that combining GSI treatment with the mTOR inhibitor, rapamycin, limits human leukemic growth *in vivo* and increases the overall survival. Moreover, the combination treatment is effective following only one GSI dose, indicating that lower concentrations of GSI may prove effective when administered in combination with other anti-leukemic agents. Similarly, work by Chan et al show that GSI and rapamycin synergize to limit human T-ALL cell line growth *in vitro* [326]. We extend their *in vitro* findings and show that Notch

and mTOR pathway inhibition limits human leukemic growth *in vivo*, when tested in a mouse xenograft setting. Thus, whether GSI and rapamycin will prove efficacious remains to be tested in mouse T-ALL models.

Notch receptors and ligands are found upregulated in multiple human cancers (reviewed in [329]) and expression of activated *Notch* alleles results in T-ALL like disease [122,216,330] and induction of mammary tumors in mice [331]. In addition to cell autonomous effects, Notch pathway inhibition may also have anti-angiogenic activity [332-335] and thereby render a 'double hit' to the malignant cell. Thus, Notch inhibitors may have enormous potential in targeted cancer therapy.

Materials and Methods

Mouse and Human T-ALL Cell Lines

Murine T-ALL cell lines were cultured in RPMI with 10% FBS, 1% glutamine, penicillin/ streptomycin, 50μM β mercaptoethanol at 37 C under 5% CO_2. Human T-ALL cell lines were cultured in RPMI with 10% FBS, 1% glutamine, penicillin/ streptomycin at 37 C under 5% CO_2. To inhibit Notch1 signaling, cells were plated at $1x10^6$ in a 10cm dish in the presence of either MRK-003 (Merck Research Laboratories, Boston, MA) at 1μM, rapamycin at 10nM (LC Laboratories, Woburn, MA), or a combination of MRK-003 and rapamycin. Mock treated cells were cultured with DMSO at a final concentration of 0.01%. All mouse procedures performed in these experiments have been approved by the University of Massachusetts Medical School Institutional Animal Care and Use Committee (IACUC).

GSI efficacy studies

A cohort of *Tal1/Ink4a/Arf +/-* transgenic mice was generated (n= 30) and monitored daily for the onset of leukemia as described previously [61]. Once disease became evident (respiratory distress, decrease in activity, weight loss, ruffled coat) leukemic *Tal1/Ink4a/Arf +/-* mice were randomly assigned to the vehicle or GSI treatment groups (vehicle cohort n=14, GSI cohort n=16). Leukemic mice were administered either a 150mg/kg dose of freshly prepared MRK-003 (dissolved in 0.5% methylcellulose) or a comparable volume of 0.5% methylcellulose by oral gavage. Mice were treated for three consecutive days followed by a rest period of four days. Mice were continuously treated with this regimen throughout the study period and euthanized when deemed moribund by

a third party blinded to the treatment group. Survival data was plotted using Kaplan-Meyer survival curves and statistical analysis performed using SPSS software. To examine the effects on human leukemic growth, female CD1 *nu/nu* mice (Charles River Laboratories, Wilmington, MA) were inoculated with human TALL-1 cells (Deutsche Sammlung von Mikroorganismen und Zellkulturen (DSMZ) Braunschweig, Germany) three days after an intraperitoneal inoculation of 100mg/kg cyclophosphamide (no. C0768-1G; Sigma Aldrich, St. Louis, MO) to facilitate tumor growth. TALL-1 cells were implanted at a concentration $5x10^6$ cells diluted in 100µl of 50% matrigel (no. CB-40230C; Fisher Scientific, Pittsburgh, PA)/50% PBS. When tumors reached $200mm^3$, mice were randomized into groups (n=12) of equal average tumor volume. MRK-003 was dosed at either 0 or 150 mg/kg by oral gavage once a week. Rapamycin (rapamune) was administered by oral gavage daily at a concentration of either 0 or 20 mg/kg. Tumors were callipered and body weights were recorded twice weekly for the duration of study. Mice were euthanized when tumors reached the maximum volume allowed by IACUC guidelines. Survival data was plotted as a Kaplan-Meyer survival curve using Prism Graphpad software (GraphPad Software, San Diego, CA). Repeated measures analysis of variance was used for the comparison of tumor growth inhibition. MRK-003 levels in plasma, and in tumor were measured by High-Pressure Liquid Chromotography using Cohesive Technologies pump and auto-sampler (Thermo Scientific, Waltham, MA) equipped with a reversed-phase column (Atlanis C18, 3µm, 3 x 20mm; Waters, Milford, MA) and linear water/ANC gradient (5-90% organic in 3 minutes) containing 0.1% formic acid at a flow rate of 850 µL/min. The protonated molecules were fragmented by

collision-induced dissociation with nitrogen as a collision gas. The collision energy voltage was set at 35V and 48V for GSI and internal standard respectively. The data were acquired and processed by Analyst 1.4.1 software (AB/MDS Sciex, Foster City, CA).

TUNEL staining

To quantify apoptotic cells, leukemic mice treated with a 150mg/kg dose of MRK-003 or 0.5% methylcellulose orally for three days, were euthanized and a post-mortem examination was performed. Paraffin embedded tumor sections were analyzed for apoptosis using the ApopTag Plus peroxidase TUNEL kit (Chemicon, Temecula, CA). Approximately, 10 fields from each slide were counted and compared to the serial section not treated with the TdT enzyme. Wilcoxon's rank sum test was used to determine statistical significance [324]. Images were taken using an Olympus BX41 microscope (Olympus Imaging America, Center Valley, PA) with a 20x or 40x lenses. The images were acquired with an Evolution MP 5.0 camera (Media Cybernetics, Bethesda, MD) and Q capture Pro 5.1 acquisition software.

Immunohistochemistry

Paraffin embedded tumor sections were analyzed for phospho-S6 ribosomal protein expression (1:75; Cell Signaling Technology, Beverly, MA). Automated staining was performed using the ChromoMap Kit on the Discovery XT (Ventana Medical System) under standard conditions. Periodic Acid Schiff (PAS) staining of mouse duodenum was conducted as previously described [201]. Images were taken using a Carl Zeiss Imager.Z1 Plan-Apochromat (Carl Zeiss, Jena, Germany) with a 20X objective lens. The

images were acquired using a Carl Zeiss AxioCam HRc camera and the imaging-acquisition software used was Carl Zeiss AxioVision Rel. 4.6.

Flow cytometry

To determine the effects of GSI and/or rapamycin treatment on the cell cycle, mouse and human leukemic cells were pelleted by centrifugation for 10 minutes at 2000 rpm, washed in PBS, and resuspended in 70% ice-cold ethanol. Cells were fixed overnight and then stained with propidium iodide. DNA content was analyzed by flow cytometry (FACScan; BD Biosciences, San Jose, CA). Data was analyzed using FlowJo version 7.0 (TreeStar, Ashland, OR). To quantify the effects of GSI on primary tumors, thymic masses isolated directly from *Tal1* transgenic animals were treated *ex vivo* with GSI or vehicle and then were stained with FITC-Annexin V/PI and analyzed by flow cytometry (BD Biosciences, San Jose, CA).

For intracellular-S6-Ribosomal staining, cells from bone marrow or spleens of leukemic animals were fixed directly with 1.5% paraformaldehyde for 10 minutes at room temperature. Cells were pelleted by centrifugation at 500g for 5 minutes and incubated in 100% ice cold methanol at 4°C for 10 minutes to 16 hrs. Cells were washed twice with intracellular staining buffer (PBS, 0.5% BSA, 0.02% sodium aside) and then incubated with antibodies for 30 minutes at room temperature. Cells were then washed with Intracellular staining buffer and measured by flow cytometry. Data was analyzed using FlowJo software (Tree Star Inc., Ashland, OR).

RNA Analysis

RNA was extracted from murine T-ALL cell lines and primary thymic masses treated with vehicle or MRK-003 using Trizol. cDNA was synthesized using Superscript First - Strand Synthesis System (Invitrogen, Carlsbad, CA). To determine the effects of MRK-003 treatment on Notch1 target genes, quantitative RT-PCR was performed using *Deltex1* and *Hes1* primers as described previously[59]. To determine Notch1 target gene expression in primary tumors, quantitative PCR was performed using c-*Myc, Hes1, Pre-T α, Deltex1* primers designed using Primer Express software (Applied Biosystems, Foster City, CA). The primer sequences are as follows; c-Myc forward, 5'-CTGTTTGAAGGCTGGATTTCCT-3'; c-Myc reverse, 5'-CAGCACCGACAGACGCC-3'. Hes1 forward 5' - AAGACGGCCTCTGAGCACA -3'; Hes1 reverse 5' – CCTTCGCCTCTTCTCCATGAT – 3'. *Pre-Tα* forward 5'-CTGCTTCTGGGCGTCAGGT- 3'; *Pre-Tα* reverse 5'-TGCCTTCCATCTACCAGCAGT-3'. *Deltex1* forward 5' TGCCTGGTGGCCATGTACT-3'; *Deltex1* reverse 5'-GACACTGCAGGCTGCCATC-3'. The copy number obtained for the gene of interest was normalized to the copy number for *ß-Actin.*

Western Blot Analysis

Murine leukemic cells lines were lysed in 20mM Tris buffer pH 7.4 containing 0.14 M NaCl, 1% NP-40, 10% glycerol, 1mM sodium orthovanadate and protease inhibitors and protein concentrations determined using the Bradford assay (Bio-Rad, Hercules, CA). Thirty five micrograms of total protein was resolved on a 10% SDS-PAGE gel,

transferred to a nitrocellulose membrane, blocked for 1h with a 50 mM Tris buffer, pH 7.5, containing 0.15 M NaCl, 0.05% Tween 20 (TBST), and 5% (wt/vol) non fat dry milk, and probed overnight at 4°C with buffer containing primary antibodies. After three 10 min washes in TBST, the filters were incubated for 1h in blocking buffer containing horseradish peroxidase-conjugated secondary antibodies. After three 10 min washes in TBST, proteins were detected by enhanced chemiluminescence (Pierce, Rockford, IL). The following antibodies used for immunoblotting were purchased from Cell Signaling Technology, Beverly, CA; phospho-p70 S6 kinase T389 (#9205), p70 S6 kinase (#9202), phospho-Akt S473 (#9271), Akt (#9272), phospho-S6 ribosomal S240/244 (#2215), S6 ribosomal (#2217), phospho-4E-BP1 S65 (#9451), 4E-BP-1 (#9452), PTEN antibody (#9552), $Notch^{IC}$ Val1744 (#2421). Blots were stripped and reprobed with β-Actin (#A5441; Sigma, St. Louis, MO) to control for equal loading.

***In vitro* Vialight Assay**

The human T-ALL cell line, TALL-1 was obtained from Deutsche Sammlung von Mikroorganismen und Zellkulturen (DSMZ, Braunschweig, Germany) were plated at a concentration of $1x10^4$ in 80µl of growth media in a flat bottom 96 well plate. Approximately, 10µl of MRK-003 (at concentrations ranging from 0-50µM) and 10µl of rapamycin (EMD Biosciences, # 553210-1mg) at either 0, 1nM, or 100nM concentrations were then added to each well. On day four, new media and drug was added by spinning the plate and replacing 75µl per well with fresh drug and media. Plates were read seven days after seeding cells following the Vialight Plus (# LT07-22; Lonza Bioscience, Basel, Switzerland) manufacturer's protocol.

MTT Analysis

In a 96 well flat bottom plate approximately $1x10^4$ cells/ 200μL of a cell suspension was plated and treated for 72 hours with vehicle, 1nM rapamycin, increasing concentrations of MRK-003 (10^{-5} -10^{1}μM) or both rapamycin and MRK-003. Following treatment 20μl of a 5mg/ml 3-(4,5-dimethylthiazol-2-yl)-2,5-diphenyl tetrazolium bromide (MTT) solution (Sigma Aldrich, St. Louis, MO) was added and incubated for 4 hours at 37°C. The plate was then spun at 2000rpm for 5 minutes and the media was removed. The reagent was solubilized with 100 μl of dimethyl sulfoxide (Sigma Aldrich, St. Louis, MO) and incubated for 10 minutes at room temperature. Plates were then analyzed at A_{490} wavelength. Data is plotted as percent apoptosis. This value was determined by comparing the absorbance reading of each set of test wells to a set of control wells in which no drug was added and baseline proliferation was recorded. The following equation was used to determine effect on growth: ([absorbance of control – absorbance of test]/ absorbance of control) x100.

Figure 8. MRK-003 is a potent γ-secretase inhibitor that represses Notch1 target gene expression and induces apoptosis *in vitro*. (A) Mouse leukemic cell lines were treated with 1μM MRK-003 for the times periods indicated and *Hes1* and *Deltex*1 expression examined using RT-PCR. Glyceraldehyde-3-phosphate dehydrogenase (*Gapdh*) was used as an internal control. **(B)** Three murine leukemic lines (720, 135, 5151) were treated for 72 hours with 1μM DAPT, 1μM MRK-003, or DMSO at a final concentration of 0.01%. Cells were harvested and stained with PI and DNA content measured by flow cytometry. **(C)** Thymic masses isolated directly from *Tal1/Ink4a/Arf*+/- transgenic animals were left untreated or were treated *ex vivo* with 1μM DAPT, 1μM MRK-003, or DMSO for 3 days. Cells were then stained with FITC-Annexin V/PI and analyzed by flow cytometry. Three independent tumors were analyzed, one representative experiment is shown. Statistics were analyzed using a Kruskal-Wallis test.

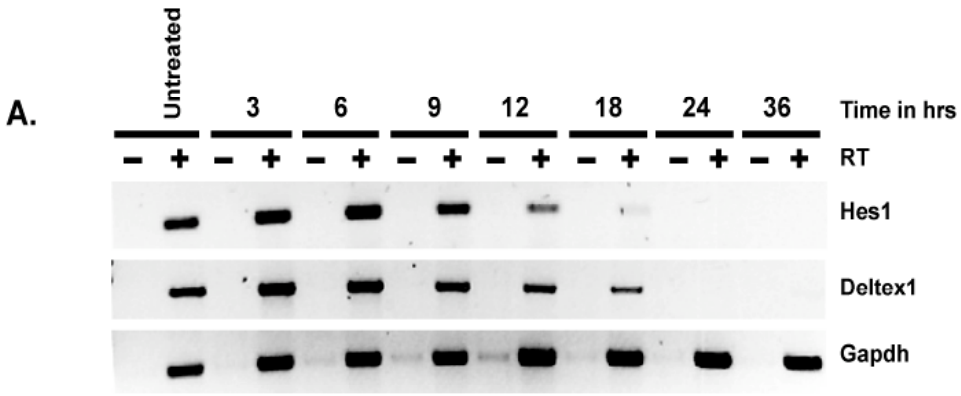
A.
Untreated
3
6
9
12
18
24
36
Time in hrs
RT
Hes1
Deltex1
Gapdh

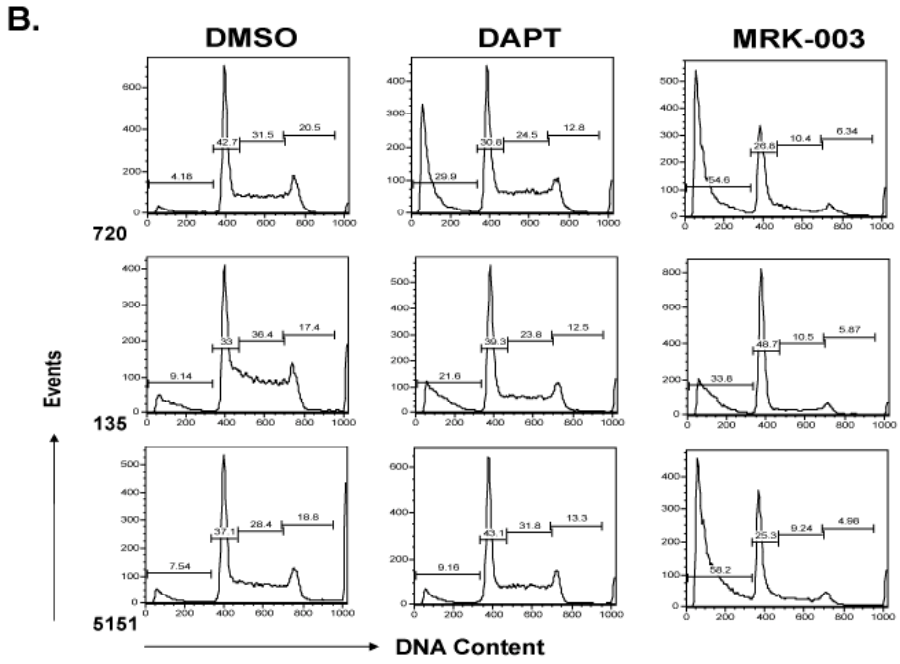
B.
DMSO
DAPT
MRK-003
720
135
5151
Events
DNA Content

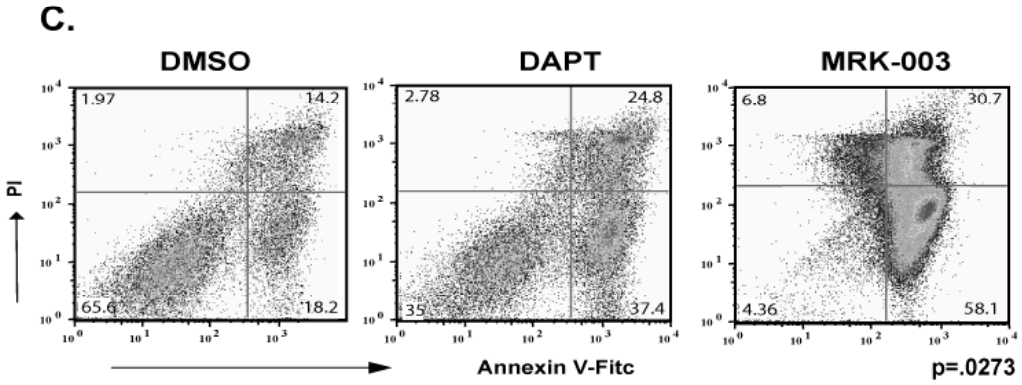
C.
DMSO
DAPT
MRK-003
PI
Annexin V-Fitc
1.97
14.2
65.6
18.2
2.78
24.8
35
37.4
6.8
30.7
4.36
58.1
p=.0273

Figure 9. GSI treatment prolongs survival in a mouse T-ALL model. **(A)** Effective compound levels in MRK-003 treated mice**.** Compound serum levels were analyzed 1-5 days following continuous dosing of MRK-003 treatment. Effective and stable compound levels (1 -10μM) were detected in the serum of treated mice after 12 hours at each drug concentration tested. **(B)** Plasma levels decrease during 4-day rest period. Mice were treated for three days with 150 mg/kg of MRK-003. Following treatment, serum was analyzed for compound levels. **(C)** Intermittent GSI dosing minimizes "on-target" gastrointestinal toxicity. To define a GSI dosing regimen with limited/no associated toxicity, mice were administered vehicle (V) or 150 mg/kg MRK-003 by oral gavage everyday (R1) or for three days followed by a four day rest period (R2). Mice were monitored daily for loss of body weight and for evidence of diarrhea. **(D)** Extended survival in MRK-003-treated leukemic mice. Near end stage diseased *Tal1/Ink4a/Arf+/-* mice were treated with 150mg/kg of MRK-003 (n=16 mice) or 0.5% methylcellulose (n=14 mice) orally for three days and rested for four days until mice were deemed moribund. Median survival for T-ALL mice treated with vehicle is 3 days, and 18 days for GSI treated mice (p value < 0.005).

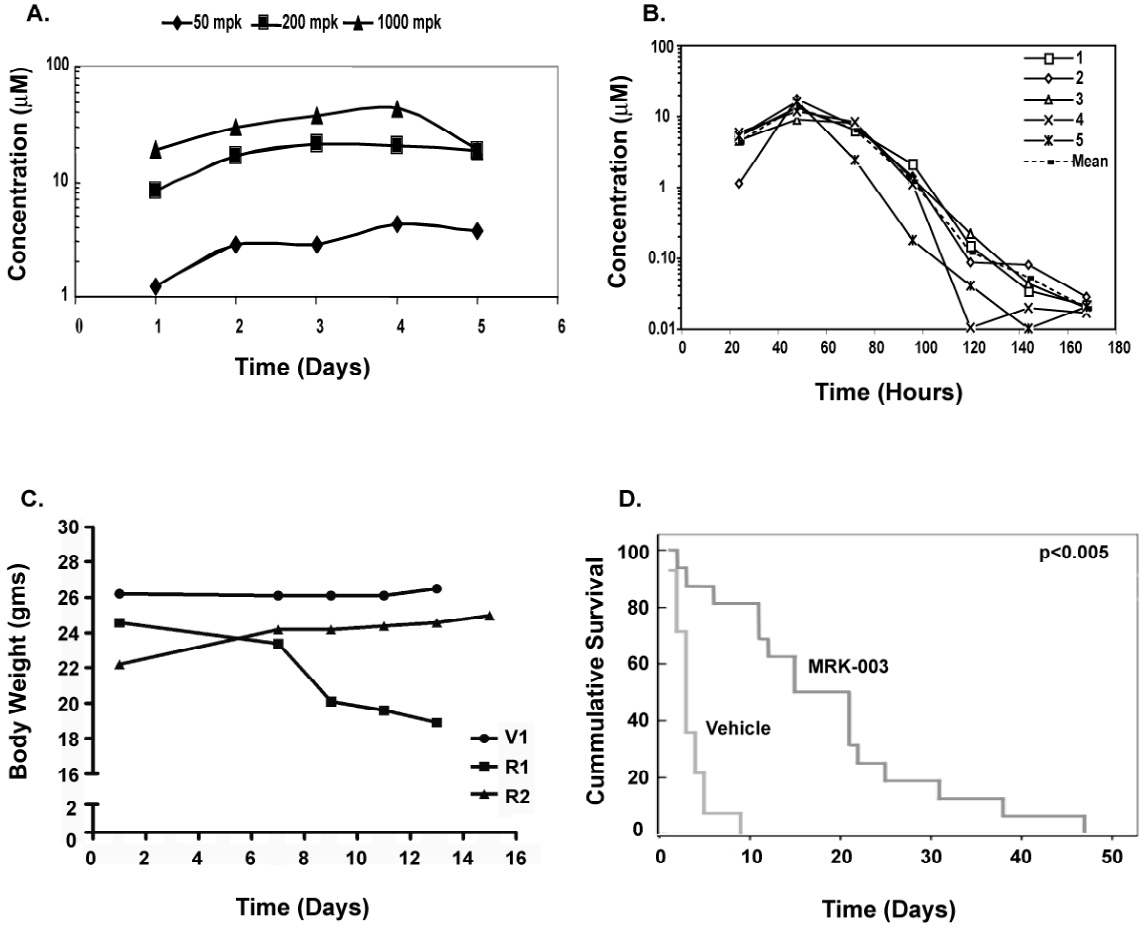

Figure 10. GSI induced gut metaplasia is reduced during the four day rest period. FVB mice were treated with either vehicle (0.5% methylcellulose) or MRK-003 at 150mg/kg, once daily for three consecutive days. Intestines were harvested at indicated times ranging from 6 hours to 96 hours following the last dose and gut metaplasia was detected by PAS staining (visualized as red clusters). Scale bar, 100μM.

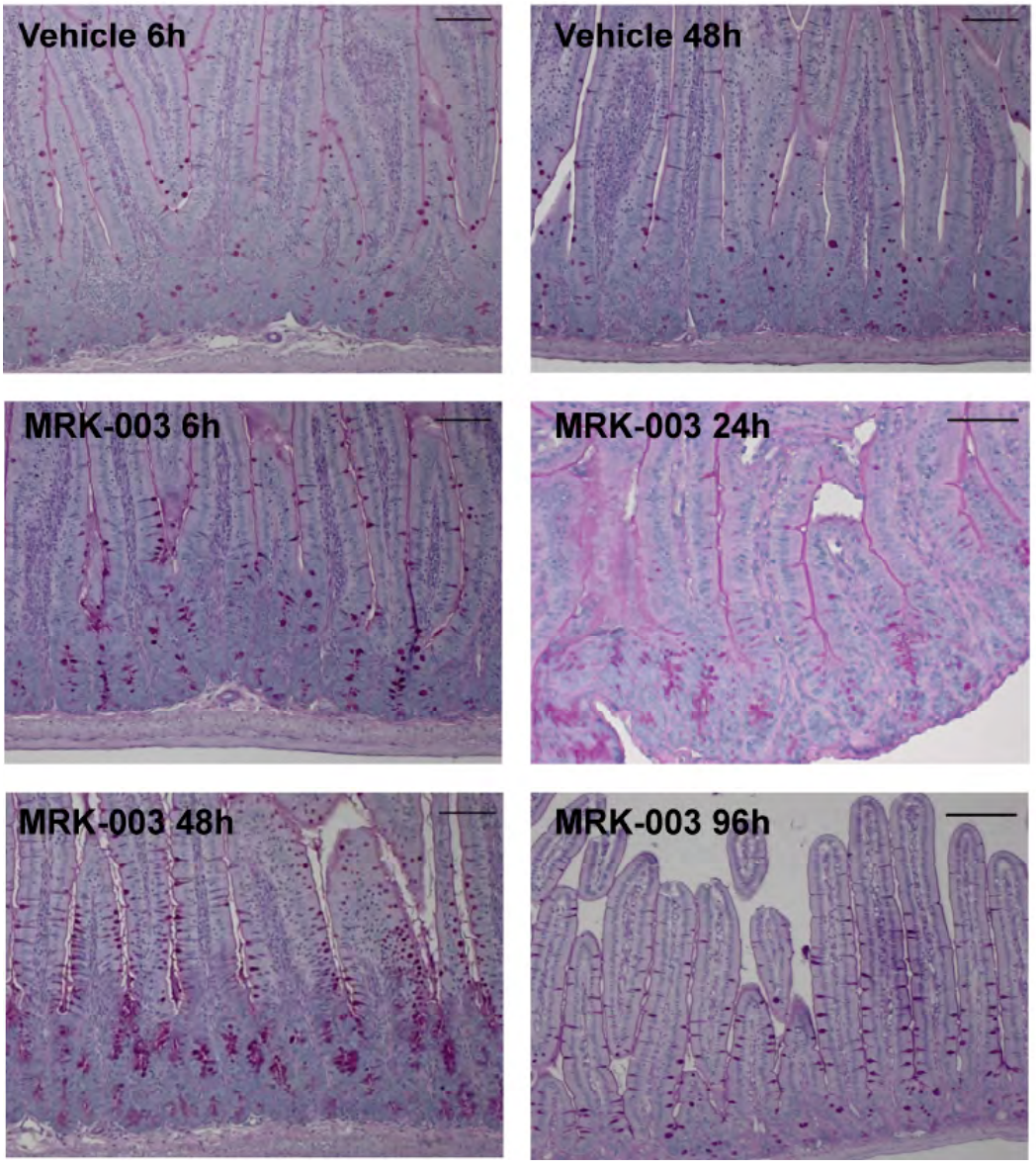

Table 1. Body weight is maintained in mice treated with successive cycles of intermittent GSI dosing.

Vehicle Treated					MRK-003 Treated				
Mouse Number	Weight (Enrollment)	Weight (Sacrifice)	Days Treated	Weight Change	Mouse Number	Weight (Enrollment)	Weight (Sacrifice)	Days Treated	Weight Change
6837	21.0	21.2	4	0.2	6818	19.1	19.4	47	0.3
6851	26.5	24.3	3	-2.2	6827	22.2	24.0	15	1.8
6856	21.5	19.7	9	-1.8	6838	21.4	17.6	12	-3.8
6893	25.2	23.7	3	-1.5	6835	16.4	15.9	3	-0.5
6819	23.4	22.9	5	-0.5	6805	31.1	28.9	6	-2.2
6812	21.5	20.2	3	-1.3	6803	30.2	30.2	31	0
6854	31.1	30.3	3	-0.8	6831	24.1	23.9	11	-0.2
6857	28.9	29.1	5	0.2	6841	23.2	22.5	2	-0.7
6839	24.2	23.1	2	-1.1	6894	21.0	22.0	25	1.0
6821	29.2	29.5	3	0.3					
Average	**25.6**	**24.4**	**4**	**-0.9**	**Average**	**23.2**	**22.7**	**16.9**	**-0.5**

Figure 11. GSI treatment induces apoptosis of leukemic cells *in vivo*. (A) Leukemic mice were treated with a 150mg/kg dose of MRK-003 or with vehicle for three days. Tumor sections were fixed in 10% buffered formalin and number of apoptotic cells quantified using TUNEL assay. **(B)** Bar graph representing the fold change in TUNEL positive cells compared to vehicle. Ten independent fields/section were counted to obtain the representative value.

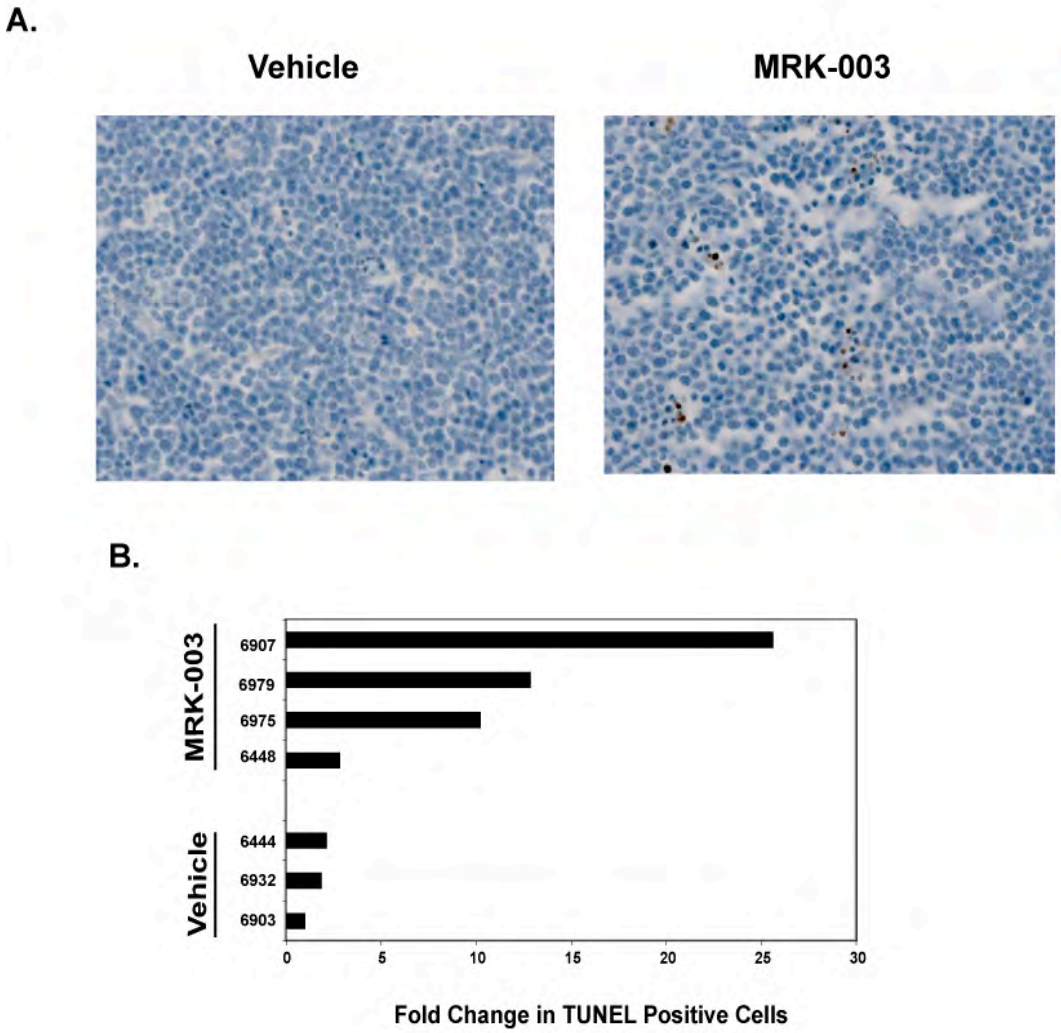

Figure 12. GSI-treated tumors do not appear to develop GSI resistance. Thymomas from MRK-003 or vehicle treated mice were harvested from the animals at sacrifice and converted to *in vitro* culture. (**A)** Leukemic cell lines from vehicle and GSI treated mice were treated for 48 hours with 1 μM MRK-003 or DMSO carrier. Cell lysates were examined for intracellular Notch1 levels by immunoblotting with intracellular Notch1 (anti-Notch1^{IC} Val1744) and anti-β Actin antibodies. **(B)** Leukemic cell lines, generated from vehicle and GSI treated mice, were treated with vehicle or 1μM MRK-003 for 3 and 6 days. Cells were then assayed for DNA content by staining with propidium iodide followed by flow cytometry. The figure is a representative experiment using cell line 6838.

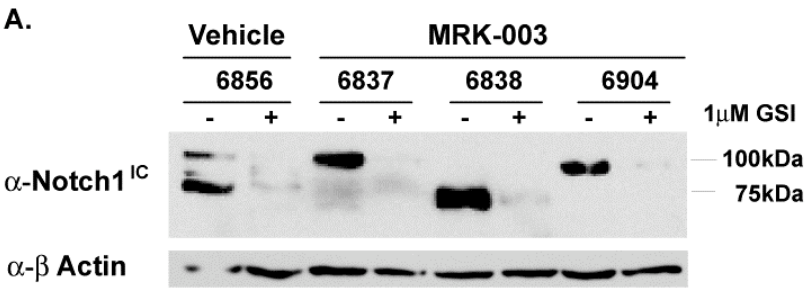

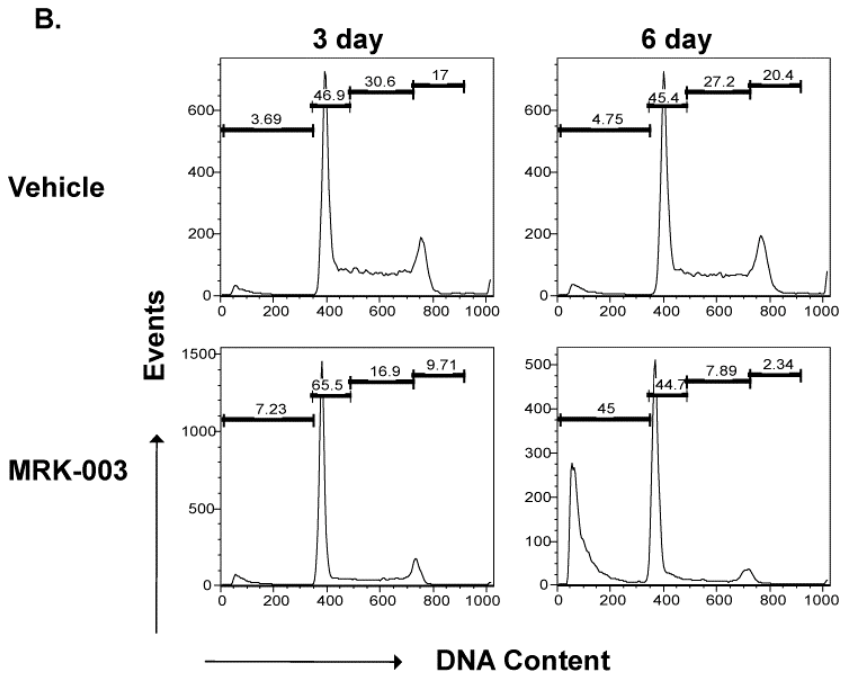

Figure 13. Notch1 target genes are repressed in GSI treated leukemic *Tal1/Ink4a/Arf+/-* mice. At sacrifice, thymomas were harvested from vehicle and MRK-003 treated mice and *c-Myc* **(A),** *Pre-T* α **(B),** *Deltex1* **(C),** and *Hes1* **(D)** expression quantified using real time PCR. The copy number for each gene was normalized to the copy number for β Actin. The following result is an average of three independent experiments. The mouse T-ALL cell line 720 was treated *in vitro* with 1μM MRK-003 or DMSO for 72 hours and used as a positive control in these experiments.

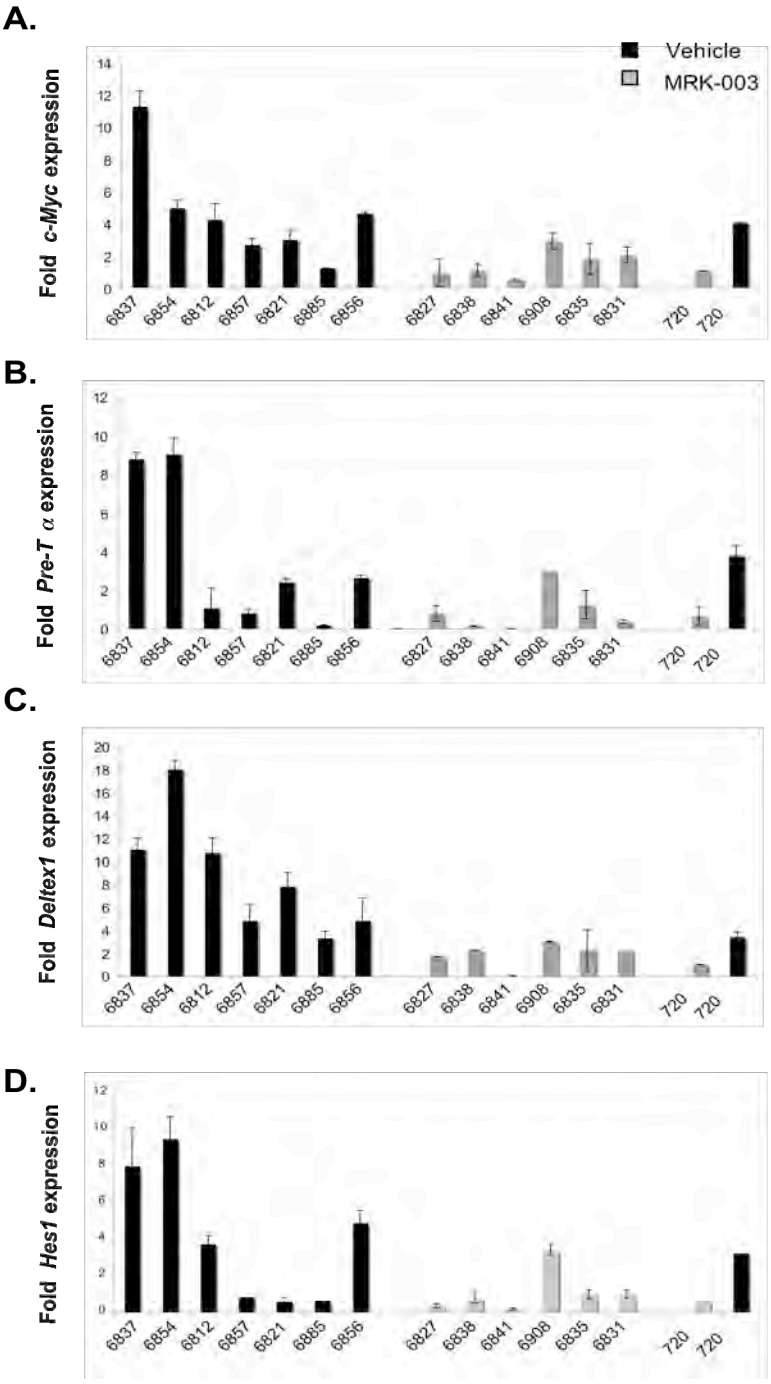

Figure 14. mTOR activity is detected in primary murine leukemic cells. (A) Thymomas from untreated mice were harvested at sacrifice and tumor sections were fixed in 10% buffered formalin. Sections were then stained with antibodies to phospho-S6 ribosomal protein (p-S6RP) or phospho-Akt (Ser473). Scale bars are 50μM. **(B)** At sacrifice, thymomas were made into single cell suspensions. Cells were then treated *ex vivo* with DMSO or 10nM rapamycin for time points indicated. Cells were then harvested, stained with an intracellular p-S6RP antibody, and analyzed by FACS.

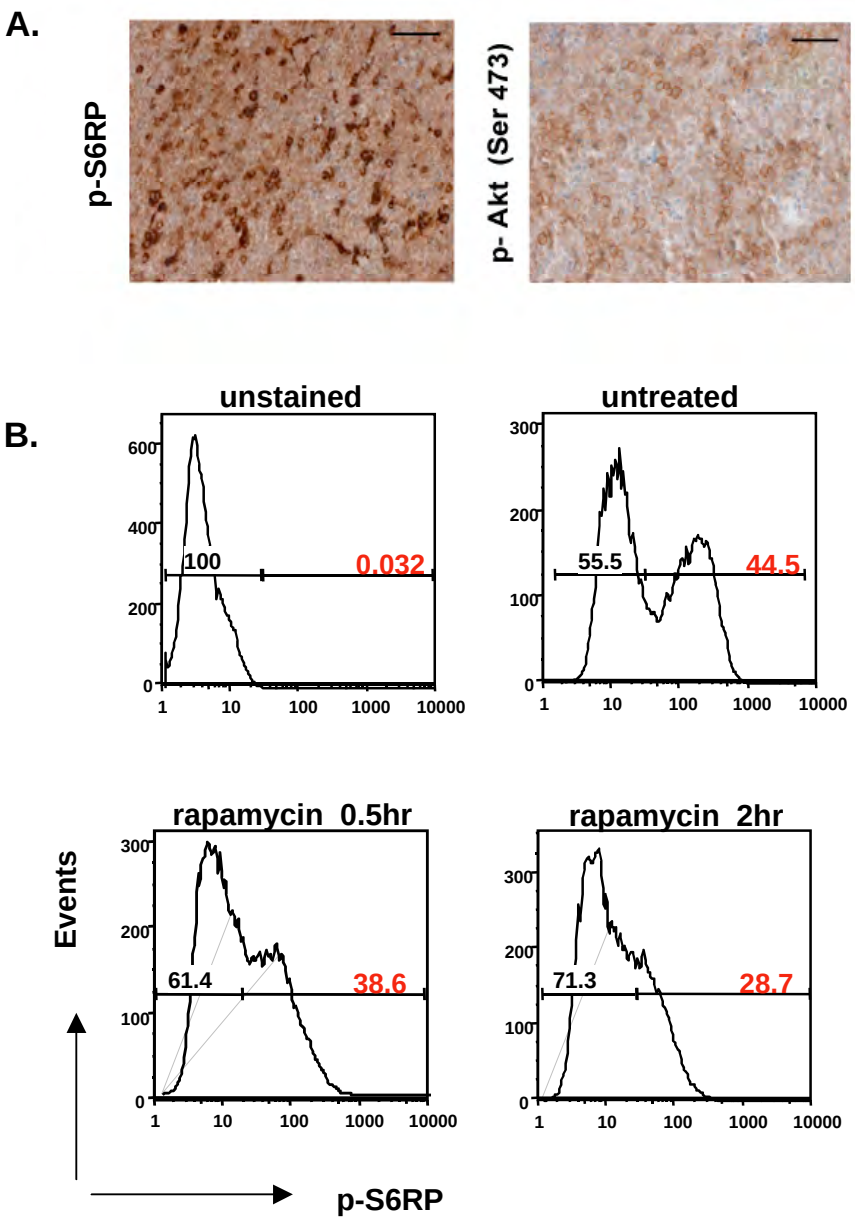

Table 2. GSI sensitivity does not correlate with PTEN expression.

Cell Line	Genotype	PTEN Expression	p-AKT Activation	p70S6 K Activation	Notch1 Status	GSI
130	Tal1/HEB+/-	+	-	+	PEST Truncation	Sensitive
135	Tal1/HEB+/-	-	+	+	PEST Truncation	Sensitive
720	Tal1/HEB+/-	+	-	+	PEST Truncation	Sensitive
2869	Tal1/Ink4a/Arf+/-	+	-	+	No mutation	Sensitive
2912	Tal1/Ink4a+/-	+	-	+	No mutation	Sensitive
2913	Tal1/Ink4a+/-	+	-	+	No mutation	Sensitive
3569	Tal1/Ink4a/Arf+/-	-	+	+	Het Mut. L to P 1699	Sensitive
5010	Tal1/+	-	+	+	No mutation	Resistant
5046	Tal1/+	-	+	+	N.D.	Sensitive
5151	Tal1/+	-	+	+	Het truncation	Sensitive

Figure 15. Notch1 positively regulates the Akt/ mTOR pathway in murine T-ALL cell lines. (A) Reduced level of mTOR substrates are observed when murine T-ALL cell lines are treated with GSI. Primary murine leukemic lines were treated with 1μM MRK-003 or DMSO for 48 hours. mTOR activity was assayed by immunoblotting cell lysates with anti-phospho-p70 S6 kinase or phospho-S6 ribosomal antibodies. p70 S6 kinase and S6 ribosomal were used as loading controls **(B)** Notch1 regulates Akt activity in some mouse T-ALL lines. Akt activity was assayed by immunoblotting cell lysates with anti-phospho-Akt Ser 473 antibody. Akt was used as a loading control. Fold reductions in kinase activity were determined by densitometry and represent ratios (phospho/total) normalized to DMSO treated samples.

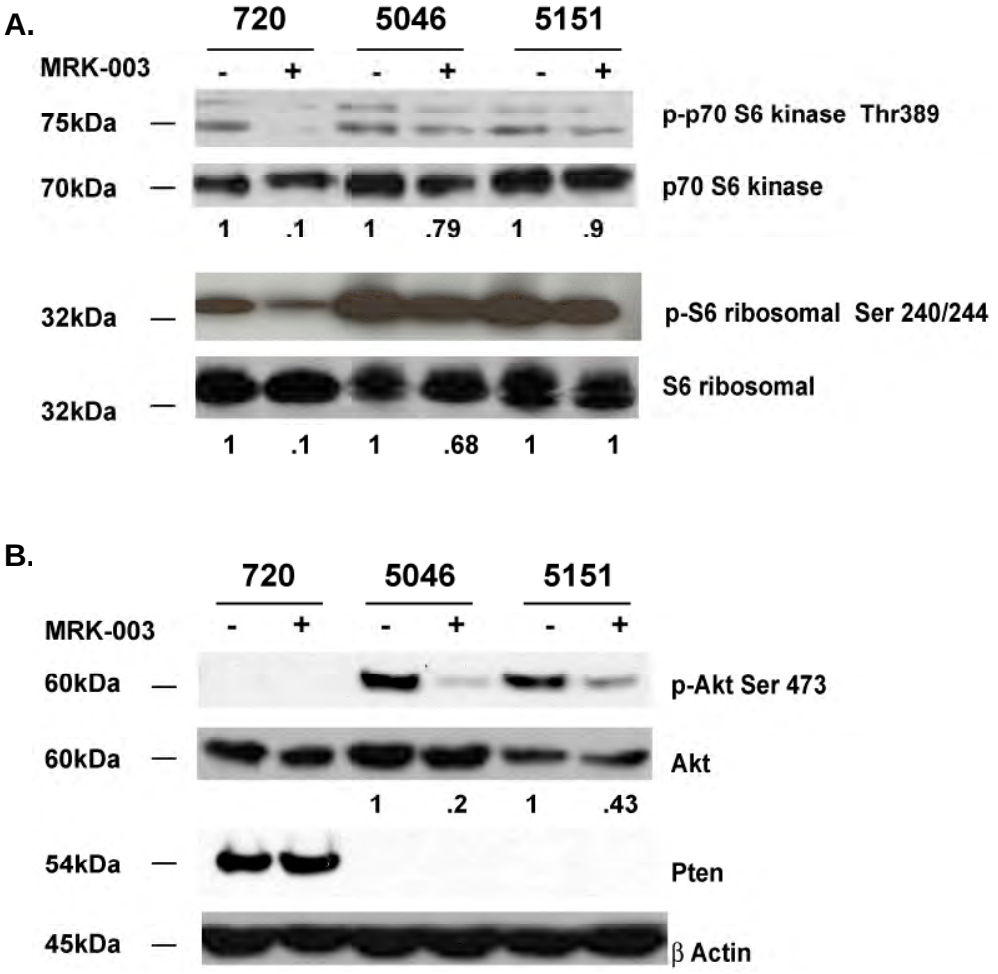

Figure 16. GSI and rapamycin treatment *in vitro* induces massive apoptosis of mouse T-ALL cells and cooperates to suppress mTOR activity. (A) Mouse T-ALL cell lines, 135, 5046, and 5151, were treated with DMSO, 1μM MRK-003, 10nM rapamycin, or with 1μM MRK-003 and 10nM rapamycin for 24 hours. Cells were assayed for DNA content by staining with PI followed by flow cytometry. **(B)** mTOR activity is ablated when mouse T-ALL lines are treated with GSI and rapamycin. Mouse T-ALL lines, 720 and 5046, were treated with DMSO, 1μM MRK-003, 10nM rapamycin, or with 1μM MRK-003 and 10nM rapamycin and mTOR kinase activity assayed by immunoblotting the cell lysates with phospho-p70 S6 kinase antibody after 18 hours. Total p70 S6 kinase was used as a loading control. Fold reductions in kinase activity were determined by densitometry and represent ratios (phospho/total) normalized to DMSO treated samples. **(C)** At low pharmacologic doses, MRK-003 and rapamycin appear to have synergistic effects on mouse leukemic growth. Mouse T-ALL lines, 720 and 5046, were treated for 72 hours with 1nM rapamycin, increasing concentrations of MRK-003 (10^{-5}–10^{1}μM), or rapamycin and MRK-003 and growth was assayed by MTT analysis. The above is a representative of three independent experiments using cell line 720.

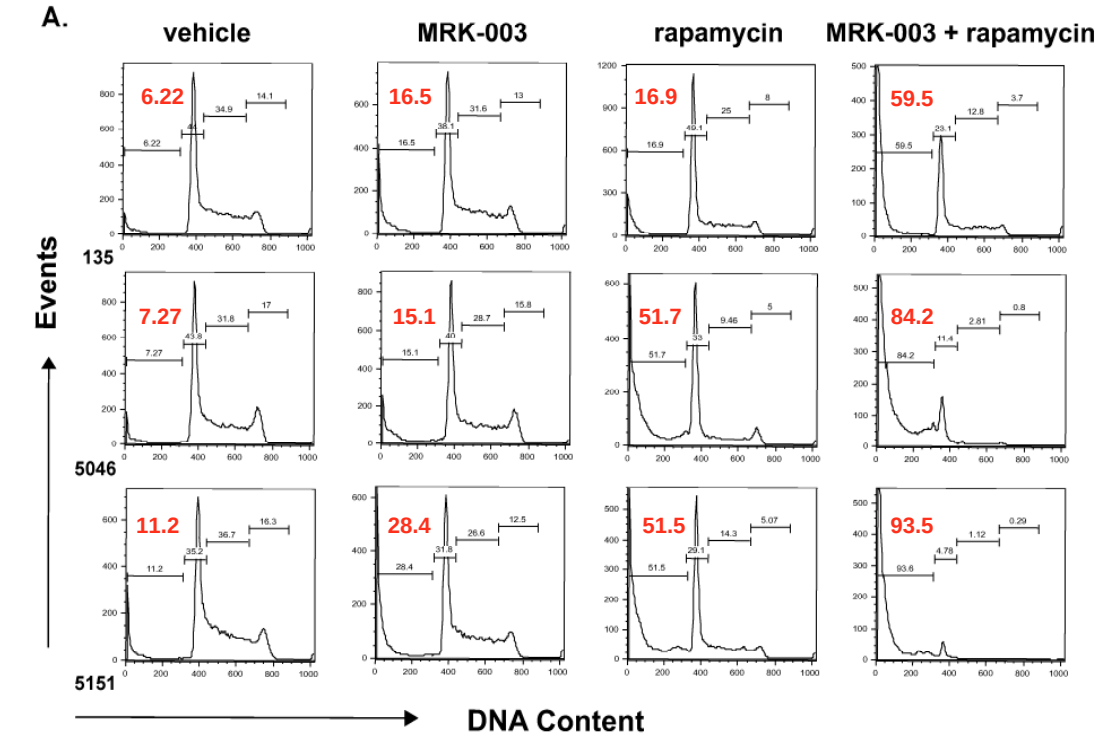
A.
vehicle
MRK-003
rapamycin
MRK-003 + rapamycin
Events
135
5046
5151
DNA Content
6.22
16.5
16.9
59.5
7.27
15.1
51.7
84.2
11.2
28.4
51.5
93.5

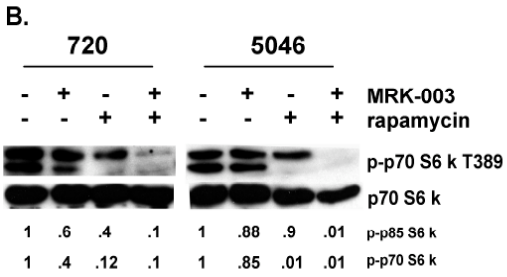
B.
720
5046
MRK-003
rapamycin
p-p70 S6 k T389
p70 S6 k
1 .6 .4 .1 1 .88 .9 .01 p-p85 S6 k
1 .4 .12 .1 1 .85 .01 .01 p-p70 S6 k

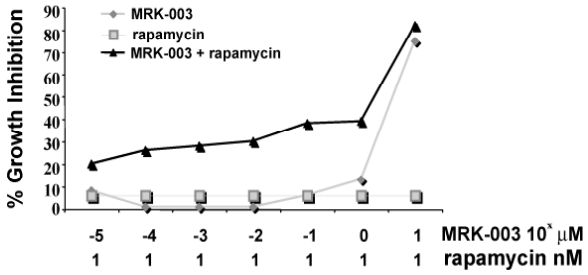
C.
MRK-003
rapamycin
MRK-003 + rapamycin
% Growth Inhibition
MRK-003 10^x μM
rapamycin nM

Figure 17. GSI and rapamycin treatment inhibits human T-ALL growth and extends survival. (A). GSI and rapamycin treatment inhibits human T-ALL growth *in vitro*. Human T-ALL cell line (TALL-1) were treated with 0, 0.5, 1, 5, 10, or 50 μM of MRK-003 in addition to 0, 1, or 100 nM of rapamycin and ATP activity quantified using the Vialight Assay Kit. **(B)** The combination treatment (GSI and rapamycin) inhibits human T-ALL growth *in vivo* more effectively than treatment with either agent. CD1 *nu/nu* mice were injected with human T-ALL cell line, TALL-1. When tumors reached 200mm^3, xenograft mice were treated with vehicle, rapamycin, MRK-003, or a combination of MRK-003 and rapamycin for three weeks. MRK-003 was dosed at either 0 or 150 mg/kg PO once a week. Rapamycin was dosed at either 0 or 20 mg/kg PO daily. Following treatment, tumors were callipered and body weight was recorded. Bar graph indicates relative tumor volumes at sacrifice. The following statistics were analyzed by a t-test; vehicle vs. rapamycin (p=0.0012), vehicle vs. MRK-003 (p=0.3252), rapamycin vs. rapamycin + MRK-003 (p=0.00192), MRK-003 vs. rapamycin + MRK-003 (p=0.0001). **(C)** GSI and rapamycin treatment inhibits human T-ALL growth *in vivo* and increased overall survival. Following three weeks of treatment with vehicle, MRK-003 (150mg/kg/week), rapamycin (20mg/kg daily), or MRK-003 and rapamycin, T-ALL-1 xenograft mice were monitored for tumor recurrence. Tumor free survival was compiled on a Kaplan-Meier survival plot. Data was analyzed by a logrank test (p=0.058).

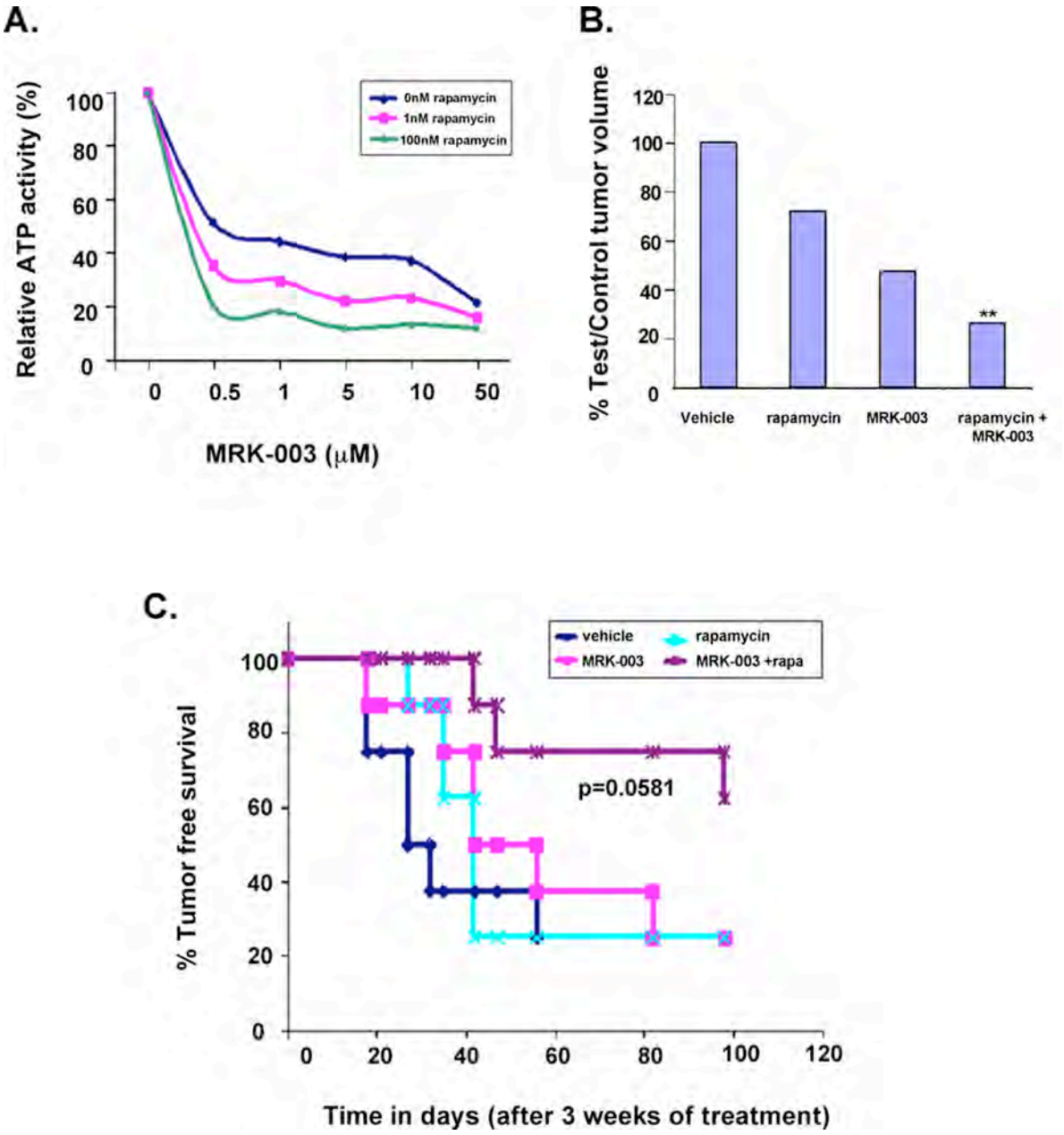
A.
Relative ATP activity (%)
100
80
60
40
20
0
0nM rapamycin
1nM rapamycin
100nM rapamycin
0
0.5
1
5
10
50
MRK-003 (μM)
B.
% Test/Control tumor volume
120
100
80
60
40
20
0
**
Vehicle
rapamycin
MRK-003
rapamycin + MRK-003
C.
% Tumor free survival
100
80
60
40
20
0
vehicle
rapamycin
MRK-003
MRK-003 +rapa
p=0.0581
0
20
40
60
80
100
120
Time in days (after 3 weeks of treatment)

CHAPTER IV

Early Thymic Progenitors are Enriched in Leukemia-Initiating Potential

Figure Contribution:

Kathleen Cullion performed all of the experiments presented in this chapter, excluding Table 3. Kathleen Cullion generated the material for the evaluation of the Notch1 mutational status of preleukemic progenitors, however, the sequencing and mutational analysis was performed by Jessica Tatarek.

Introduction

Overexpression of TAL1 is found in 60% of human T-ALL patients and approximately 80% of these patients also co-express LMO proteins [28]. Thus, TAL1 and LMO gene activation are common genetic events in human T-ALL. TAL1 expression is associated with a poor prognosis compared to other subtypes of T-ALL, with a 5-year survival of 43% [28]. These findings highlight the need for new therapeutic strategies for TAL1+ T-ALL patients.

Leukemia-initiating cells (L-ICs) are a relatively rare population of leukemic cells that like normal stem cells, have the ability to both self-renew and differentiate. L-ICs have been suggested to be refractory to current therapy [336-338], suggesting that therapeutic relapse may result from a failure to eradicate the L-IC population. Therefore, the high rate of relapse observed in TAL1+ T-ALL patients might suggest that current therapies fail to eliminate the L-IC population. However, whether a majority of T-ALL patients harbor a L-IC population remains controversial [302,303,339].

To address whether murine T-ALL harbors L-ICs, we used a mouse model of T-ALL in which the *Tal1* and *Lmo2* oncogenes are misexpressed during mouse thymocyte development by the proximal Lck promoter. We find that *Tal1/Lmo2* transgenic mice exhibit thymocyte developmental arrest that results in significant expansion of DN3/DN4 thymic progenitor populations. Using a Transgenic Notch Reporter mouse (TNR) to detect Notch active cells, we find increased Notch activity in these expanded preleukemic DN3/4 progenitors. These preleukemic DN3/4 progenitors are also oligoclonal and harbor *Notch1* mutations. By analyzing *Tal1/Lmo2* tumors that arise between 4-to-6

months, we demonstrate that DN3-like and DN4-like progenitors are maintained within the tumor. We find the tumor-associated DN3-like progenitors enriched in the ability to initiate leukemia in syngeneic mice compared to the more differentiated DP leukemic blasts. These studies support the idea that mouse T-ALL harbors a leukemia-initiating cell (L-IC) population and suggests that the L-ICs are enriched within the tumor-associated progenitor populations.

Results

DN3/4 thymic progenitor population is expanded in preleukemic *Tal1/Lmo2* mice.

Ectopic Tal1 expression in the thymus interferes with E47/Heb function and leads to repression of E47/Heb-regulated genes that are critical for thymocyte development. Consequently, thymocyte differentiation is perturbed in *Tal1* transgenic mice [58]. Typically the differentiation arrest occurs in the DN stage of development, resulting in an accumulation of DN thymic progenitors. Greater than 40% of T-ALL patients coexpress both TAL1 and LMO1/2 oncogenes [28]. Coexpression of *Tal1* and *Lmo1 or 2* oncogenes in murine thymocytes via the proximal *Lck* promoter accelerates leukemogenesis and interferes with thymocyte maturation to the DP stage (Figure 18A and [51]).

We observed a significant reduction in the overall thymic cellularity in 4-to-6 week old preleukemic *Tal1/Lmo2* mice compared to littermate controls (Figure 18B). While all thymocyte subpopulations could be detected, preleukemic *Tal1/Lmo2* mice had significant increases in the percentage of DN thymic progenitors (range 32.4% to 63%) compared to littermate controls (range 1.92% to 2.9%)($p<0.005$), suggesting that thymocyte development may be arrested in the DN thymic progenitor stage. The differentiation block was associated with a 2-fold decrease in the percentage of double positive (DP) thymocytes, as well as a 3-fold decrease in CD4 single positive (SP) thymocytes (Figure 18A).

Further analysis of the DN population in the preleukemic animals revealed an expansion of DN3 and DN4 progenitors. Although the percentage of DN3 and DN4 cells was not statistically different between preleukemic and control littermates, preleukemic

Tal1/Lmo2 animals had a 2-fold increase in the absolute number of the DN3 and DN4 thymic progenitors (Figure 18C p=0.05). The differentiation arrest observed in *Tal1/Lmo1* and *Tal1/Lmo2* animals was greater than that described in animals that expressed *Tal1* only [58], suggesting that Lmo proteins may cooperate with Tal1 to arrest thymocyte development.

Preleukemic *Tal1/Lmo2* thymocytes exhibit aberrant Notch1 expression.

Spontaneous gain of function *Notch1* mutations are common secondary events in murine T-ALL models [228-230]. While it has been suggested that these gain of function mutations occur during the preleukemic phase [229,340], the precise nature of the target cell remained unclear. To monitor Notch activity during leukemogenesis, we mated our *Tal1/Lmo2* mice with the Transgenic Notch Reporter (TNR) mouse line. The TNR mouse contains a transgene with four CSL-binding sites, a minimal SV40 promoter, followed by an enhanced green fluorescent protein (GFP) sequence [315,341]. The TNR mouse has been shown by others to accurately reflect Notch activity during early thymocyte development, angiogenesis, and hair follicle formation [315,316,341,342]. In the wild type thymus, we observed the highest percentage of Notch active cells in DN progenitors (Figure 19A). Within the DN population in TNR/+ mice, we detected increases in Notch active cells in the DN2 to DN3 stage, followed by repression of Notch signaling as cells progressed to DN4 (Figure 19B). Consistent with these results, a similar pattern of Notch expression is found when DN thymocytes are sorted and expression of *Notch1* and Notch1 target genes are measured [114,315]. We also detected Notch active cells in the DN population of

preleukemic *Tal1/Lmo2* animals (39%-58%) (Figure 19A). The proportion of GFP+ DN thymocytes in preleukemic animals was significantly greater than that observed in TNR/+ littermates (46.35% compared to 14.17%; $p<0.05$). No significant increase in Notch active cells was observed in the DP, CD4SP, or CD8SP populations isolated from *Tal1/Lmo2* preleukemic or control mice (Figure 19A).

Notch1 expression and transcriptional activity are tightly regulated during thymocyte development. *Notch1* expression peaks at the DN3 stage and then decreases as thymocytes mature to the DN4 stage [114]. In preleukemic *Tal1/Lmo2* mice we observed a significant increase in the percentage of Notch-active, GFP+ DN3/4 progenitors (Figure 19B). Although Notch1 expression and therefore activity are normally downregulated at the DN4 stage, we detect marked expansion of GFP+ DN4 progenitors in the mice predisposed to leukemia (Figure 19B).

The sustained Notch1 activity in preleukemic *Tal1/Lmo2* thymic progenitors suggested that *Notch1* mutations may occur at a high frequency in these mice. To test this possibility, the GFP+ DN3 and DN4 cells from three preleukemic *Tal1/Lmo2* mice were examined for the presence of *Notch1* mutations. Preliminary studies performed by Jess Tatarek in the lab have detected multiple *Notch1* mutations in both the DN3 and DN4 preleukemic populations (data summarized, Table 3). All of the mutations identified are found within the PEST region of *Notch1* and result in insertions that introduce STOP codons or alter the reading frame. These types of mutations result in truncation of the Notch1 protein (data not shown) and can contribute to increased Notch1 protein stability. Although all of the mutations identified are similar in that they are predicted to result in

truncation of the PEST domain of Notch1, this analysis revealed the presence of a number of different *Notch1* mutations within the DN3 and DN4 progenitor populations. These findings demonstrate that *Notch1* is frequently mutated in preleukemic *Tal1/Lmo2* DN3 and DN4 progenitors, thereby explaining the increased Notch1 activity detected in preleukemic mice.

To further evaluate the double negative populations expanded in preleukemic mice, we assessed the clonality of Notch1 active DN3 and DN4 progenitors. mRNA was isolated from wild type thymocytes or sorted preleukemic GFP+ DN3 or DN4 cells and TCRβ gene expression was determined by PCR. In wild type thymocytes, we detect rearrangements in 15 of the 22 TCRβ families tested, confirming the polyclonality of the wild type thymus (Figure 19C). In each of the three *Tal1/Lmo2* preleukemic mice examined, the DN3 and DN4 preleukemic subpopulations appear oligoclonal, consisting of 3-6 predominant TCRβ rearranged clones (Figure 19C and data not shown). Interestingly, the types of TCRβ rearrangements differed among the three mice examined, but were identical between the DN3 and DN4 progenitors within each mouse. This analysis suggests that the increases in absolute numbers of DN progenitors in preleukemic animals may reflect the expansion of these Notch1 active clones.

***Tal1/Lmo2* tumors contain thymic progenitors and this population is maintained upon transplant.**

To test whether *Tal1/Lmo2* tumors contained a stem cell or progenitor-like population, we stained *Tal1/Lmo2* tumors with CD4, CD8 or with a lineage cocktail (CD4,

CD8, B220, GR1, Mac1) and then stained the lineage negative cells with CD44 and CD25 antibodies. We analyzed 25 *Tal1/Lmo2* tumors and found that most (24/25) were heterogeneous (Figure 20A, Table 4). Tumors consisted of undifferentiated DN and differentiated DP or SP cells that maintain expression of the *Tal1* and *Lmo2* transgenes. In 22 of the tumors where the DN population was further analyzed, 16 tumors (72%) contained a predominant DN3-like or DN3-like and DN4-like population of cells (Figure 20A, Table 4). Similarly a DN population has been noted in other mouse T-ALL models and in human T-ALL samples suggesting that this maybe a common feature of mouse and human T-ALL [51,302].

The maintenance of the DN3-like and DN4-like progenitors within mouse T-ALL, suggests these cells may be required to initiate disease in recipient mice. To test this idea, we transplanted 5 different *Tal1/Lmo2* tumors into syngeneic mice and monitored the mice for disease. All injected mice developed disease and immunophenotyping of the resultant tumors revealed that in all cases the thymic progenitors were maintained, suggesting that this progenitor population may harbor leukemia-initiating cells (Figure 20B).

To determine if the immunophenotypic heterogeneity reflects functional differences among *Tal1/Lmo2* tumor cells, we performed a series of limiting dilution experiments. Three *Tal1/Lmo2* tumors were injected as serial dilutions into syngeneic mice and recipient mice were monitored for the onset of leukemia. The first tumor analyzed, 8129, required injection of between 5,000 and 50,000 cells to initiate disease in recipient mice (Table 5). We also found that injecting fewer leukemic cells from this

tumor resulted in an increase in disease latency, as injection of $5x10^6$ cells resulted in disease in approximately 26 days, while injection of 50,000 to 5,000 cells resulted in disease in 41 or 53 days, respectively (Table 5). These data indicate that the L-IC population in this tumor is quite rare (Table 5, estimated L-IC frequency of 1:30,735). Consistently, this tumor was comprised of primarily DP blasts and DN3-like and DN4-like precursors made up 1.3% of the tumor. While an increase in disease latency was also observed when serial dilutions of leukemic blasts isolated from tumor 1002 were injected into recipient mice, this tumor appeared to harbor L-ICs at a higher frequency than tumor 8129. When evaluating tumor 1002, injection of 500 to 5000 tumor cells was capable of initiating leukemia in 2/8 and 7/8 recipient mice, respectively (Table 5). Thus, in this tumor the L-IC frequency was much greater and estimated to be 1:2,209. Unlike tumor 8129, this *Tal1/Lmo2* tumor contained significantly more undifferentiated DN3-like and DN4-like precursors (56.8% compared to 1.3%)(data not shown). The third *Tal1/Lmo2* tumor analyzed, 8159, resembled 8129 and required injection of 5000 to 50,000 cells to initiate disease. These data suggest that in this mouse T-ALL model, not all leukemic cells appear capable of initiating leukemia. Moreover, the frequency of L-ICs is variable among tumors and may correlate with the number of tumor-associated thymic progenitors.

Tumor-associated progenitors are enriched in disease initiation potential.

While the presence of a leukemic initiating cell (L-IC) population has been well documented in AML, whether ALL is driven by a rare L-IC remains controversial [302,303,339]. To determine whether tumor-associated thymic progenitors are enriched in

disease initiating potential, the DN3-like population from three independent *Tal1/Lmo2* tumors was sorted, along with DP blasts, and injected as serial dilutions into recipient mice. The purity of the DN3-like and DP tumor cells ranged between 98.4-99.4% (data not shown). Mice injected with unsorted tumor cells developed disease within 24-37 days, as expected. 19/20 mice injected with DP cells failed to develop disease, irrespective of the number of DP leukemic blasts injected (Figure 21A). However, 1 of 10 mice injected with $1x10^4$ DP cells did develop disease. In contrast, 8/9 mice injected with 10^4 DN3-like cells and 5/9 mice injected with 10^3 DN3-like cells developed leukemia within 35-60 days (Figure 21A). Collectively, these data suggest that the tumor-associated thymic progenitors are enriched in leukemia-initiating potential.

It is possible that the DN3-like and DN4-like cells maintained within the tumor are altered DP cells that are unable to express CD4 and CD8 co-receptors. The *Pre-Tα* gene encodes the surrogate TCRα protein that associates with the TCRβ chain to form the pre-TCR. *Pre-Tα* mRNA expression increases during DN development, is highest in DN3 and DN4 progenitors and declines in DP thymocytes [343]. Therefore, we compared *Pre-Tα* expression levels in the sorted tumor subpopulations from three independent tumors. In two of the three tumors analyzed, the DN3-like (CD4-, CD8-, CD44-, CD25+) and the DN4-like (CD4-, CD8-, CD44-, CD25-) tumor cells expressed higher *Pre-Tα* expression levels than the DP leukemic blasts (Figure 21B). These data support the idea that tumor-associated DN3 and DN4 cells may more closely resemble DN3 and DN4 thymic progenitors than DP thymocytes.

L-ICs have two unique features, the ability to self-renew and generate more L-ICs, while retaining the capacity to differentiate into cells with limited self-renewal potential. These features manifest in an immunophenotypically and functionally heterogeneous tumor. To determine whether the sorted tumor-associated DN3 cells retained differentiation potential and generated DP and SP tumor cells, we examined the tumors harvested from recipient mice injected with purified DN3 tumor cells. The transplanted tumors resemble the primary tumor and contain undifferentiated DN3-like and DN4-like progenitor cells as well as more differentiated DP leukemic cells (Figure 21C). Thus, the tumor-associated DN3 thymic progenitors are enriched in L-IC potential and retain differentiation potential.

Discussion

Here, we have studied leukemia progression in a *Tal1/Lmo2* mouse T-ALL model. We show that expression of these two oncogenes arrests thymocyte differentiation at the DN3-DN4 transition and selects for accrual of additional mutations, including gain of function *Notch1* mutations. These thymic progenitors are maintained in most *Tal1/Lmo2* tumors and when tumor-associated, are enriched in leukemia-initiating potential.

In models of T-ALL and other hematological malignancies, differentiation arrest is a common feature and several studies have indicated that differentiation arrest is central to the development of leukemia (as reviewed in [344]). In preleukemic *Tal1/Lmo2* mice, the DN3-DN4 transition is severely perturbed due to a sequestration and repression of the E47/Heb heterodimer ([58] and K. Draheim manuscript in preparation). E proteins enforce proliferation checkpoints and regulate the expression of *Rag1/2* and *Pre-Tα* [345], genes that are essential for thymocyte development. T-ALL models driven by an E2A deficiency are also characterized by an expansion of DN3 thymic progenitors and acquisition of *Notch1* mutations [231]. Thus, the differentiation arrest may select for progenitors with increased Notch1 activity. Consistent with this idea, we detect gain of function *Notch1* mutations and elevated Notch activity within preleukemic *Tal1/Lmo2* DN3 and DN4 progenitors. Aberrant Notch1 signaling has been demonstrated to stimulate thymocyte expansion and can promote DP thymocyte differentiation [346]. Hence, aberrant activation of the Notch1 pathway during the DN3 to DN4 transition may contribute to the preleukemic progenitor expansion and the L-IC activity of cells within this population.

By evaluating TCRβ rearrangements, we demonstrate that increases in the absolute number of DN3 and DN4 progenitors preleukemically may be the result of clonal expansion. Although these preleukemic populations harbor identical TCRβ rearrangements, we find that a majority of the *Notch1* mutations identified preleukemically are different among the DN3 and DN4 thymic subsets. The fact that many of the expanded clones harbor different *Notch1* mutations may suggest that *Notch1* mutations are not responsible for progenitor differentiation or expansion. Alternatively, these data may reflect the continued pressure of preleukemic DN3 and DN4 cells to select for *Notch1* mutations that result in increased thresholds of Notch1 signaling. Further evaluation of the potency of each Notch1 mutation within the preleukemic DN3 and DN4 thymic subsets is currently ongoing in the lab.

The cancer stem cell model predicts that the heterogeneity observed within most clonal tumors reflects an organizational hierarchy, with some cells having greater self-renewal potential and the capability to initiate tumor growth. In the *Tal1/Lmo2* mouse model, clonal tumors appear hierarchically organized, and contain both undifferentiated DN3-like and DN4-like cells and more differentiated DP and SP blasts. This heterogeneity is also observed in infiltrated lymph nodes/organs and importantly is maintained upon transplant. In addition to being immunophenotyically heterogeneous, we also demonstrate that *Tal1/Lmo2* tumor cells are functionally heterogeneous and have evidence of a L-IC population. Titration analyses reveal that compared to the more differentiated DP blasts, tumor-associated DN3 cells are enriched in leukemia-initiating potential, suggesting this tumor population harbors L-ICs.

Although this study suggests that in this mouse T-ALL model the tumor-associated thymic progenitors have acquired extensive proliferative capabilities and maintain differentiation potential, titration analysis reveal the L-IC population comprises only a subset of the tumor-associated DN3 cells. These data suggest that further purification of this population is required to better define the L-IC in this model. These findings also highlight the importance of evaluating the L-IC frequency in other tumor populations that reside within these *Tal1/Lmo2* tumors, including the DN2 and DN4 tumor-associated progenitors. Evaluation of these other populations is essential, as the frequency of L-ICs observed within the tumor-associated DN3 population may simply reflect the presence of contaminating progenitors from another tumorigenic subset.

Following the further purification of the L-IC population in this murine T-ALL model, a critical unanswered question from these studies becomes, what specific pathways are activated within this L-IC enriched population and contribute to L-IC activity. Our preleukemic studies support the notion that aberrant Notch1 activity at this developmental stage may confer “stem cell-like” properties on committed thymic progenitors. If aberrant Notch1 signaling contributes to L-IC activity, Notch pathway inhibition may reduce L-IC activity in this model. It is also possible that aberrant Notch1 signaling alone in committed thymic progenitors is not sufficient to confer “stem cell-like” properties on these cells and that additional mutations are required for L-IC activity. This possibility would predict that Notch inhibition will have little or no effect on L-IC activity, a question we are currently examining the effects of Notch inhibition on leukemia-initiating activity.

Other critical signaling pathways, including NFκB and Akt/mTOR, may be co-opted by sustained Notch1 signaling during this thymocyte development stage and may contribute to the survival, extensive proliferation, and escape from the differentiation arrest that is required for complete leukemic transformation.

During thymocyte development, nuclear factor-κB (NFκB) is activated following pre-TCR signaling to promote survival of late DN3-DN4 thymocytes [86]. Aberrant NF-κB activation is observed in preleukemic *Tal1* thymocytes, *Tal1* tumors, and in human T-ALL cell lines [347,348]. Recent studies indicate that constitutively active NOTCH1 transcriptionally regulates NF-κB and contributes to aberrant activation of this pathway in T-ALL [348]. Given that NF-κB may be able to substitute for pre-TCR signaling [86] and promotes survival of thymocytes, it is possible that Notch1-mediated NF-κB activation is critical to leukemia development. The Akt/mTOR pathway also provides critical pro-survival signals to thymocytes during β selection [118]. Similarly, aberrant Akt/mTOR activation is found in both primary T-ALL samples and T-ALL cell lines, and is in part Notch1 regulated [326,349]. Therefore, it is possible that the NF-κB and/or the Akt/mTOR pathways may become activated by Notch1 and contribute to leukemic transformation. Both the NF-κB and Akt/mTOR pathways are aberrantly active in a number of malignancies and are required for the maintenance of L-ICs in AML[350,351]. Interestingly, these pathways are not active in normal HSCs, therefore pharmacologic inhibition of either pathway may reduce L-ICs and bulk AML cells, but have little effect on normal HSC maintenance. It remains to be tested whether the NF-κB or Akt pathways are active in T-ALL L-ICs and are required for L-IC maintenance.

In addition to deregulated Notch1 signaling, mutations in other regulators of stem cell quiescence may contribute to L-IC activity in this model. Loss of *p16(INK4A)* and *p14(ARF),* and *PTEN* are common genetic events in human T-ALL [352]. The *Ink4a/Arf* locus is epigenetically silenced in hematopoietic stem cells and when expressed, inhibits stem cell self-renewal [353]. Deletion of these genes, or overexpression of negative regulators, such as Bmi1, contributes to aberrant self-renewal in leukemogenesis [354,355]. PTEN has also been implicated in HSC and cancer stem cell self-renewal [356-361]. Whether *Pten* or *Ink4a/Arf* loss contributes mouse L-IC activity and/or frequency remains unknown, but will be considered in future experiments.

Materials and Methods

Mouse Studies

A cohort of *Tal1/Lmo2* transgenic mice was generated and monitored daily for the onset of leukemia as described previously (Draheim and Kelliher, manuscript in preparation). To generate the *Tal/Lmo2/TNR* cohort, *Tal/Lmo2* mice were mated with *TNR/+* mice (STOCK Tg(Cp-EGFP)25Gaia/J # 005854, Jackson Laboratories, Bar Harbor, ME). *Tal1/Lmo2/TNR* mice are maintained on a mixed background ((C57BL/6J x SJL/J)F2 x FVB/N). To control for differences in genetic background all preleukemic studies were performed using *TNR/+* control littermates. For mouse transplantation studies, *Tal1/Lmo2* tumor (FVB/N) cells were washed in PBS and mixed with wild type FVB/N thymocytes as carrier cells. Cells were injected via intraperitoneal injection into recipient FVB/N mice (6-8 weeks old, Jackson Lab, Bar Harbor, ME) and mice were monitored daily for cachexia, lethargy, and/or ruffled coat. Diseased animals were sacrificed and histopathological examination was performed. L-IC frequency was determined using *Poisson* distribution statistics and the L-Calc Version 1.1 software program (StemCell Technologies, Inc., Vancouver, Canada).

Flow cytometry

Thymomas isolated directly from *Tal1/Lmo2* leukemic animals were made into single cell suspensions by mincing with glass slides. Approximately $1x10^6$ tumor cells were stained with CD4-Cy5Pe and CD8-PE or with a lineage cocktail consisting of CD4-PE, CD8-PE, B220-PE, GR1-PE, MAC1-PE. Lineage negative cells were then stained with CD44-APC and CD25-Cy7Pe (BD Pharmingen, San Diego, CA). Flow cytometric

analysis was performed on the FACS Caliber and FACS Aria (Becton Dickinson, Franklin Lakes, NJ) and sorting was performed using BD FACSVantage (Becton Dickinson, Franklin Lakes, NJ). Data was analyzed using Flow-Jo (Tree Star Inc., Ashland, OR).

RNA Analysis

RNA was extracted from murine preleukemic thymocytes or thymomas using Trizol. cDNA was synthesized using Superscript First - Strand Synthesis System (Invitrogen, Carlsbad, CA). To determine the effects of Notch1 target gene expression on pre-leukemic thymic subsets, cDNA was quantitated using the SYBR green kit (Qiagen, Valencia, CA). Specific c-*Myc*, *Deltex1,* and *Pre-Tα* primers were designed using Primer Express software (Applied Biosystems, Foster City, CA): c-Myc forward, 5'-CTGTTTGAAGGCTGGATTTCCT-3'; c-Myc reverse, 5'-CAGCACCGACAGACGCC-3'. *Pre-Tα* forward 5'-CTGCTTCTGGGCGTCAGGT- 3'; *Pre-Tα* reverse 5'-TGCCTTCCATCTACCAGCAGT-3'. *Deltex1* forward 5' TGCCTGGTGGCCATGTACT-3'; *Deltex1* reverse 5'-GACACTGCAGGCTGCCATC-3'. The copy number obtained for gene of interest was normalized to the copy number for *ß-Actin*.

Mutational Analysis

To determine the Notch1 mutational status, DNA isolated from preleukemic sorted thymic populations or mouse T-ALL cells was amplified by PCR with, Pfu1 Taq (Strategene, Ceder Creek, TX) with primers specific for exon 34 of the *Notch1* gene [230]. PCR products were run on a 1.5% agarose gel, purified (QIAquick Gel Extraction Kit,

Qiagen, Valencia, CA), and cloned into the TOPO TA cloning vector (Invitrogen, Carlsbad, CA) for sequencing using the universal M13 primers.

TCR repertoire analysis

To determine clonality, rearrangements of the TCRβ chain were assayed by standard qualitative PCR analysis, using Pfu1 Taq (Strategene, Ceder Creek, TX) and primers specific for mouse TCR Vβ1-Vβ18 genes and constant region as described in [362]. Vβ1 – Vβ18 primers were each paired with a the following Vβ constant primer. Vβ - 5'-GGCTCAAACAAGGAGACCTTGGGTGG - 3'. The amplification was performed using a Strategene Robocycler Gradient 96 starting with a 2 minute 94°C denaturation, followed by 30 cycles consisting of 20 seconds at 94°C, 12 seconds at 55°C, and 30 seconds at 68°C and a final elongation step of 10 minutes at 68°C. PCR products were purified on a 2% agarose gel, subcloned and confirmed by sequencing.

Figure 18. Thymic progenitors are expanded in preleukemic *Tal1/Lmo2* mice (A) Thymocytes from four-to-six week old wild type or preleukemic *Tal1/Lmo2* mice were made into single cell suspensions. Cells were stained with CD4-Cy5Pe and CD8-PE or with a lineage cocktail consisting of CD4-PE, CD8-PE, B220-PE, GR1-PE, MAC1-PE. Lineage negative cells were then stained with CD44-APC and CD25-Cy7Pe and analyzed by flow cytometry. **(B)** Decreased thymic cellularity in preleukemic *Tal1/Lmo2* mice. Thymocytes were counted and total thymic cellularity was determined. **(C)** The absolute number of DN3 and DN4 progenitors is increased in *Tal1/Lmo2* mice. The absolute number in each thymic subset was determined by multiplying the percentage of each thymic subset by the total thymic cellularity.

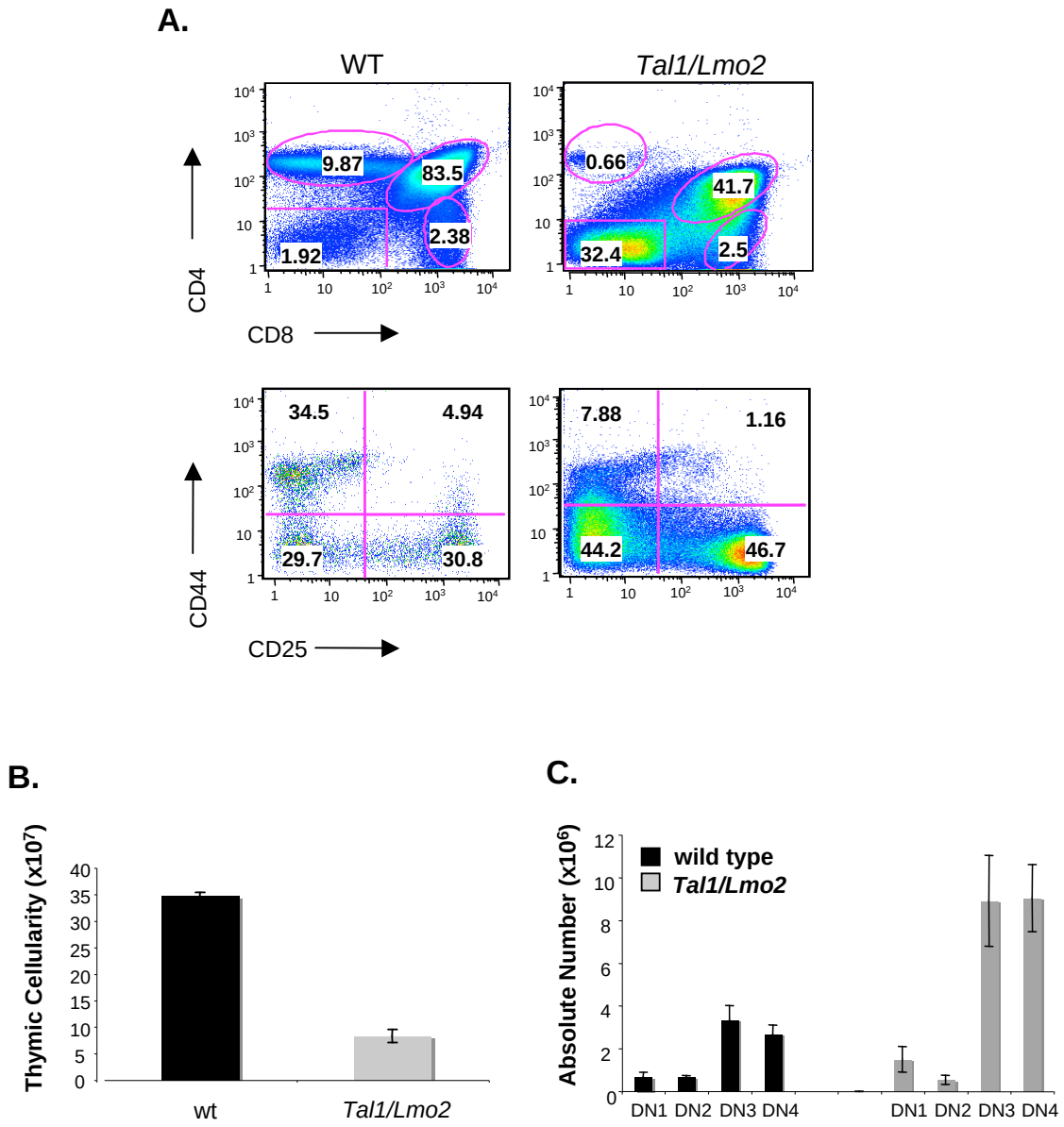

Figure 19. Notch1-active thymic progenitors are expanded in preleukemic *Tal1/Lmo2* mice. (A) Six-to-eight week old *TNR/+* or *Tal1/Lmo2/TNR* mice were sacrificed and thymocytes stained with CD4, CD8 antibodies. DP, SP, and DN populations were analyzed for percent GFP+ cells by flow cytometry. **(B)** Lineage negative cells were stained with CD25 and CD44 antibodies and GFP+ was analyzed by flow cytometry. The percent GFP+ cells in the DN1, DN2, DN3, and DN4 progenitor populations are shown. **(C)** Using specific primers for Vβ1-18, TCRVβ mRNA expression was examined in wild type and sorted GFP+ DN3 and 4 thymic progenitors isolated from preleukemic *Tal1/Lmo2* mice.

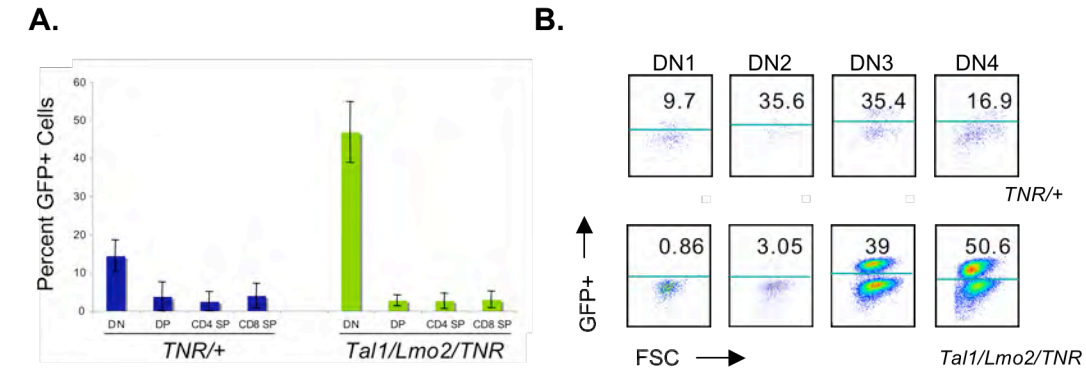

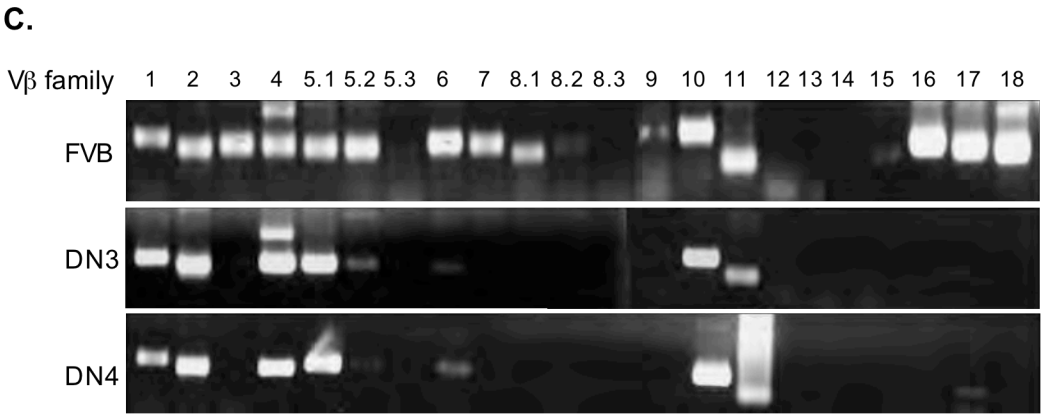

Table 3. Mutational analysis of preleukemic DN3 and DN4 populations

Mouse #	Thymic Subset	# of Clones Sequenced	% of Clones with Mutations	# of Unique Mutations	# of Common Mutations in DN3, 4
9401	DN3	40	47%	6	2
	DN4	40	42%	11	
9448	DN3	20	35%	6	1
	DN4	14	36%	1	
2	DN3	20	55%	5	1
	DN4	14	43%	4	

Figure 20. Immunophenotypic heterogeneity among mouse *Tal1/Lmo2* tumors. (A) Wild type thymocytes and 25 *Tal1/Lmo2* tumors were stained with CD4 and CD8 antibodies and the lineage negative tumor cells were stained with CD25 and CD44 antibodies and analyzed by flow cytometry. Four representative *Tal1/Lmo2* tumors are shown. **(B)** Tumor-associated thymic progenitors are maintained upon transplant. *Tal1/Lmo2* tumor cells were then injected via subcutaneous injection into recipient mice. At sacrifice, the immunophenotype of the transplanted tumor was reanalyzed by flow cytometry and compared to the primary tumor. Five tumors were analyzed, one representative tumor is shown.

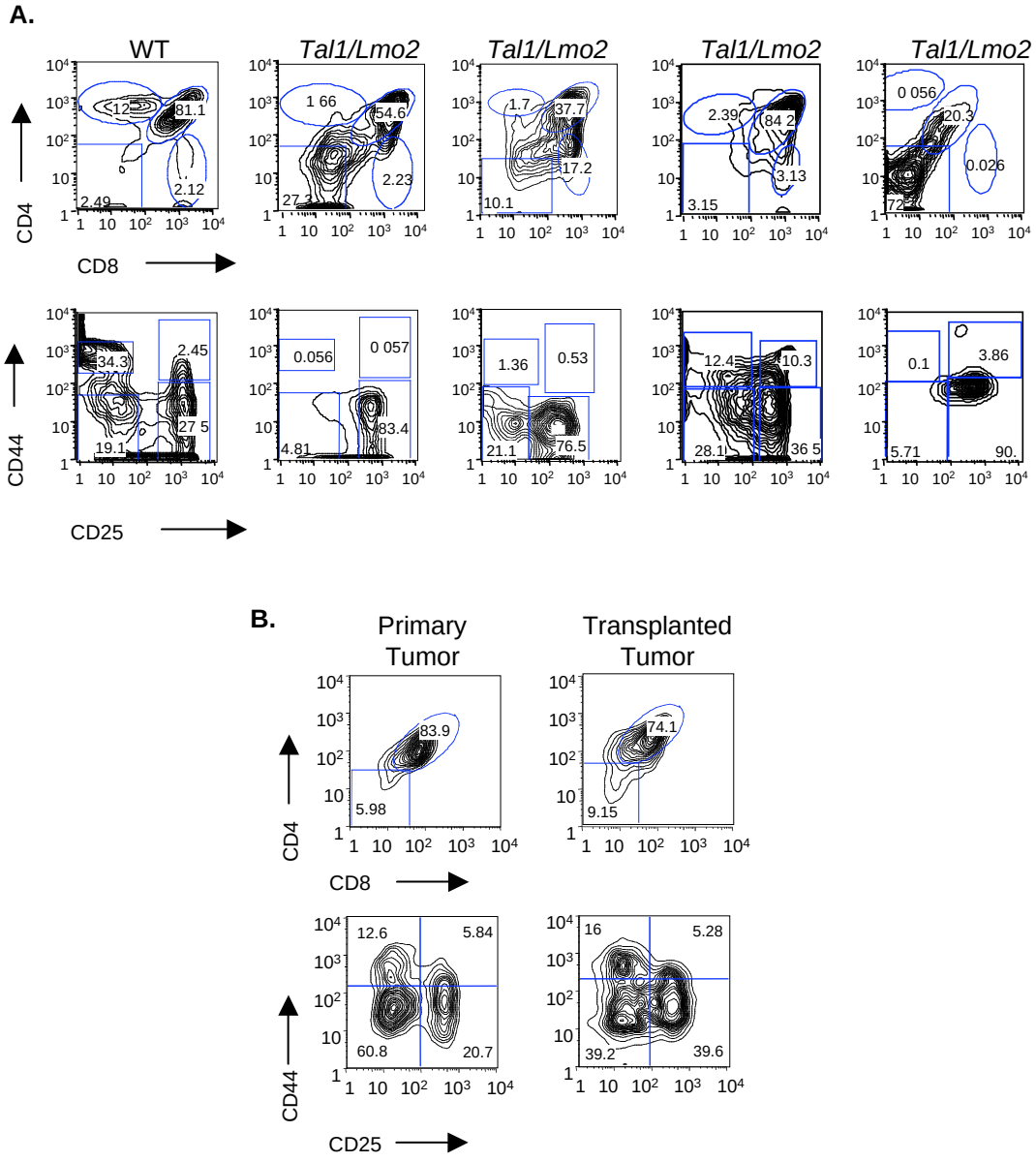

Table 4. *Tal1/Lmo2* tumors are immunophenotypically heterogeneous

Animal Number	Genotype	Phenotype	% DN	Predominant DN Subtype	Latency
1001	*Tal1/Lmo2 5*	DP,CD8SP	20	DN3	91
1002	*Tal1/Lmo2 5*	DP,DN	58	DN3,4	93
1004	*Tal1/Lmo2 5*	CD8SP	16	DN3	91
1007	*Tal1/Lmo2 5*	DP,CD8SP	18	DN3	124
1078	*Tal1/Lmo2 5*	CD8SP,DN	21	DN3,4	100
1099	*Tal1/Lmo2 5*	DP,DN	35.9	DN3,4	101
8115	*Tal1/Lmo2 5*	DP,DN	27.2	DN3	89
8129	*Tal1/Lmo2 5*	DP	2.83	DN2 (3)	128
8159	*Tal1/Lmo2 5*	CD4SP,DN	20	N.D.	93
8164	*Tal1/Lmo2 5*	All CD8SP-DN		DN2	161
8179	*Tal1/Lmo2 5*	DP	3.15	DN1,2,3,4	119
8181	*Tal1/Lmo2 5*	DP,DN	72	DN3	212
8308	*Tal1/Lmo2 5*	DP,CD8SP	1.2	DN4	60
8361	*Tal1/Lmo2 5*	DP	4	DN3,4	145
8382	*Tal1/Lmo2 19*	DP,DN	40	DN3,4	111
8383	*Tal1/Lmo2 19*	CD8SP	4.6	DN3,4	135
8602	*Tal1/Lmo2 5*	DP,DN,CD8SP	40	DN2 (3,4)	88
8613	*Tal1/Lmo2 5*	DP	3	DN3,4	120
8647	*Tal1/Lmo2 5*	DP	6	DN4	109
8653	*Tal1/Lmo2 5*	DP	4	DN3	109
8655	*Tal1/Lmo2 5*	DP,CD8SP	2.73	DN3,4	N.D.
8683	*Tal1/Lmo2 5*	DP	15.8	DN1,2	109
8734	*Tal1/Lmo2 19*	DP,CD8SP	4	N.D.	135
8757	*Tal1/Lmo2 5*	DP	19	DN3,4	112
9053	*Tal1/Lmo2 19*	DP	6	DN3,4	109

Table 5. Functional heterogeneity among *Tal1/Lmo2* tumor cells

	# of Tumor Bearing Mice (Disease Latency)			
Dilution	**8129**	**1002**	**8159**	**Summary**
$5x10^6$	4/4 (26)	8/8 (10)	-	12/12
$5x10^5$	3/3 (29)	8/8 (13)	-	11/11
$5x10^4$	3/4 (41)	8/8 (18)	2/3 (35)	13/15
$5x10^3$	1/4 (53)	7/8 (26)	1/3 (41)	9/15
$5x10^2$	-	2/8 (35)	0/2 (-)	2/10
Est. L-IC frequency	1:30,735	1:2,209	N.D.	

Figure 21. Early thymic progenitors are enriched in disease initiating potential. Tumor cells from *Tal1/Lmo2* mice were stained with CD4, CD8 antibodies and lineage negative cells were stained with CD25 and CD44 antibodies. **(A)** *Tal1/Lmo2* tumor cells were left unsorted or sorted into DN3 or DP populations by flow cytometry. Cells were then serially injected into recipient mice with carrier cells (wild type thymocytes) and mice monitored for disease. Three independent *Tal1/Lmo2* tumors were analyzed. **(B)** Pre-Tα mRNA expression levels in purified into DP or DN3/DN4 tumor cells were quantified using real time PCR. Copy number was normalized to β Actin using the ΔΔCT method. Three tumors were analyzed. An average of three independent experiments on one *Tal1/Lmo2* tumor is shown. **(C)** DN3 tumor cells retain differentiation potential. Tumors stained with CD4, CD8 antibodies and lineage negative cells were stained with CD25 and CD44 antibodies and analyzed by flow cytometry to compare the immunophenotype of tumors initiated by injection of whole tumor cells or purified DN3 tumor cells. Three *Tal1/Lmo2* tumors were re-examined, one representative tumor is shown.

A.

Tumor Cell Population	# of Tumor Cells Injected	# of Tumor Bearing Mice			
		Exp. 1	Exp. 2	Exp. 3	Summary
Unsorted Tumor	$5x10^6$	2/2	2/2	2/2	8/8
Unsorted Tumor	$5x10^5$	2/2	2/2	2/2	8/8
DN3-like	1 or $5x10^4$	3/3 (5)	3/3 (1)	2/3 (1)	8/9
DN3-like	1 or $5x10^3$	2/3 (5)	1/3 (1)	1/3 (1)	4/9
DP	1 or $5x10^4$	0/4 (5)	0/3 (1)	1/3 (1)	1/10
DP	1 or $5x10^3$	0/4 (5)	0/3 (1)	0/3 (1)	0/10

(5) = $5x10^x$, (1) = $1x10^x$ tumor cells injected

B.

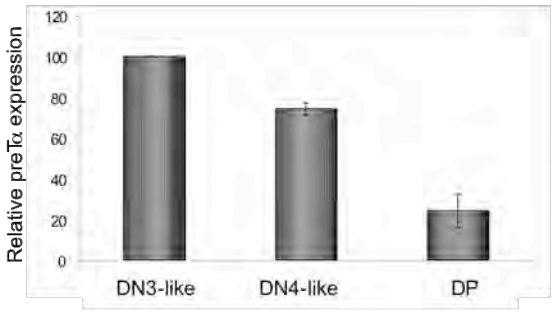

C.

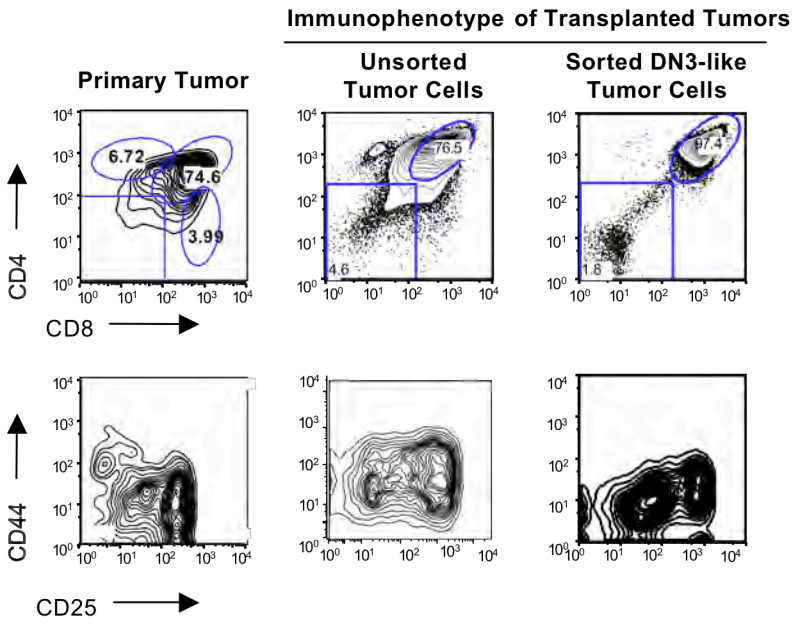

CHAPTER V

DISCUSSION

Mutations affecting the Notch1 signaling pathway are common in T-ALL and it has been well documented that aberrant Notch1 signaling is critical for leukemic growth. Yet precisely how Notch1 mediates leukemogenesis remains unclear. Work addressed in this thesis examines the effects of Notch1 inhibition on leukemic growth *in vivo*, tests a requirement for Notch1 in leukemia initiation, and evaluates the contribution of Lef1 and the Akt/mTOR pathway in human and mouse T-ALL.

The data presented in this thesis support the idea that targeted therapies for T-ALL could include Notch inhibition. We demonstrate that GSIs can be chronically administered to mice *in vivo*. Using an intermittent GSI dosing schedule, we minimize the intestinal toxicity associated with chronic Notch inhibition and importantly extend survival of near end stage leukemic mice (Figure 9). Therefore, similar to effects seen *in vitro*, murine T-ALL growth remains Notch1 dependent *in vivo*.

Our analysis also reveals that mouse T-ALL is driven by a relatively rare L-IC population, suggesting that targeted therapies for T-ALL must be evaluated for anti-L-IC activity. In *Tal1/Lmo2* tumors, the L-ICs appear enriched within the committed thymic progenitor population compared to more differentiated DP blasts (Figure 21). However, titration analyses reveal the L-IC population comprises only a subset of the tumor-associated DN3 cells within a tumor. Future studies will include further purification of the tumor-associated DN3 population by staining with cell surface proteins commonly found on either hematopoietic stem cells or other L-ICs. In addition, future experiments will include rigorous evaluation of the frequency of L-ICs within other tumorigenic populations.

As demonstrated in other hematopoietic malignancies, the frequency of L-ICs may vary significantly according to the initiating and cooperating oncogenes [363]. Therefore, in the future we will also compare L-IC frequencies among *Tal1/Lmo2*, *Tal1/Ink4a/Arf*, and *Tal1* only mice. We will also test whether L-IC frequency correlates with disease latency observed among the various mouse models. Lastly, a more defined L-IC population would also facilitate the study of the specific genes/pathways that promote the extensive proliferation capacity of this population.

While this work was in progress, two distinct L-IC populations were identified in pediatric T-ALL patients. In one report, L-ICs appear enriched in the CD34+/CD4- or CD34+/CD7- population, suggesting a primitive HSC or multipotent progenitor drives human T-ALL growth [303]. In contrast, another group failed to detect CD34 expression on L-ICs and concluded CD34 might not be a reliable L-IC marker in T-ALL [302]. This group does not immunophenotypically characterize the L-IC population but finds the population of cells with L-IC activity have the same γ and β TCR clonal rearrangements as the primary patient sample, indicating that L-ICs may reside within the T-cell committed progenitor population [302]. These studies clearly indicate further analysis of the L-IC population(s) in T-ALL patients is required. Using the NSG model, developed during my thesis work (Appendix), we will examine primary pediatric T-ALL samples for L-IC activity. A better understanding of L-ICs in human T-ALL will allow direct comparison of L-IC frequencies among pediatric T-ALL samples. This model will also be useful in determining whether L-ICs increase upon therapeutic relapse and whether L-IC frequency correlates with event free survival.

A recent report implicates Notch1 as a key regulator of L-IC activity in human T-ALL [302]. Our studies identify mutations that result in the truncation of the PEST domain of Notch1 in both preleukemic DN3 and DN4 progenitors (Table 3). We also demonstrate that when these progenitors are tumor-associated, they appear enriched in L-IC activity (Figure 21). Therefore, similar to what has been described in human T-ALL samples, it is possible that gain of function Notch1 mutations contribute to the L-IC activity in murine T-ALL. Experiments designed to test the sensitivity of preleukemic Notch1-active progenitors to GSI as well as the effects of GSI treatment on the L-IC activity of tumor-associated progenitors are currently ongoing in the lab. Preliminary data suggest Notch inhibition may reduce the L-IC activity of tumor-associated thymic progenitors. In 2 of 3 tumors tested, GSI treatment for 48 hours *in vitro* reduced the absolute number of tumor-associated DN3-cells approximately 3.5-fold and delayed the onset of leukemia by 12 days, on average. Whether prolonged GSI treatment will be sufficient to eradicate leukemia-initiating activity remains a current focus of this thesis research.

Our preleukemic studies reveal an expansion of Notch1 active thymic progenitors. C-Myc is directly regulated by Notch1 in thymocyte development and in leukemia and has been shown to contribute to both normal and cancer stem cell functions [59,163,238,364]. Thus, we hypothesize that activation of the Notch1-c-Myc pathway confers limitless proliferation potential to thymic progenitors. Interestingly, many of the pathways identified in this thesis to be regulated by Notch1, all have a common connection and effect c-Myc expression. Lef/Tcf family members can promote c-Myc expression through direct transcriptional regulation [365]. While the Akt/mTOR pathway can inhibit Gsk3β-

mediated inactivation of c-Myc and also affects c-Myc translation. Therefore, it is possible that Notch1 acts primarily by deregulating c-Myc expression levels in T-ALL.

Interestingly, the preleukemic Notch active progenitors were oligoclonal, which could indicate that while Notch1 may drive thymic expansion, additional mutations including loss of *Ink4a/Arf*, *Pten*, or other mutations that potentiate c-Myc activity may be required for complete leukemic transformation. In the future it will be important to elucidate the genes/pathways specifically activated in L-ICs. To accomplish this we will compare the gene-expression profiling of wild type DN3 and DP thymocytes to the DN3-like and DP leukemic cells isolated from *Tal1/Lmo2* tumors.

Comparative analysis of gene-expression profiles and annotated pathway analysis between tumor maintained DN3-like and DP blasts will likely yield many potential targets. Therefore, our analysis will be limited to genes that show statistically significant differential expression and are at least two-fold over or underexpressed between the two groups. We will prioritize our study to include genes that are associated with self-renewal, cell cycle, differentiation, DNA repair and to genes that regulate transcription and chromatin. Previous studies have identified L-IC populations to be enriched in gene expression signatures similar to those associated with embryonic stem cells or malignancies with poor prognosis [363,366]. To identify potentially important genes, we will compare our data with these previously published data sets. Genes identified in this screen will be validated using quantitative PCR. We will also compare the tumor-associated DN3 cells to normal DN3 and DP thymocytes. This gene expression analysis may reveal tumor maintained L-ICs resemble wild type DN3s rather than DP blasts. This

finding would support the suggestion that the L-IC originated within these progenitors and the genes that differ between the two populations may reveal candidate genes required for L-IC activity.

Data presented in this thesis also identified genes and pathways directly regulated by Notch1. Using a cell line in which intracellular Notch1 expression is doxycycline regulated, we identified Lef1 as a direct transcriptional target of Notch1 in mouse T-ALL cells (Figure 5). Lef1 has since been shown to contribute to leukemic expansion of murine T-ALL cell lines [321]. However, unlike c-Myc, Lef1 expression is unable to completely rescue leukemic cells from the effects of Notch inhibition (Figure 6). These data suggest that Lef1 contributes, but is not sufficient for leukemic growth and survival. Interestingly, recent data suggest the role of LEF1 in human ALL might be even more complex. A high-resolution genome wide analysis performed on pediatric ALL samples detected *LEF1* deletions in 1.56% of B-ALL and 8% of T-ALL cases examined [352]. In a follow up study, highly focal deletions of *LEF1* were detected in 10.6% primary T-ALL patient samples. This locus was then sequenced in the same 45 cases and heterozygous mutations were observed in an additional 6% of T-ALL patients (A. Gutierrez, personal communication). These data indicate that there is selection for *LEF1* loss, raising the possibility LEF1 may function as a tumor suppressor in a subset of T-ALL patients.

This thesis research also demonstrates that Notch1 positively regulates the Akt/mTOR pathway in murine T-ALL cells (Figure 15). Although Notch1 inhibition reduces the phosphorylation of mTOR targets, mTOR kinase activity can be detected in GSI treated leukemic cells. We demonstrate that treatment with both GSI and rapamycin

induces massive apoptosis of leukemic cells *in vitro* and ablates mTOR activity. Moreover, we show that the administration of GSI and rapamycin significantly limits human T-ALL cell line growth *in vivo* and prolongs survival in a xenograft model (Figure 17). Importantly, we also demonstrate that at low doses, GSIs synergize with rapamycin to induce apoptosis of mouse and human T-ALL cells. GSIs have been shown to synergize with dexamethasone and sensitize glucocorticoid-resistant T-ALL cells lines and primary samples to glucocorticoid-induced apoptosis [200]. Collectively, these studies suggest that when given in combination, rapamycin, dexamethasone, and lower doses of GSIs may prove efficacious. These findings have urged the evaluation of GSI combination therapy in a phase 1 trial of relapsed T-ALL patients (T. Look and A. Gutierrez, personal communication).

The treatment of both murine and human T-ALL cell lines with rapamycin alone, results in G1 arrest and/or apoptosis *in vitro*, suggesting that the mTOR pathway is also critical for leukemic growth. Emerging evidence also suggests that this pathway controls both normal stem cell homeostasis and may also contribute to the self-renewal activities of leukemia- or cancer-initiating cells [356-361]. In a mouse T-ALL model driven by conditional *Pten* deletion, rapamycin selectively prevented the generation or maintenance of L-ICs [360]. These data suggest that much of the effects of the *Pten* deficiency on L-IC self-renewal may be mTOR dependent. Currently, it remains unknown whether rapamycin treatment alone or in combination with GSIs affects L-IC activity, a question we will address in future studies.

While this work was in progress, members of the PI3K/AKT/mTOR pathway have been reported mutated or deleted in T-ALL patients. mTOR, which is regulated by NOTCH1 in T-ALL, is also a substrate for the E3ligase, FBXW7 [180,326,349]. Mutations in the substrate recognition domain of FBXW7 are common in T-ALL and could contribute to increased mTOR stability and activity. In addition, genetic mutations affecting the PI3K/AKT/mTOR pathway directly are found in approximately 40% of T-ALL patients. Gain of function mutations affecting *RAS, PI3K, AKT* as well as inactivating mutations in *PTEN*, *SHIP1*, and *NF1* have also been reported (Figure 3) [367-369]. PTEN also appears negatively regulated by NOTCH1 via HES1 in human T-ALL cell lines [327]. In PTEN wild type cells, GSI-mediated NOTCH1 inhibition restores PTEN signaling and reduces AKT activity. However, some cell lines have homozygous loss of PTEN, which renders cells primarily addicted to the PI3K/Akt/mTOR pathway and consequently GSI resistant. In murine T-ALL, no correlation between Pten loss and GSI resistance has been observed. In fact, in samples with Pten loss, Akt phosphorylation was reduced following Notch inhibition (Figure 15), suggesting that in murine T-ALL, Notch1 positively regulates Akt and mTOR in a Pten independent manner.

Future Directions:

In the future we need to further define the murine and human L-ICs in our T-ALL models. This effort should reveal the pathways and/or genes activated in L-ICs. This gene set would be predicted to contribute to leukemic self-renewal and may reveal new therapeutic targets. An additional priority will be to test whether L-IC frequency

correlates with the molecular subtype of T-ALL (TAL1, LMO, TLX1/3, NOTCH1, PTEN) in both murine and human samples.

These data support the idea that new state of the art mechanisms to specifically target the Notch1 pathway are essential. To date there are a number of approaches proposed to inhibit Notch signaling including GSIs and ADAM inhibitors that prevent receptor cleavage, monoclonal antibodies that interfere with receptor/ligand binding, and small molecules that specifically disrupt the protein-protein interactions required for Notch-dependent transactivation. For T-ALL, future studies should also include investigation of cell specific methods of Notch inhibition. To date, a number of novel methods for cell specific siRNA delivery have been developed. These include encapsulating siRNA particles in β1,3-D-glucan to promote efficient uptake in murine macrophages [370] and tethering siRNA sequences to the CD7 receptor to allow for uptake by T-cells [371]. For treatment of T-ALL, cell specific Notch pathway inhibition is likely to increase the therapeutic window and decrease toxicities.

Figure 22. A proposed model of leukemia initiation. When *Tal1* and *Lmo2* are misexpressed in DN thymocytes, E47/Heb heterodimers are disrupted and the expression of E47/Heb regulated genes reduced. This causes a DN3-DN4 arrest in thymocyte development. To overcome the arrest, DN3 progenitors may mutate the Notch1 receptor, which allows for progenitor expansion and possibly aberrant self-renewal capabilities. Most likely through additional mutations listed above, preleukemic DN3 progenitors are able to expand and differentiate, resulting in a heterogeneous tumor.

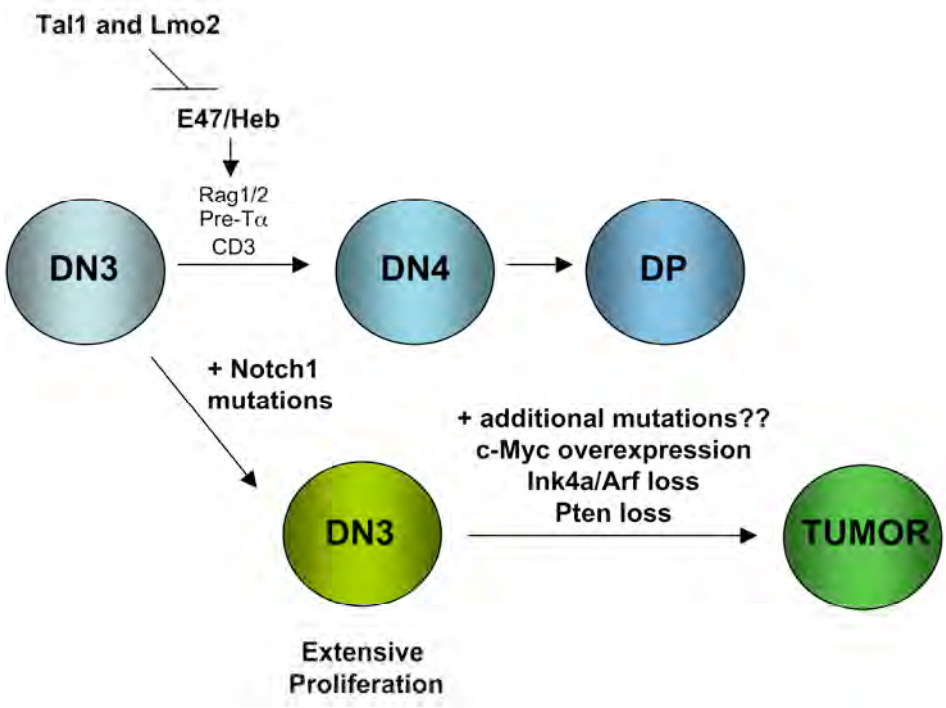

APPENDIX

Generation of the Human T-ALL/NSG Model

Figure Contribution:

Kathleen Cullion was responsible for all of the experiments presented in this chapter. Assistance was received for intracardiac and intraveneous injections as well as daily monitoring of the NSG mice from members of the Greiner Lab.

Introduction

The development of an animal model that permits engraftment of primary human leukemic blasts would allow for a better understanding of the molecular characteristics driving leukemic growth and ultimately to improved treatment strategies for the disease. Currently for T-ALL, experiments designed to test the effects of drug therapies are performed on cultured human T-ALL cell lines *in vitro* and in mouse xenograft systems. These human T-ALL cell lines were derived from relapsed patients many years ago and unlike primary T-ALL samples, these cell lines have frequent p53 mutations, suggesting that p53 function is impaired in these cell lines [372]. Therefore, it is possible that drug responses obtained using these cultured cell lines might not accurately reflect drug responses of primary T-ALL samples. Therefore, we have generated a new human T-ALL mouse model by engrafting immunodeficient NOD*/scid/IL2γ-/-* (NSG) mice with primary pediatric T-ALL cells. NSG mice have no functional T or B-cells and have a targeted mutation that leads to an IL-2 receptor common γ chain deficiency [373]. NSG mice also have a complete absence of natural killer (NK) cells and more severe adaptive and innate immune deficiency, which results in a significant increase in the engraftment of human cells compared to NOD/SCID mice [373,374]. Here, we demonstrate that primary T-ALL leukemic blasts can be engrafted in this mouse strain, allowing for the expansion of leukemic blasts and the identification of L-ICs. Moreover, therapeutic efficacy can be tested on primary leukemic samples in this preclinical model, as opposed to established cell lines.

Results

NOD/scid/IL2γ-/- mice engrafted with human T-ALL cells develop disease

To test whether primary T-ALL leukemic blasts could be engrafted into immunodeficient mice, we transferred $5x10^6$ blasts from human peripheral blood into NOD/scid/IL2γ-/- (NSG) mice. To determine optimal conditions for engraftment, neonates and adult NSG mice were left unirradiated or irradiated with 1 and 2 Gy, respectively. We then transferred leukemic blasts into either 1-2 day old NSG neonates by intracardiac injection or NSG adult mice by intravenous injection. Mice were monitored and were sacrificed upon symptom presentation (ruffled coat, weight loss, and hunched posture). We found the transfer of leukemic cells into NSG neonates resulted in a more rapid induction of disease, as NSG neonates developed disease in approximately 49 days (Table 6, average of non-irradiated and irradiated). Adult NSG animals also developed disease, but required a longer latency of 78 days (Table 6, average of non-irradiated and irradiated). Irradiation prior to the transfer of leukemic blasts did not affect either disease latency or level of engraftment. Therefore, the following studies were performed on non-irradiated NSG adult mice.

To evaluate the level of engraftment, cells from the bone marrow and spleens of diseased animals were stained with anti-human CD45 antibodies and analyzed by flow cytometry. Cytospin preparations of bone marrow cells were stained with Wright Giemsa stain. We found approximately 95% of bone marrow (Figure 23A) and 90% of the spleen (data not shown) consisted of human CD45 positive cells. Wright Giemsa analysis of the bone marrow revealed the presence of large blast-like cells with predominantly nuclear

staining and little cytoplasm (Figure 23A). Human CD45 positive cells infiltrated mouse thymus, liver, and spleen (Figure 23B). Histopathological examination of mouse tissues revealed organ infiltration of lymphoblasts and destruction of normal tissue architecture.

Level of engraftment and immunophenotype remain unchanged following secondary engraftment.

To determine whether the properties of the disease or level of engraftment changed upon serial transfer, serial transplantations were performed using cells isolated from the bone marrow of primary recipient NSG mice engrafted with patient samples. All 40 secondary recipients developed disease with little difference in level of disease engraftment observed (Figure 24, 91% vs. 99%). Similar percentages of anti-human CD45+ double negative (DN) and anti-human CD45+ double positive (DP) blasts were detected in the spleens and bone marrow of primary and secondary recipients (Figure 24), indicating that passage through NSG mice did not result in a change in immunophenotype. These data are consistent with other published findings that report no changes in level of engraftment, immunophenotype, or clonality following transfer into primary, secondary, or tertiary recipients [303].

Characteristics of primary T-ALL patients engrafted into NSG mice.

Unsorted cells from 5 T-ALL patients were evaluated for their ability to engraft into NSG mice (Table 7). In 3/5 patients (05-386, 06078-061, 202-67-64), primary leukemic cells were successfully engrafted in recipient mice. The level of engraftment

was similar, ranging from 82-95% in the bone marrow (Figure 25 A-C). Of the three patients that have successfully serially transferred, one patient (202-67-64, Figure 25C) was obtained as a cryogenically frozen sample. This sample achieved similar levels of engraftment and similar disease latency as fresh samples, suggesting both fresh and frozen leukemic blasts can be engrafted into NSG recipients.

In patient 05-418, 4/6 NSG primary recipient mice developed disease and human CD45+ cells were noted in the bone marrow and spleens of recipient mice. However, cells harvested from primary NSG recipients did not resemble the original patient sample (Figure 25D). Upon arrival, 05-418 was predominantly CD4 SP (96%) and 4% of the tumor consisted of DN cells. No CD8SP or DP cells were detected in this leukemic sample. However, the cells harvested from primary NSG recipient mice have detectable CD4 and CD8 SP cells, raising the possibility that CD8 positive cells may reflect graft versus host (GVH) disease. These cells were transferred to secondary NSG recipients and thus far, have not resulted in disease in these mice, as of 8 months post injection. These data indicate that the cells isolated from the primary NSG recipient mice were most likely not leukemic blasts, as they did not serial transfer. Patient 05-456 was recently received and injected into primary NSG recipients, as of 60 days post injection, no adult recipient mice have developed disease as of yet.

Future Experiments

The ability to engraft primary T-ALL blasts allows both for expansion of primary human leukemic cells for subsequent studies and establishes a preclinical model to test

novel treatment regimens. Preliminary evidence shows that combinations of Notch, mTOR, and P13K inhibitors, along with dexamethasone may have clinical efficacy in T-ALL [326,327,349]. An additional feature of this model is the ability to monitor kinetics and progression of human disease. Using the T-ALL NSG model, human CD45-positive leukemic blasts can be detected as early as 2 weeks post injection in the peripheral blood (Figure 26). This allows disease to be monitored overtime, which can provide a measure of leukemogenicity and can allow for administration of drugs to approximately the same amount of leukemic blasts when regimens are tested using different patient samples.

The development of this model will also allow for the study of L-IC activity in human T-ALL samples. Currently, there are only a few reports that have measured L-IC frequency in primary T-ALL samples and have done so using NOD/SCID mice. There is growing evidence that using NOD/SCID mice might underestimate L-IC frequency due to poor engraftment ability. The use of the more highly immunocompromised NSG mouse, may prove to be a more accurate measure of L-IC activity [375].

Materials and Methods

Primary leukemic blasts

Primary leukemic T-ALL samples were collected from patients treated at Dana-Farber Cancer Institute (Boston, MA) or at Johns Hopkins Medical Center (Baltimore, MD) and were obtained under signed consent in accordance with the Declaration of Helsinki and approval from the Institutional Review Board of the University of Massachusetts Medical School. Total human peripheral blood leukocytes were purified by Ficoll gradient separation (GE Healthcare Lifesciences, Pittsburgh, PA). Viability was assessed by trypan blue exclusion.

Mice

NOD.Cg-Prkdc^{scid} Il2rγ^{tm1Wjl}/SzJ (abbreviated NSG, stock # 005557) were obtained from Jackson Laboratories (Bar Harbor, ME). Mice were housed at the University of Massachusetts Medical School under specific pathogen free conditions in accordance with Federal and Institutional IACUC guidelines. Mice are given autoclaved food and maintained on acidified, autoclaved water and sulphamethoxazole-trimethoprim medicated water (Goldline Laboratories, Ft. Lauderdale, FL) provided on alternate weeks.

In vivo engraftment

Adult recipient NSG mice were inoculated by tail vein injection with 5x10^6 cells in maximum volume of 500µl of PBS. Neonates were inoculated by intra-cardiac injections with 1-5x10^6 cells in a maximum volume of 50µl. Mice were returned to their cages and

examined daily for well-being. At the first signs of morbidity (weight loss, ruffled fur, lethargy) mice were euthanized.

Immunohistochemistry

At sacrifice liver, kidney, and spleen were fixed in 10% neutral buffered formalin, embedded in paraffin, and 5μm tissue sections were cut. Sections were stained with hematoxylin and eosin for histological evaluation at the DERC Transgenic Core Laboratory at the University of Massachusetts Medical School. Immunohistochemical staining was also performed using human CD45 antibodies (BD Pharmingen, San Diego, CA.) Images were taken using a Carl Zeiss Imager.Z1 Plan-Apochromat (Carl Zeiss, Jena, Germany) with a 20X objective lens. The images were acquired using a Carl Zeiss AxioCam HRc camera and the imaging-acquisition software used was Carl Zeiss AxioVision Rel. 4.6.

Flow cytometry

To determine percent engraftment and to characterize the immunophenotype of patient samples, spleen and bone marrow were harvested from NSG mice were stained with the following antibodies; anti-human CD45-PerCP, anti-mouse Ly5-APC, anti-human CD4-PE, anti-human CD8-FITC, anti-human CD20- FITC (BD Pharmingen, San Diego, CA). Cells were stained for 30–45 minutes, washed and fixed with 2% paraformaldehyde prior to analysis. Samples were analyzed using BD FACSCalibur or FACSVantage machines and data analyzed using FlowJo software (Tree Star Inc., Ashland, OR).

To monitor engraftment, mice were bled via intraocular bleeding at time points indicated for complete blood count (CBC) differential and for FACS analysis. Blood for CBC and

differential was run using the Heska CBC/Diff Veterinary Hematology System (Heska AG, Fribourg, Switzerland). For FACS analysis, 100µl of blood was stained as described above for 30-45 minutes. Cells were then washed with FACS buffer and red blood cells were lysed by incubating with BD FACS Lysing Solution for 5 minutes (BD Biosciences, San Jose, CA). Cells were then washed with FACS staining buffer and were analyzed using BD FACScalibur or FACSVantage machines and data analyzed using FlowJo software (Tree Star Inc., Ashland, OR).

Table 6. Irradiation does not affect disease latency or percent engraftment.

Method	# of mice	Time to Disease	% Human CD45+ Blast
Non-Irrad. Neonate	4/4	52.6 +/- 4.1	84.4 +/- 5.4
Irrad. Neonate	4/4	45.3 +/- 9.0	82.3 +/- 5.1
Non-Irrad. Adult	4/4	78.3 +/- 1.5	93.2 +/- 3.0
Irrad. Adult	5/5	79.2 +/- 4.0	93.0 +/- 3.0

Figure 23. NOD/*scid*/IL2Rγ-/- (NSG) mice engrafted with primary pediatric human T-ALL cells develop disease. (A) Adult NSG mice were irradiated with 2 Gy and then injected intravenously with $5x10^6$ primary human T-ALL leukemic blasts. Bone marrow cells from diseased mice were harvested from femurs and cells were stained with anti-human CD45 antibody and analyzed by flow cytometry. Cytospin of bone marrow cells harvested from a leukemic NSG mouse were stained with Wright-Giemsa. **(B)** Tumor sections of primary NSG recipient mice were stained with an anti-human CD45 antibody to identify human leukemic cells in the mouse thymus, liver, and spleen. Leukemic blasts in thymus, liver, and spleen were identified by H&E staining (panel below).

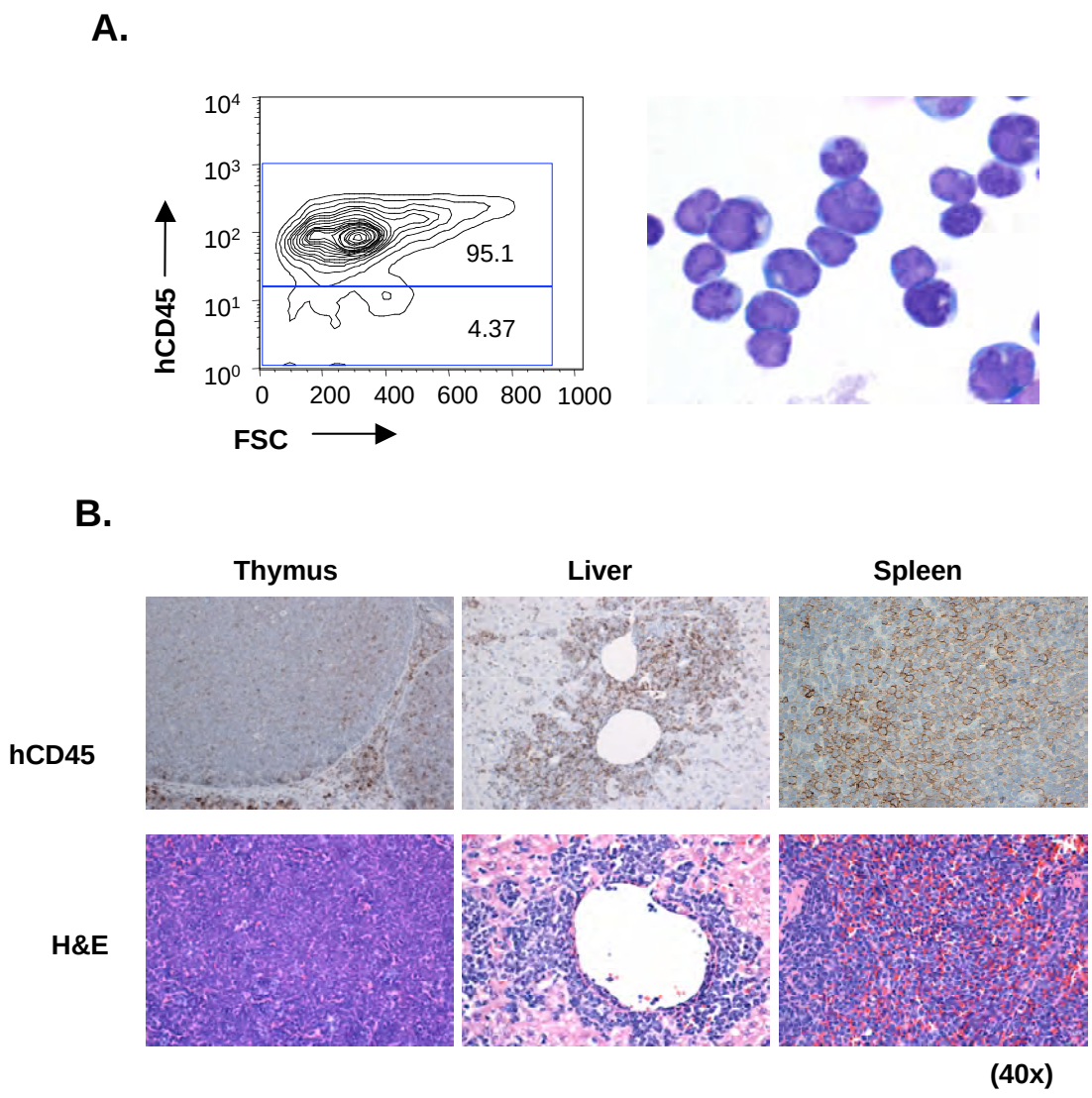

Figure 24. Phenotypic analysis of bone marrow from primary and secondary NSG recipient mice. Human T-ALL cells from patient 05-386 were injected into primary NSG recipients and monitored for the onset of disease. At sacrifice, bone marrow cells from primary recipients were injected into secondary (NSG) recipients. Bone marrow from primary and secondary NSG recipients was stained with CD45, CD4 and CD8 antibodies and analyzed by flow cytometry.

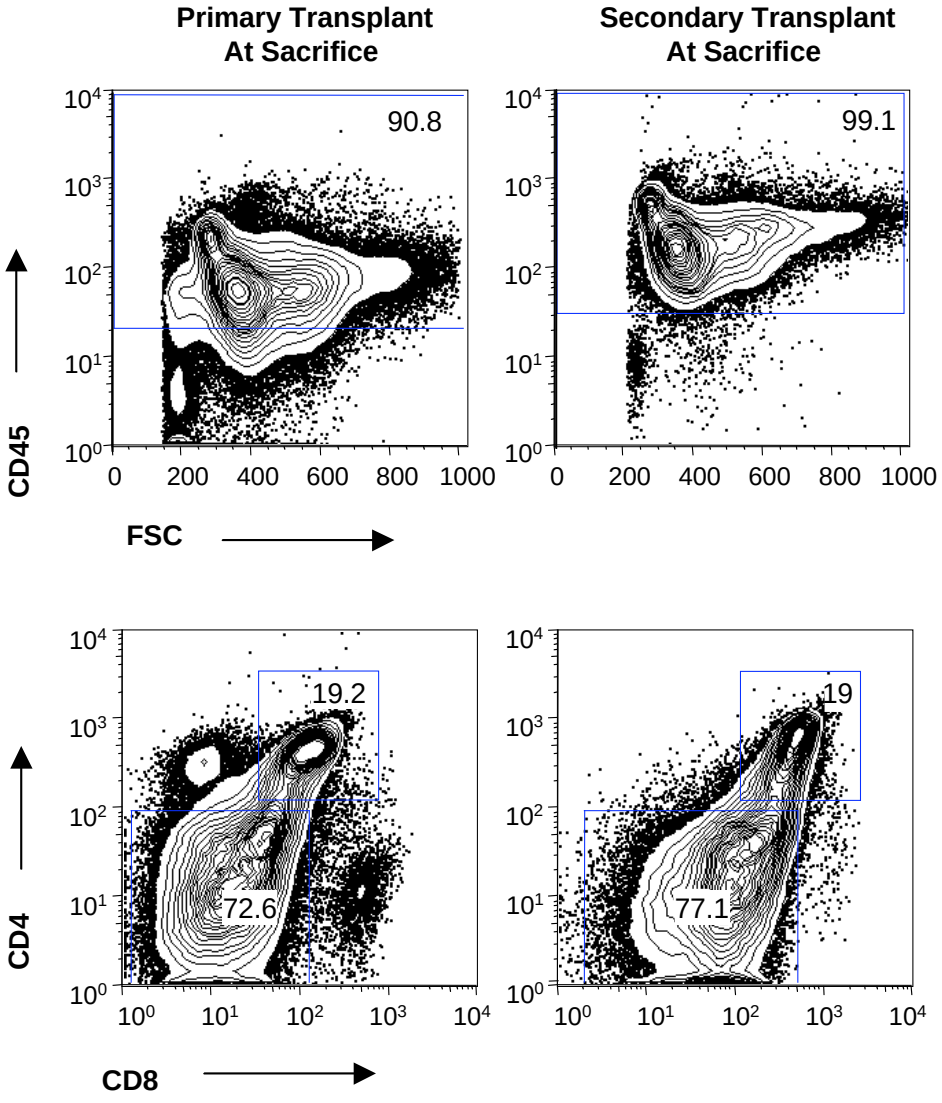

Table 7. Characteristics of patient samples engrafted into NSG mice.

Patient Sample	WBC Count k/mcl	Marker Expression (dx)	TAL1 Expression	Notch1 Expression	Fresh vs Frozen	Engraftment Status
05-386	118	CD45, CD34, CD2, CD7, CD117, CD4, CD8	+	+	Fresh	Quaternary
05-418	400	CD45, CD7, sCD3, TdT, CD21,CD4, CD11b, CD71, CD10, CD1a, CD58	-	-	Fresh	Secondary*
06-078-061	500	CD45, CD2, CD5, CD7, CD4,CD8, TdT	N.D.	N.D.	Fresh	Secondary
202-67-64	700	CD45, CD1, CD2, CD3, CD5,CD7, CD99, TdT, CD34, CD38	+	+	Frozen	Secondary
05-456	Bone marrow	CD45, CD2, CD3, CD5, CD7,CD8, CD10, TdT	N.D.	N.D.	Fresh	Primary

*Suspect graft versus host

Figure 25. Primary patient samples engrafted into NSG mice. Leukemic blasts were isolated from the peripheral blood/ or bone marrow biopsy from primary T-ALL patients. $5x10^6$ leukemic blasts were injected into NSG mice and mice were monitored for disease. Upon sacrifice, spleens from leukemic mice were minced and stained with anti-human CD45 or anti-CD4 and anti-CD8 antibodies and analyzed by flow cytometry. CD4 and CD8 are gated on CD45+ cells. Patient samples isolated include **(A)** 05-386, **(B)** 06-078-061, **(C)** 202-67-64, and **(D)** 05-418.

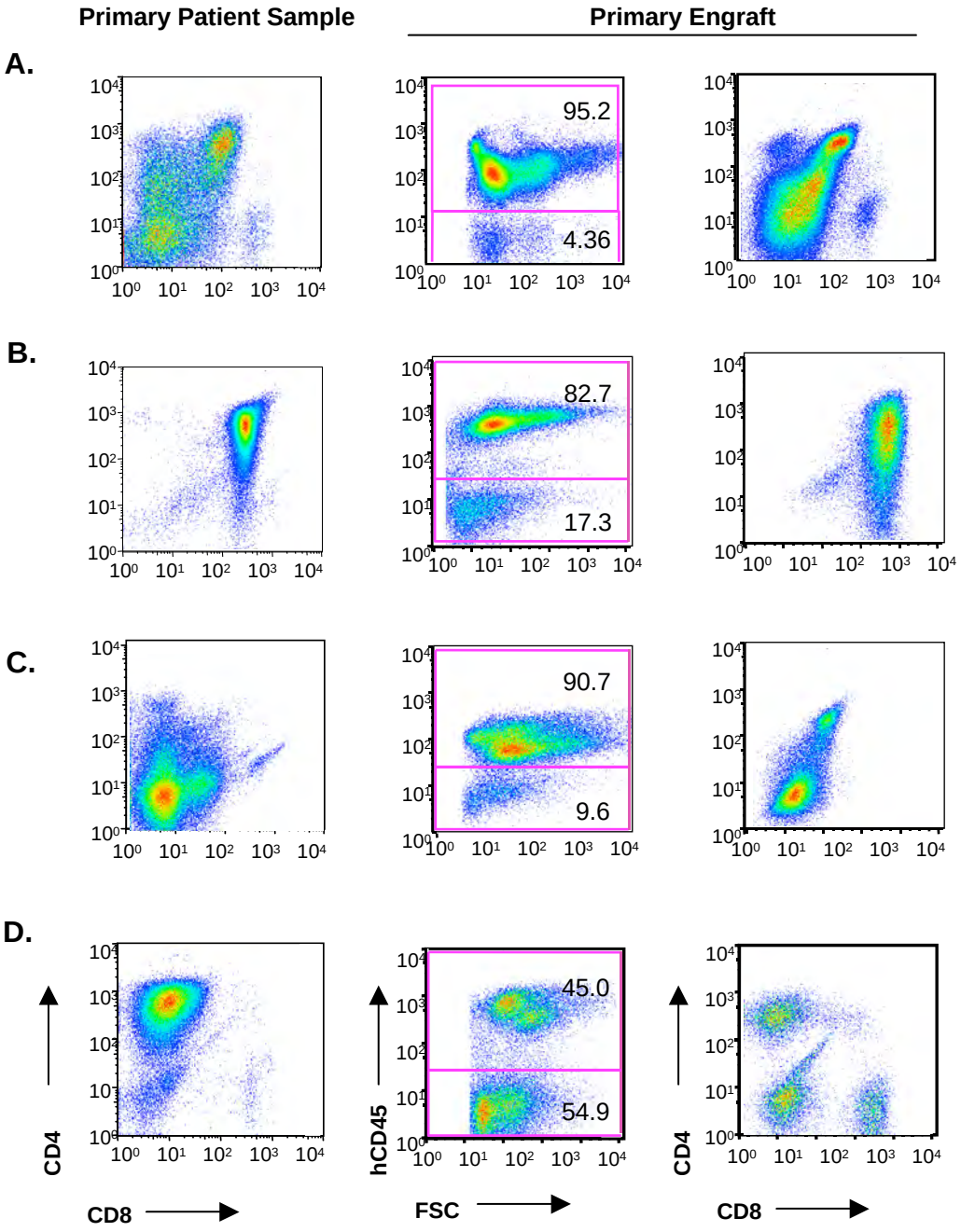

Figure 26. Human CD45-positive leukemic blasts can be monitored in peripheral blood of recipient mice. Peripheral blood from engrafted NSG recipient mice was obtained by eye bleed at time points indicated. Peripheral blood was stained with anti-human CD45 or anti-mouse Ly5 antibodies and analyzed by flow cytometry. White blood cells counts were monitored in engrafted NSG recipient mice at 4 and 6 weeks post-injection.

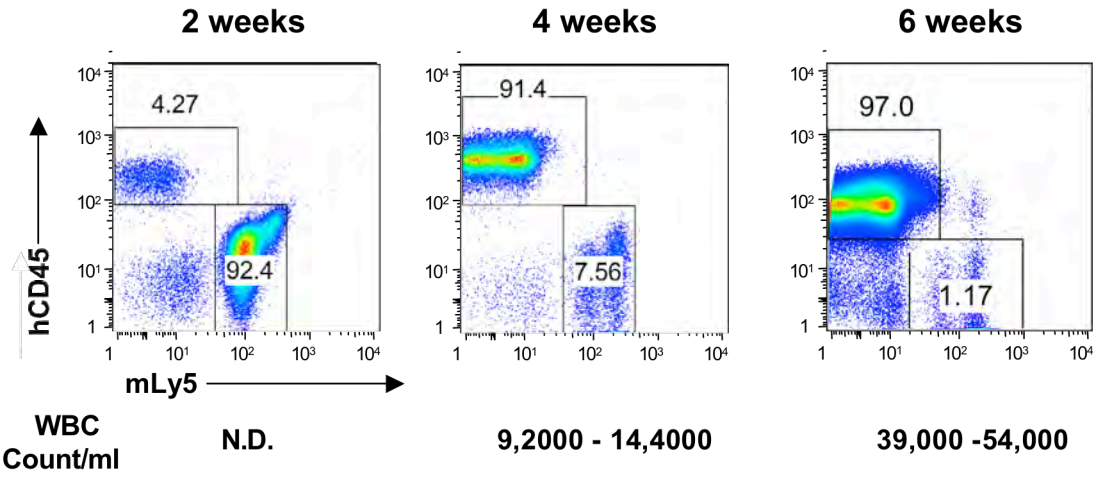

References

1. Downing JR, Shannon KM. Acute leukemia: a pediatric perspective. Cancer Cell. 2002;2:437-445.
2. Goldberg JM, Silverman LB, Levy DE, et al. Childhood T-cell acute lymphoblastic leukemia: the Dana-Farber Cancer Institute acute lymphoblastic leukemia consortium experience. J Clin Oncol. 2003;21:3616-3622.
3. Pui CH, Schrappe M, Ribeiro RC, Niemeyer CM. Childhood and adolescent lymphoid and myeloid leukemia. Hematology Am Soc Hematol Educ Program. 2004:118-145.
4. Thiel E, Kranz BR, Raghavachar A, et al. Prethymic phenotype and genotype of pre-T (CD7+/ER-)-cell leukemia and its clinical significance within adult acute lymphoblastic leukemia. Blood. 1989;73:1247-1258.
5. Ferrando AA, Neuberg DS, Staunton J, et al. Gene expression signatures define novel oncogenic pathways in T cell acute lymphoblastic leukemia. Cancer Cell. 2002;1:75-87.
6. Bernard O, Lecointe N, Jonveaux P, et al. Two site-specific deletions and t(1;14) translocation restricted to human T-cell acute leukemias disrupt the 5' part of the tal-1 gene. Oncogene. 1991;6:1477-1488.
7. Bernard OA, Busson-LeConiat M, Ballerini P, et al. A new recurrent and specific cryptic translocation, t(5;14)(q35;q32), is associated with expression of the Hox11L2 gene in T acute lymphoblastic leukemia. Leukemia. 2001;15:1495-1504.
8. Chen Q, Cheng JT, Tasi LH, et al. The tal gene undergoes chromosome translocation in T cell leukemia and potentially encodes a helix-loop-helix protein. EMBO J. 1990;9:415-424.
9. Cheng JT, Yang CY, Hernandez J, Embrey J, Baer R. The chromosome translocation (11;14)(p13;q11) associated with T cell acute leukemia. Asymmetric diversification of the translocational junctions. J Exp Med. 1990;171:489-501.
10. Clappier E, Cuccuini W, Kalota A, et al. The C-MYB locus is involved in chromosomal translocation and genomic duplications in human T-cell acute leukemia (T-ALL), the translocation defining a new T-ALL subtype in very young children. Blood. 2007;110:1251-1261.
11. Dube ID, Kamel-Reid S, Yuan CC, et al. A novel human homeobox gene lies at the chromosome 10 breakpoint in lymphoid neoplasias with chromosomal translocation t(10;14). Blood. 1991;78:2996-3003.
12. Hatano M, Roberts CW, Minden M, Crist WM, Korsmeyer SJ. Deregulation of a homeobox gene, HOX11, by the t(10;14) in T cell leukemia. Science. 1991;253:79-82.
13. Kennedy MA, Gonzalez-Sarmiento R, Kees UR, et al. HOX11, a homeobox-containing T-cell oncogene on human chromosome 10q24. Proc Natl Acad Sci U S A. 1991;88:8900-8904.
14. Lu M, Gong ZY, Shen WF, Ho AD. The tcl-3 proto-oncogene altered by chromosomal translocation in T-cell leukemia codes for a homeobox protein. EMBO J. 1991;10:2905-2910.
15. McGuire EA, Hockett RD, Pollock KM, Bartholdi MF, O'Brien SJ, Korsmeyer SJ. The t(11;14)(p15;q11) in a T-cell acute lymphoblastic leukemia cell line activates

multiple transcripts, including Ttg-1, a gene encoding a potential zinc finger protein. Mol Cell Biol. 1989;9:2124-2132.
16. Mellentin JD, Smith SD, Cleary ML. lyl-1, a novel gene altered by chromosomal translocation in T cell leukemia, codes for a protein with a helix-loop-helix DNA binding motif. Cell. 1989;58:77-83.
17. Schrappe M, Reiter A, Zimmermann M, et al. Long-term results of four consecutive trials in childhood ALL performed by the ALL-BFM study group from 1981 to 1995. Berlin-Frankfurt-Munster. Leukemia. 2000;14:2205-2222.
18. Silverman LB, Gelber RD, Dalton VK, et al. Improved outcome for children with acute lymphoblastic leukemia: results of Dana-Farber Consortium Protocol 91-01. Blood. 2001;97:1211-1218.
19. Pui CH, Evans WE. Treatment of acute lymphoblastic leukemia. N Engl J Med. 2006;354:166-178.
20. Asnafi V, Buzyn A, Le Noir S, et al. NOTCH1/FBXW7 mutation identifies a large subgroup with favorable outcome in adult T-cell acute lymphoblastic leukemia (T-ALL): a Group for Research on Adult Acute Lymphoblastic Leukemia (GRAALL) study. Blood. 2009;113:3918-3924.
21. Breit S, Stanulla M, Flohr T, et al. Activating NOTCH1 mutations predict favorable early treatment response and long-term outcome in childhood precursor T-cell lymphoblastic leukemia. Blood. 2006;108:1151-1157.
22. Begley CG, Aplan PD, Denning SM, Haynes BF, Waldmann TA, Kirsch IR. The gene SCL is expressed during early hematopoiesis and encodes a differentiation-related DNA-binding motif. Proc Natl Acad Sci U S A. 1989;86:10128-10132.
23. Cheng JT, Hsu HL, Hwang LY, Baer R. Products of the TAL1 oncogene: basic helix-loop-helix proteins phosphorylated at serine residues. Oncogene. 1993;8:677-683.
24. Elwood NJ, Green AR, Melder A, Begley CG, Nicola N. The SCL protein displays cell-specific heterogeneity in size. Leukemia. 1994;8:106-114.
25. Kallianpur AR, Jordan JE, Brandt SJ. The SCL/TAL-1 gene is expressed in progenitors of both the hematopoietic and vascular systems during embryogenesis. Blood. 1994;83:1200-1208.
26. Drake CJ, Brandt SJ, Trusk TC, Little CD. TAL1/SCL is expressed in endothelial progenitor cells/angioblasts and defines a dorsal-to-ventral gradient of vasculogenesis. Dev Biol. 1997;192:17-30.
27. Green AR, Lints T, Visvader J, Harvey R, Begley CG. SCL is coexpressed with GATA-1 in hemopoietic cells but is also expressed in developing brain. Oncogene. 1992;7:653-660.
28. Ferrando AA, Look AT. Gene expression profiling in T-cell acute lymphoblastic leukemia. Semin Hematol. 2003;40:274-280.
29. Mouthon MA, Bernard O, Mitjavila MT, Romeo PH, Vainchenker W, Mathieu-Mahul D. Expression of tal-1 and GATA-binding proteins during human hematopoiesis. Blood. 1993;81:647-655.
30. Tremblay M, Herblot S, Lecuyer E, Hoang T. Regulation of pT alpha gene expression by a dosage of E2A, HEB, and SCL. J Biol Chem. 2003;278:12680-12687.

31. Robb L, Lyons I, Li R, et al. Absence of yolk sac hematopoiesis from mice with a targeted disruption of the scl gene. Proc Natl Acad Sci U S A. 1995;92:7075-7079.
32. Shivdasani RA, Mayer EL, Orkin SH. Absence of blood formation in mice lacking the T-cell leukaemia oncoprotein tal-1/SCL. Nature. 1995;373:432-434.
33. Porcher C, Swat W, Rockwell K, Fujiwara Y, Alt FW, Orkin SH. The T cell leukemia oncoprotein SCL/tal-1 is essential for development of all hematopoietic lineages. Cell. 1996;86:47-57.
34. Mikkola HK, Klintman J, Yang H, et al. Haematopoietic stem cells retain long-term repopulating activity and multipotency in the absence of stem-cell leukaemia SCL/tal-1 gene. Nature. 2003;421:547-551.
35. Robb L, Elwood NJ, Elefanty AG, et al. The scl gene product is required for the generation of all hematopoietic lineages in the adult mouse. EMBO J. 1996;15:4123-4129.
36. Visvader JE, Fujiwara Y, Orkin SH. Unsuspected role for the T-cell leukemia protein SCL/tal-1 in vascular development. Genes Dev. 1998;12:473-479.
37. Hsu HL, Cheng JT, Chen Q, Baer R. Enhancer-binding activity of the tal-1 oncoprotein in association with the E47/E12 helix-loop-helix proteins. Mol Cell Biol. 1991;11:3037-3042.
38. Hsu HL, Wadman I, Baer R. Formation of in vivo complexes between the TAL1 and E2A polypeptides of leukemic T cells. Proc Natl Acad Sci U S A. 1994;91:3181-3185.
39. Voronova AF, Lee F. The E2A and tal-1 helix-loop-helix proteins associate in vivo and are modulated by Id proteins during interleukin 6-induced myeloid differentiation. Proc Natl Acad Sci U S A. 1994;91:5952-5956.
40. Lecuyer E, Herblot S, Saint-Denis M, et al. The SCL complex regulates c-kit expression in hematopoietic cells through functional interaction with Sp1. Blood. 2002;100:2430-2440.
41. Valge-Archer VE, Osada H, Warren AJ, et al. The LIM protein RBTN2 and the basic helix-loop-helix protein TAL1 are present in a complex in erythroid cells. Proc Natl Acad Sci U S A. 1994;91:8617-8621.
42. Wadman IA, Osada H, Grutz GG, et al. The LIM-only protein Lmo2 is a bridging molecule assembling an erythroid, DNA-binding complex which includes the TAL1, E47, GATA-1 and Ldb1/NLI proteins. EMBO J. 1997;16:3145-3157.
43. Huang S, Qiu Y, Stein RW, Brandt SJ. p300 functions as a transcriptional coactivator for the TAL1/SCL oncoprotein. Oncogene. 1999;18:4958-4967.
44. Huang S, Qiu Y, Shi Y, Xu Z, Brandt SJ. P/CAF-mediated acetylation regulates the function of the basic helix-loop-helix transcription factor TAL1/SCL. EMBO J. 2000;19:6792-6803.
45. Huang S, Brandt SJ. mSin3A regulates murine erythroleukemia cell differentiation through association with the TAL1 (or SCL) transcription factor. Mol Cell Biol. 2000;20:2248-2259.
46. Fitzgerald TJ, Neale GA, Raimondi SC, Goorha RM. c-tal, a helix-loop-helix protein, is juxtaposed to the T-cell receptor-beta chain gene by a reciprocal chromosomal translocation: t(1;7)(p32;q35). Blood. 1991;78:2686-2695.

47. Aplan PD, Lombardi DP, Kirsch IR. Structural characterization of SIL, a gene frequently disrupted in T-cell acute lymphoblastic leukemia. Mol Cell Biol. 1991;11:5462-5469.
48. Aplan PD, Lombardi DP, Reaman GH, Sather HN, Hammond GD, Kirsch IR. Involvement of the putative hematopoietic transcription factor SCL in T-cell acute lymphoblastic leukemia. Blood. 1992;79:1327-1333.
49. Begley CG, Green AR. The SCL gene: from case report to critical hematopoietic regulator. Blood. 1999;93:2760-2770.
50. Bash RO, Hall S, Timmons CF, et al. Does activation of the TAL1 gene occur in a majority of patients with T-cell acute lymphoblastic leukemia? A pediatric oncology group study. Blood. 1995;86:666-676.
51. Aplan PD, Jones CA, Chervinsky DS, et al. An scl gene product lacking the transactivation domain induces bony abnormalities and cooperates with LMO1 to generate T-cell malignancies in transgenic mice. EMBO J. 1997;16:2408-2419.
52. Larson RC, Osada H, Larson TA, Lavenir I, Rabbitts TH. The oncogenic LIM protein Rbtn2 causes thymic developmental aberrations that precede malignancy in transgenic mice. Oncogene. 1995;11:853-862.
53. Robb L, Rasko JE, Bath ML, Strasser A, Begley CG. scl, a gene frequently activated in human T cell leukaemia, does not induce lymphomas in transgenic mice. Oncogene. 1995;10:205-209.
54. Goardon N, Schuh A, Hajar I, et al. Ectopic expression of TAL-1 protein in Ly-6E.1-htal-1 transgenic mice induces defects in B- and T-lymphoid differentiation. Blood. 2002;100:491-500.
55. Kelliher MA, Seldin DC, Leder P. Tal-1 induces T cell acute lymphoblastic leukemia accelerated by casein kinase IIalpha. EMBO J. 1996;15:5160-5166.
56. O'Neil J, Billa M, Oikemus S, Kelliher M. The DNA binding activity of TAL-1 is not required to induce leukemia/lymphoma in mice. Oncogene. 2001;20:3897-3905.
57. Rothenberg EV, Moore JE, Yui MA. Launching the T-cell-lineage developmental programme. Nat Rev Immunol. 2008;8:9-21.
58. O'Neil J, Shank J, Cusson N, Murre C, Kelliher M. TAL1/SCL induces leukemia by inhibiting the transcriptional activity of E47/HEB. Cancer Cell. 2004;5:587-596.
59. Sharma VM, Calvo JA, Draheim KM, et al. Notch1 contributes to mouse T-cell leukemia by directly inducing the expression of c-myc. Mol Cell Biol. 2006;26:8022-8031.
60. Larson RC, Lavenir I, Larson TA, et al. Protein dimerization between Lmo2 (Rbtn2) and Tal1 alters thymocyte development and potentiates T cell tumorigenesis in transgenic mice. EMBO J. 1996;15:1021-1027.
61. Shank-Calvo JA, Draheim K, Bhasin M, Kelliher MA. p16Ink4a or p19Arf loss contributes to Tal1-induced leukemogenesis in mice. Oncogene. 2006;25:3023-3031.
62. Chervinsky DS, Zhao XF, Lam DH, Ellsworth M, Gross KW, Aplan PD. Disordered T-cell development and T-cell malignancies in SCL LMO1 double-transgenic mice: parallels with E2A-deficient mice. Mol Cell Biol. 1999;19:5025-5035.
63. Wadman I, Li J, Bash RO, et al. Specific in vivo association between the bHLH and LIM proteins implicated in human T cell leukemia. EMBO J. 1994;13:4831-4839.

64. Boehm T, Foroni L, Kaneko Y, Perutz MF, Rabbitts TH. The rhombotin family of cysteine-rich LIM-domain oncogenes: distinct members are involved in T-cell translocations to human chromosomes 11p15 and 11p13. Proc Natl Acad Sci U S A. 1991;88:4367-4371.
65. Royer-Pokora B, Loos U, Ludwig WD. TTG-2, a new gene encoding a cysteine-rich protein with the LIM motif, is overexpressed in acute T-cell leukaemia with the t(11;14)(p13;q11). Oncogene. 1991;6:1887-1893.
66. Rabbitts TH. LMO T-cell translocation oncogenes typify genes activated by chromosomal translocations that alter transcription and developmental processes. Genes Dev. 1998;12:2651-2657.
67. Hacein-Bey-Abina S, von Kalle C, Schmidt M, et al. A serious adverse event after successful gene therapy for X-linked severe combined immunodeficiency. N Engl J Med. 2003;348:255-256.
68. Hacein-Bey-Abina S, Von Kalle C, Schmidt M, et al. LMO2-associated clonal T cell proliferation in two patients after gene therapy for SCID-X1. Science. 2003;302:415-419.
69. Osawa M, Hanada K, Hamada H, Nakauchi H. Long-term lymphohematopoietic reconstitution by a single CD34-low/negative hematopoietic stem cell. Science. 1996;273:242-245.
70. Cheshier SH, Morrison SJ, Liao X, Weissman IL. In vivo proliferation and cell cycle kinetics of long-term self-renewing hematopoietic stem cells. Proc Natl Acad Sci U S A. 1999;96:3120-3125.
71. Morrison SJ, Wandycz AM, Hemmati HD, Wright DE, Weissman IL. Identification of a lineage of multipotent hematopoietic progenitors. Development. 1997;124:1929-1939.
72. Kondo M, Weissman IL, Akashi K. Identification of clonogenic common lymphoid progenitors in mouse bone marrow. Cell. 1997;91:661-672.
73. Zuniga-Pflucker JC, Lenardo MJ. Regulation of thymocyte development from immature progenitors. Curr Opin Immunol. 1996;8:215-224.
74. Godfrey DI, Kennedy J, Suda T, Zlotnik A. A developmental pathway involving four phenotypically and functionally distinct subsets of CD3-CD4-CD8- triple-negative adult mouse thymocytes defined by CD44 and CD25 expression. J Immunol. 1993;150:4244-4252.
75. Benz C, Martins VC, Radtke F, Bleul CC. The stream of precursors that colonizes the thymus proceeds selectively through the early T lineage precursor stage of T cell development. J Exp Med. 2008;205:1187-1199.
76. Ceredig R, Rolink T. A positive look at double-negative thymocytes. Nat Rev Immunol. 2002;2:888-897.
77. Porritt HE, Rumfelt LL, Tabrizifard S, Schmitt TM, Zuniga-Pflucker JC, Petrie HT. Heterogeneity among DN1 prothymocytes reveals multiple progenitors with different capacities to generate T cell and non-T cell lineages. Immunity. 2004;20:735-745.
78. von Boehmer H, Fehling HJ. Structure and function of the pre-T cell receptor. Annu Rev Immunol. 1997;15:433-452.

79. Dudley EC, Petrie HT, Shah LM, Owen MJ, Hayday AC. T cell receptor beta chain gene rearrangement and selection during thymocyte development in adult mice. Immunity. 1994;1:83-93.
80. Saint-Ruf C, Ungewiss K, Groettrup M, Bruno L, Fehling HJ, von Boehmer H. Analysis and expression of a cloned pre-T cell receptor gene. Science. 1994;266:1208-1212.
81. Shinkai Y, Ma A, Cheng HL, Alt FW. CD3 epsilon and CD3 zeta cytoplasmic domains can independently generate signals for T cell development and function. Immunity. 1995;2:401-411.
82. Aifantis I, Gounari F, Scorrano L, Borowski C, von Boehmer H. Constitutive pre-TCR signaling promotes differentiation through Ca2+ mobilization and activation of NF-kappaB and NFAT. Nat Immunol. 2001;2:403-409.
83. Eyquem S, Chemin K, Fasseu M, Bories JC. The Ets-1 transcription factor is required for complete pre-T cell receptor function and allelic exclusion at the T cell receptor beta locus. Proc Natl Acad Sci U S A. 2004;101:15712-15717.
84. Michie AM, Zuniga-Pflucker JC. Regulation of thymocyte differentiation: pre-TCR signals and beta-selection. Semin Immunol. 2002;14:311-323.
85. Neilson JR, Winslow MM, Hur EM, Crabtree GR. Calcineurin B1 is essential for positive but not negative selection during thymocyte development. Immunity. 2004;20:255-266.
86. Voll RE, Jimi E, Phillips RJ, et al. NF-kappa B activation by the pre-T cell receptor serves as a selective survival signal in T lymphocyte development. Immunity. 2000;13:677-689.
87. Fehling HJ, Krotkova A, Saint-Ruf C, von Boehmer H. Crucial role of the pre-T-cell receptor alpha gene in development of alpha beta but not gamma delta T cells. Nature. 1995;375:795-798.
88. Mallick CA, Dudley EC, Viney JL, Owen MJ, Hayday AC. Rearrangement and diversity of T cell receptor beta chain genes in thymocytes: a critical role for the beta chain in development. Cell. 1993;73:513-519.
89. von Boehmer H, Bonneville M, Ishida I, et al. Early expression of a T-cell receptor beta-chain transgene suppresses rearrangement of the V gamma 4 gene segment. Proc Natl Acad Sci U S A. 1988;85:9729-9732.
90. Villa N, Walker L, Lindsell CE, Gasson J, Iruela-Arispe ML, Weinmaster G. Vascular expression of Notch pathway receptors and ligands is restricted to arterial vessels. Mech Dev. 2001;108:161-164.
91. Kisielow P, Miazek A. Positive selection of T cells: rescue from programmed cell death and differentiation require continual engagement of the T cell receptor. J Exp Med. 1995;181:1975-1984.
92. Kisielow P, von Boehmer H. Development and selection of T cells: facts and puzzles. Adv Immunol. 1995;58:87-209.
93. Surh CD, Sprent J. T-cell apoptosis detected in situ during positive and negative selection in the thymus. Nature. 1994;372:100-103.
94. Allman D, Aster JC, Pear WS. Notch signaling in hematopoiesis and early lymphocyte development. Immunol Rev. 2002;187:75-86.

95. Han H, Tanigaki K, Yamamoto N, et al. Inducible gene knockout of transcription factor recombination signal binding protein-J reveals its essential role in T versus B lineage decision. Int Immunol. 2002;14:637-645.
96. Radtke F, Wilson A, Stark G, et al. Deficient T cell fate specification in mice with an induced inactivation of Notch1. Immunity. 1999;10:547-558.
97. Wolfer A, Bakker T, Wilson A, et al. Inactivation of Notch 1 in immature thymocytes does not perturb CD4 or CD8T cell development. Nat Immunol. 2001;2:235-241.
98. Doerfler P, Shearman MS, Perlmutter RM. Presenilin-dependent gamma-secretase activity modulates thymocyte development. Proc Natl Acad Sci U S A. 2001;98:9312-9317.
99. Hadland BK, Manley NR, Su D, et al. Gamma -secretase inhibitors repress thymocyte development. Proc Natl Acad Sci U S A. 2001;98:7487-7491.
100. Pui JC, Allman D, Xu L, et al. Notch1 expression in early lymphopoiesis influences B versus T lineage determination. Immunity. 1999;11:299-308.
101. Jaleco AC, Neves H, Hooijberg E, et al. Differential effects of Notch ligands Delta-1 and Jagged-1 in human lymphoid differentiation. J Exp Med. 2001;194:991-1002.
102. Schmitt TM, Zuniga-Pflucker JC. Induction of T cell development from hematopoietic progenitor cells by delta-like-1 in vitro. Immunity. 2002;17:749-756.
103. Kawamata S, Du C, Li K, Lavau C. Overexpression of the Notch target genes Hes in vivo induces lymphoid and myeloid alterations. Oncogene. 2002;21:3855-3863.
104. Anderson G, Pongracz J, Parnell S, Jenkinson EJ. Notch ligand-bearing thymic epithelial cells initiate and sustain Notch signaling in thymocytes independently of T cell receptor signaling. Eur J Immunol. 2001;31:3349-3354.
105. Felli MP, Maroder M, Mitsiadis TA, et al. Expression pattern of notch1, 2 and 3 and Jagged1 and 2 in lymphoid and stromal thymus components: distinct ligand-receptor interactions in intrathymic T cell development. Int Immunol. 1999;11:1017-1025.
106. Harman BC, Jenkinson EJ, Anderson G. Entry into the thymic microenvironment triggers Notch activation in the earliest migrant T cell progenitors. J Immunol. 2003;170:1299-1303.
107. Hasserjian RP, Aster JC, Davi F, Weinberg DS, Sklar J. Modulated expression of notch1 during thymocyte development. Blood. 1996;88:970-976.
108. Milner LA, Kopan R, Martin DI, Bernstein ID. A human homologue of the Drosophila developmental gene, Notch, is expressed in CD34+ hematopoietic precursors. Blood. 1994;83:2057-2062.
109. Vercauteren SM, Sutherland HJ. Constitutively active Notch4 promotes early human hematopoietic progenitor cell maintenance while inhibiting differentiation and causes lymphoid abnormalities in vivo. Blood. 2004;104:2315-2322.
110. Allman D, Sambandam A, Kim S, et al. Thymopoiesis independent of common lymphoid progenitors. Nat Immunol. 2003;4:168-174.
111. Balciunaite G, Ceredig R, Rolink AG. The earliest subpopulation of mouse thymocytes contains potent T, significant macrophage, and natural killer cell but no B-lymphocyte potential. Blood. 2005;105:1930-1936.

112. Sambandam A, Maillard I, Zediak VP, et al. Notch signaling controls the generation and differentiation of early T lineage progenitors. Nat Immunol. 2005;6:663-670.
113. Tan JB, Visan I, Yuan JS, Guidos CJ. Requirement for Notch1 signals at sequential early stages of intrathymic T cell development. Nat Immunol. 2005;6:671-679.
114. Yashiro-Ohtani Y, He Y, Ohtani T, et al. Pre-TCR signaling inactivates Notch1 transcription by antagonizing E2A. Genes Dev. 2009;23:1665-1676.
115. Maillard I, Tu L, Sambandam A, et al. The requirement for Notch signaling at the beta-selection checkpoint in vivo is absolute and independent of the pre-T cell receptor. J Exp Med. 2006;203:2239-2245.
116. Tanigaki K, Tsuji M, Yamamoto N, et al. Regulation of alphabeta/gammadelta T cell lineage commitment and peripheral T cell responses by Notch/RBP-J signaling. Immunity. 2004;20:611-622.
117. Wolfer A, Wilson A, Nemir M, MacDonald HR, Radtke F. Inactivation of Notch1 impairs VDJbeta rearrangement and allows pre-TCR-independent survival of early alpha beta Lineage Thymocytes. Immunity. 2002;16:869-879.
118. Ciofani M, Zuniga-Pflucker JC. Notch promotes survival of pre-T cells at the beta-selection checkpoint by regulating cellular metabolism. Nat Immunol. 2005;6:881-888.
119. Garcia-Peydro M, de Yebenes VG, Toribio ML. Sustained Notch1 signaling instructs the earliest human intrathymic precursors to adopt a gammadelta T-cell fate in fetal thymus organ culture. Blood. 2003;102:2444-2451.
120. Washburn T, Schweighoffer E, Gridley T, et al. Notch activity influences the alphabeta versus gammadelta T cell lineage decision. Cell. 1997;88:833-843.
121. Deftos ML, Huang E, Ojala EW, Forbush KA, Bevan MJ. Notch1 signaling promotes the maturation of CD4 and CD8 SP thymocytes. Immunity. 2000;13:73-84.
122. Robey E, Chang D, Itano A, et al. An activated form of Notch influences the choice between CD4 and CD8 T cell lineages. Cell. 1996;87:483-492.
123. Witt CM, Hurez V, Swindle CS, Hamada Y, Klug CA. Activated Notch2 potentiates CD8 lineage maturation and promotes the selective development of B1 B cells. Mol Cell Biol. 2003;23:8637-8650.
124. Amsen D, Antov A, Jankovic D, et al. Direct regulation of Gata3 expression determines the T helper differentiation potential of Notch. Immunity. 2007;27:89-99.
125. Fang TC, Yashiro-Ohtani Y, Del Bianco C, Knoblock DM, Blacklow SC, Pear WS. Notch directly regulates Gata3 expression during T helper 2 cell differentiation. Immunity. 2007;27:100-110.
126. Skokos D, Nussenzweig MC. CD8- DCs induce IL-12-independent Th1 differentiation through Delta 4 Notch-like ligand in response to bacterial LPS. J Exp Med. 2007;204:1525-1531.
127. Minter LM, Turley DM, Das P, et al. Inhibitors of gamma-secretase block in vivo and in vitro T helper type 1 polarization by preventing Notch upregulation of Tbx21. Nat Immunol. 2005;6:680-688.
128. Bellavia D, Campese AF, Alesse E, et al. Constitutive activation of NF-kappaB and T-cell leukemia/lymphoma in Notch3 transgenic mice. EMBO J. 2000;19:3337-3348.

129. Krebs LT, Xue Y, Norton CR, et al. Characterization of Notch3-deficient mice: normal embryonic development and absence of genetic interactions with a Notch1 mutation. Genesis. 2003;37:139-143.
130. Saito T, Chiba S, Ichikawa M, et al. Notch2 is preferentially expressed in mature B cells and indispensable for marginal zone B lineage development. Immunity. 2003;18:675-685.
131. Morgan JF. Soil Solution. Science. 1917;45:19.
132. Artavanis-Tsakonas S, Rand MD, Lake RJ. Notch signaling: cell fate control and signal integration in development. Science. 1999;284:770-776.
133. Lubman OY, Korolev SV, Kopan R. Anchoring notch genetics and biochemistry; structural analysis of the ankyrin domain sheds light on existing data. Mol Cell. 2004;13:619-626.
134. Lissemore JL, Starmer WT. Phylogenetic analysis of vertebrate and invertebrate Delta/Serrate/LAG-2 (DSL) proteins. Mol Phylogenet Evol. 1999;11:308-319.
135. Fitzgerald K, Wilkinson HA, Greenwald I. glp-1 can substitute for lin-12 in specifying cell fate decisions in Caenorhabditis elegans. Development. 1993;119:1019-1027.
136. Logeat F, Bessia C, Brou C, et al. The Notch1 receptor is cleaved constitutively by a furin-like convertase. Proc Natl Acad Sci U S A. 1998;95:8108-8112.
137. Rebay I, Fleming RJ, Fehon RG, Cherbas L, Cherbas P, Artavanis-Tsakonas S. Specific EGF repeats of Notch mediate interactions with Delta and Serrate: implications for Notch as a multifunctional receptor. Cell. 1991;67:687-699.
138. Kurooka H, Kuroda K, Honjo T. Roles of the ankyrin repeats and C-terminal region of the mouse notch1 intracellular region. Nucleic Acids Res. 1998;26:5448-5455.
139. Lubman OY, Ilagan MX, Kopan R, Barrick D. Quantitative dissection of the Notch:CSL interaction: insights into the Notch-mediated transcriptional switch. J Mol Biol. 2007;365:577-589.
140. Petcherski AG, Kimble J. Mastermind is a putative activator for Notch. Curr Biol. 2000;10:R471-473.
141. Tamura K, Taniguchi Y, Minoguchi S, et al. Physical interaction between a novel domain of the receptor Notch and the transcription factor RBP-J kappa/Su(H). Curr Biol. 1995;5:1416-1423.
142. Beatus P, Lundkvist J, Oberg C, Pedersen K, Lendahl U. The origin of the ankyrin repeat region in Notch intracellular domains is critical for regulation of HES promoter activity. Mech Dev. 2001;104:3-20.
143. Rechsteiner M. Regulation of enzyme levels by proteolysis: the role of pest regions. Adv Enzyme Regul. 1988;27:135-151.
144. Bettenhausen B, Hrabe de Angelis M, Simon D, Guenet JL, Gossler A. Transient and restricted expression during mouse embryogenesis of Dll1, a murine gene closely related to Drosophila Delta. Development. 1995;121:2407-2418.
145. Lindsell CE, Shawber CJ, Boulter J, Weinmaster G. Jagged: a mammalian ligand that activates Notch1. Cell. 1995;80:909-917.

146. Vooijs M, Schroeter EH, Pan Y, Blandford M, Kopan R. Ectodomain shedding and intramembrane cleavage of mammalian Notch proteins is not regulated through oligomerization. J Biol Chem. 2004;279:50864-50873.
147. Brou C, Logeat F, Gupta N, et al. A novel proteolytic cleavage involved in Notch signaling: the role of the disintegrin-metalloprotease TACE. Mol Cell. 2000;5:207-216.
148. De Strooper B, Annaert W, Cupers P, et al. A presenilin-1-dependent gamma-secretase-like protease mediates release of Notch intracellular domain. Nature. 1999;398:518-522.
149. De Strooper B. Aph-1, Pen-2, and Nicastrin with Presenilin generate an active gamma-Secretase complex. Neuron. 2003;38:9-12.
150. Fortini ME. Gamma-secretase-mediated proteolysis in cell-surface-receptor signalling. Nat Rev Mol Cell Biol. 2002;3:673-684.
151. Francis R, McGrath G, Zhang J, et al. aph-1 and pen-2 are required for Notch pathway signaling, gamma-secretase cleavage of betaAPP, and presenilin protein accumulation. Dev Cell. 2002;3:85-97.
152. Yu G, Nishimura M, Arawaka S, et al. Nicastrin modulates presenilin-mediated notch/glp-1 signal transduction and betaAPP processing. Nature. 2000;407:48-54.
153. Oswald F, Tauber B, Dobner T, et al. p300 acts as a transcriptional coactivator for mammalian Notch-1. Mol Cell Biol. 2001;21:7761-7774.
154. Wu L, Sun T, Kobayashi K, Gao P, Griffin JD. Identification of a family of mastermind-like transcriptional coactivators for mammalian notch receptors. Mol Cell Biol. 2002;22:7688-7700.
155. Hsieh JJ, Zhou S, Chen L, Young DB, Hayward SD. CIR, a corepressor linking the DNA binding factor CBF1 to the histone deacetylase complex. Proc Natl Acad Sci U S A. 1999;96:23-28.
156. Kao HY, Ordentlich P, Koyano-Nakagawa N, et al. A histone deacetylase corepressor complex regulates the Notch signal transduction pathway. Genes Dev. 1998;12:2269-2277.
157. Taniguchi Y, Furukawa T, Tun T, Han H, Honjo T. LIM protein KyoT2 negatively regulates transcription by association with the RBP-J DNA-binding protein. Mol Cell Biol. 1998;18:644-654.
158. Laherty CD, Billin AN, Lavinsky RM, et al. SAP30, a component of the mSin3 corepressor complex involved in N-CoR-mediated repression by specific transcription factors. Mol Cell. 1998;2:33-42.
159. Waltzer L, Bourillot PY, Sergeant A, Manet E. RBP-J kappa repression activity is mediated by a co-repressor and antagonized by the Epstein-Barr virus transcription factor EBNA2. Nucleic Acids Res. 1995;23:4939-4945.
160. Zhou S, Fujimuro M, Hsieh JJ, et al. SKIP, a CBF1-associated protein, interacts with the ankyrin repeat domain of NotchIC To facilitate NotchIC function. Mol Cell Biol. 2000;20:2400-2410.
161. Hsieh JJ, Henkel T, Salmon P, Robey E, Peterson MG, Hayward SD. Truncated mammalian Notch1 activates CBF1/RBPJk-repressed genes by a mechanism resembling that of Epstein-Barr virus EBNA2. Mol Cell Biol. 1996;16:952-959.

162. Maillard I, Fang T, Pear WS. Regulation of lymphoid development, differentiation, and function by the Notch pathway. Annu Rev Immunol. 2005;23:945-974.
163. Weng AP, Millholland JM, Yashiro-Ohtani Y, et al. c-Myc is an important direct target of Notch1 in T-cell acute lymphoblastic leukemia/lymphoma. Genes Dev. 2006;20:2096-2109.
164. Joshi I, Minter LM, Telfer J, et al. Notch signaling mediates G1/S cell-cycle progression in T cells via cyclin D3 and its dependent kinases. Blood. 2009;113:1689-1698.
165. Moloney DJ, Panin VM, Johnston SH, et al. Fringe is a glycosyltransferase that modifies Notch. Nature. 2000;406:369-375.
166. Yang LT, Nichols JT, Yao C, Manilay JO, Robey EA, Weinmaster G. Fringe glycosyltransferases differentially modulate Notch1 proteolysis induced by Delta1 and Jagged1. Mol Biol Cell. 2005;16:927-942.
167. Hicks C, Johnston SH, diSibio G, Collazo A, Vogt TF, Weinmaster G. Fringe differentially modulates Jagged1 and Delta1 signalling through Notch1 and Notch2. Nat Cell Biol. 2000;2:515-520.
168. Qiu L, Joazeiro C, Fang N, et al. Recognition and ubiquitination of Notch by Itch, a hect-type E3 ubiquitin ligase. J Biol Chem. 2000;275:35734-35737.
169. Wilkin MB, Carbery AM, Fostier M, et al. Regulation of notch endosomal sorting and signaling by Drosophila Nedd4 family proteins. Curr Biol. 2004;14:2237-2244.
170. McGill MA, McGlade CJ. Mammalian numb proteins promote Notch1 receptor ubiquitination and degradation of the Notch1 intracellular domain. J Biol Chem. 2003;278:23196-23203.
171. Nakayama KI, Nakayama K. Regulation of the cell cycle by SCF-type ubiquitin ligases. Semin Cell Dev Biol. 2005;16:323-333.
172. Nash P, Tang X, Orlicky S, et al. Multisite phosphorylation of a CDK inhibitor sets a threshold for the onset of DNA replication. Nature. 2001;414:514-521.
173. Orlicky S, Tang X, Willems A, Tyers M, Sicheri F. Structural basis for phosphodependent substrate selection and orientation by the SCFCdc4 ubiquitin ligase. Cell. 2003;112:243-256.
174. Fryer CJ, White JB, Jones KA. Mastermind recruits CycC:CDK8 to phosphorylate the Notch ICD and coordinate activation with turnover. Mol Cell. 2004;16:509-520.
175. Gupta-Rossi N, Le Bail O, Gonen H, et al. Functional interaction between SEL-10, an F-box protein, and the nuclear form of activated Notch1 receptor. J Biol Chem. 2001;276:34371-34378.
176. Oberg C, Li J, Pauley A, Wolf E, Gurney M, Lendahl U. The Notch intracellular domain is ubiquitinated and negatively regulated by the mammalian Sel-10 homolog. J Biol Chem. 2001;276:35847-35853.
177. Tetzlaff MT, Yu W, Li M, et al. Defective cardiovascular development and elevated cyclin E and Notch proteins in mice lacking the Fbw7 F-box protein. Proc Natl Acad Sci U S A. 2004;101:3338-3345.

178. Tsunematsu R, Nakayama K, Oike Y, et al. Mouse Fbw7/Sel-10/Cdc4 is required for notch degradation during vascular development. J Biol Chem. 2004;279:9417-9423.
179. Wu G, Lyapina S, Das I, et al. SEL-10 is an inhibitor of notch signaling that targets notch for ubiquitin-mediated protein degradation. Mol Cell Biol. 2001;21:7403-7415.
180. Mao JH, Kim IJ, Wu D, et al. FBXW7 targets mTOR for degradation and cooperates with PTEN in tumor suppression. Science. 2008;321:1499-1502.
181. Mao JH, Perez-Losada J, Wu D, et al. Fbxw7/Cdc4 is a p53-dependent, haploinsufficient tumour suppressor gene. Nature. 2004;432:775-779.
182. Minella AC, Clurman BE. Mechanisms of tumor suppression by the SCF(Fbw7). Cell Cycle. 2005;4:1356-1359.
183. Wu J, Bresnick EH. Bare rudiments of notch signaling: how receptor levels are regulated. Trends Biochem Sci. 2007;32:477-485.
184. Hamada Y, Kadokawa Y, Okabe M, Ikawa M, Coleman JR, Tsujimoto Y. Mutation in ankyrin repeats of the mouse Notch2 gene induces early embryonic lethality. Development. 1999;126:3415-3424.
185. Swiatek PJ, Lindsell CE, del Amo FF, Weinmaster G, Gridley T. Notch1 is essential for postimplantation development in mice. Genes Dev. 1994;8:707-719.
186. Hrabe de Angelis M, McIntyre J, 2nd, Gossler A. Maintenance of somite borders in mice requires the Delta homologue DII1. Nature. 1997;386:717-721.
187. Xue Y, Gao X, Lindsell CE, et al. Embryonic lethality and vascular defects in mice lacking the Notch ligand Jagged1. Hum Mol Genet. 1999;8:723-730.
188. Domenga V, Fardoux P, Lacombe P, et al. Notch3 is required for arterial identity and maturation of vascular smooth muscle cells. Genes Dev. 2004;18:2730-2735.
189. Oda T, Elkahloun AG, Pike BL, et al. Mutations in the human Jagged1 gene are responsible for Alagille syndrome. Nat Genet. 1997;16:235-242.
190. Joutel A, Corpechot C, Ducros A, et al. Notch3 mutations in CADASIL, a hereditary adult-onset condition causing stroke and dementia. Nature. 1996;383:707-710.
191. Joutel A, Monet M, Domenga V, Riant F, Tournier-Lasserve E. Pathogenic mutations associated with cerebral autosomal dominant arteriopathy with subcortical infarcts and leukoencephalopathy differently affect Jagged1 binding and Notch3 activity via the RBP/JK signaling Pathway. Am J Hum Genet. 2004;74:338-347.
192. Pan Y, Lin MH, Tian X, et al. gamma-secretase functions through Notch signaling to maintain skin appendages but is not required for their patterning or initial morphogenesis. Dev Cell. 2004;7:731-743.
193. Vauclair S, Nicolas M, Barrandon Y, Radtke F. Notch1 is essential for postnatal hair follicle development and homeostasis. Dev Biol. 2005;284:184-193.
194. Yamamoto N, Tanigaki K, Han H, Hiai H, Honjo T. Notch/RBP-J signaling regulates epidermis/hair fate determination of hair follicular stem cells. Curr Biol. 2003;13:333-338.
195. Thurston G, Gale NW. Vascular endothelial growth factor and other signaling pathways in developmental and pathologic angiogenesis. Int J Hematol. 2004;80:7-20.
196. Zhong TP, Childs S, Leu JP, Fishman MC. Gridlock signalling pathway fashions the first embryonic artery. Nature. 2001;414:216-220.

197. Lawson ND, Scheer N, Pham VN, et al. Notch signaling is required for arterial-venous differentiation during embryonic vascular development. Development. 2001;128:3675-3683.
198. Krebs LT, Shutter JR, Tanigaki K, Honjo T, Stark KL, Gridley T. Haploinsufficient lethality and formation of arteriovenous malformations in Notch pathway mutants. Genes Dev. 2004;18:2469-2473.
199. Jensen J, Pedersen EE, Galante P, et al. Control of endodermal endocrine development by Hes-1. Nat Genet. 2000;24:36-44.
200. Real PJ, Tosello V, Palomero T, et al. Gamma-secretase inhibitors reverse glucocorticoid resistance in T cell acute lymphoblastic leukemia. Nat Med. 2009;15:50-58.
201. van Es JH, van Gijn ME, Riccio O, et al. Notch/gamma-secretase inhibition turns proliferative cells in intestinal crypts and adenomas into goblet cells. Nature. 2005;435:959-963.
202. Passegue E, Jamieson CH, Ailles LE, Weissman IL. Normal and leukemic hematopoiesis: are leukemias a stem cell disorder or a reacquisition of stem cell characteristics? Proc Natl Acad Sci U S A. 2003;100 Suppl 1:11842-11849.
203. Fre S, Huyghe M, Mourikis P, Robine S, Louvard D, Artavanis-Tsakonas S. Notch signals control the fate of immature progenitor cells in the intestine. Nature. 2005;435:964-968.
204. Hitoshi S, Alexson T, Tropepe V, et al. Notch pathway molecules are essential for the maintenance, but not the generation, of mammalian neural stem cells. Genes Dev. 2002;16:846-858.
205. Hitoshi S, Seaberg RM, Koscik C, et al. Primitive neural stem cells from the mammalian epiblast differentiate to definitive neural stem cells under the control of Notch signaling. Genes Dev. 2004;18:1806-1811.
206. Shen Q, Goderie SK, Jin L, et al. Endothelial cells stimulate self-renewal and expand neurogenesis of neural stem cells. Science. 2004;304:1338-1340.
207. Hadland BK, Huppert SS, Kanungo J, et al. A requirement for Notch1 distinguishes 2 phases of definitive hematopoiesis during development. Blood. 2004;104:3097-3105.
208. Kumano K, Chiba S, Kunisato A, et al. Notch1 but not Notch2 is essential for generating hematopoietic stem cells from endothelial cells. Immunity. 2003;18:699-711.
209. Robert-Moreno A, Espinosa L, de la Pompa JL, Bigas A. RBPjkappa-dependent Notch function regulates Gata2 and is essential for the formation of intra-embryonic hematopoietic cells. Development. 2005;132:1117-1126.
210. Reya T, Duncan AW, Ailles L, et al. A role for Wnt signalling in self-renewal of haematopoietic stem cells. Nature. 2003;423:409-414.
211. Varnum-Finney B, Xu L, Brashem-Stein C, et al. Pluripotent, cytokine-dependent, hematopoietic stem cells are immortalized by constitutive Notch1 signaling. Nat Med. 2000;6:1278-1281.
212. Maillard I, Koch U, Dumortier A, et al. Canonical notch signaling is dispensable for the maintenance of adult hematopoietic stem cells. Cell Stem Cell. 2008;2:356-366.

213. Mancini SJ, Mantei N, Dumortier A, Suter U, MacDonald HR, Radtke F. Jagged1-dependent Notch signaling is dispensable for hematopoietic stem cell self-renewal and differentiation. Blood. 2005;105:2340-2342.
214. Ellisen LW, Bird J, West DC, et al. TAN-1, the human homolog of the Drosophila notch gene, is broken by chromosomal translocations in T lymphoblastic neoplasms. Cell. 1991;66:649-661.
215. Capobianco AJ, Zagouras P, Blaumueller CM, Artavanis-Tsakonas S, Bishop JM. Neoplastic transformation by truncated alleles of human NOTCH1/TAN1 and NOTCH2. Mol Cell Biol. 1997;17:6265-6273.
216. Pear WS, Aster JC, Scott ML, et al. Exclusive development of T cell neoplasms in mice transplanted with bone marrow expressing activated Notch alleles. J Exp Med. 1996;183:2283-2291.
217. Beverly LJ, Capobianco AJ. Perturbation of Ikaros isoform selection by MLV integration is a cooperative event in Notch(IC)-induced T cell leukemogenesis. Cancer Cell. 2003;3:551-564.
218. Aster JC, Xu L, Karnell FG, Patriub V, Pui JC, Pear WS. Essential roles for ankyrin repeat and transactivation domains in induction of T-cell leukemia by notch1. Mol Cell Biol. 2000;20:7505-7515.
219. Malyukova A, Dohda T, von der Lehr N, et al. The tumor suppressor gene hCDC4 is frequently mutated in human T-cell acute lymphoblastic leukemia with functional consequences for Notch signaling. Cancer Res. 2007;67:5611-5616.
220. Maser RS, Choudhury B, Campbell PJ, et al. Chromosomally unstable mouse tumours have genomic alterations similar to diverse human cancers. Nature. 2007;447:966-971.
221. O'Neil J, Grim J, Strack P, et al. FBW7 mutations in leukemic cells mediate NOTCH pathway activation and resistance to gamma-secretase inhibitors. J Exp Med. 2007;204:1813-1824.
222. Thompson BJ, Buonamici S, Sulis ML, et al. The SCFFBW7 ubiquitin ligase complex as a tumor suppressor in T cell leukemia. J Exp Med. 2007;204:1825-1835.
223. Sulis ML, Williams O, Palomero T, et al. NOTCH1 extracellular juxtamembrane expansion mutations in T-ALL. Blood. 2008;112:733-740.
224. Weng AP, Ferrando AA, Lee W, et al. Activating mutations of NOTCH1 in human T cell acute lymphoblastic leukemia. Science. 2004;306:269-271.
225. Malecki MJ, Sanchez-Irizarry C, Mitchell JL, et al. Leukemia-associated mutations within the NOTCH1 heterodimerization domain fall into at least two distinct mechanistic classes. Mol Cell Biol. 2006;26:4642-4651.
226. Chiang MY, Xu L, Shestova O, et al. Leukemia-associated NOTCH1 alleles are weak tumor initiators but accelerate K-ras-initiated leukemia. J Clin Invest. 2008;118:3181-3194.
227. Bellavia D, Campese AF, Checquolo S, et al. Combined expression of pTalpha and Notch3 in T cell leukemia identifies the requirement of preTCR for leukemogenesis. Proc Natl Acad Sci U S A. 2002;99:3788-3793.

228. Dumortier A, Jeannet R, Kirstetter P, et al. Notch activation is an early and critical event during T-Cell leukemogenesis in Ikaros-deficient mice. Mol Cell Biol. 2006;26:209-220.
229. Lin YW, Nichols RA, Letterio JJ, Aplan PD. Notch1 mutations are important for leukemic transformation in murine models of precursor-T leukemia/lymphoma. Blood. 2006;107:2540-2543.
230. O'Neil J, Calvo J, McKenna K, et al. Activating Notch1 mutations in mouse models of T-ALL. Blood. 2006;107:781-785.
231. Reschly EJ, Spaulding C, Vilimas T, et al. Notch1 promotes survival of E2A-deficient T cell lymphomas through pre-T cell receptor-dependent and -independent mechanisms. Blood. 2006;107:4115-4121.
232. Lewis HD, Leveridge M, Strack PR, et al. Apoptosis in T cell acute lymphoblastic leukemia cells after cell cycle arrest induced by pharmacological inhibition of notch signaling. Chem Biol. 2007;14:209-219.
233. Weng AP, Nam Y, Wolfe MS, et al. Growth suppression of pre-T acute lymphoblastic leukemia cells by inhibition of notch signaling. Mol Cell Biol. 2003;23:655-664.
234. Cowan JW, Wang X, Guan R, et al. Growth hormone receptor is a target for presenilin-dependent gamma-secretase cleavage. J Biol Chem. 2005;280:19331-19342.
235. Hass MR, Yankner BA. A {gamma}-secretase-independent mechanism of signal transduction by the amyloid precursor protein. J Biol Chem. 2005;280:36895-36904.
236. Lammich S, Okochi M, Takeda M, et al. Presenilin-dependent intramembrane proteolysis of CD44 leads to the liberation of its intracellular domain and the secretion of an Abeta-like peptide. J Biol Chem. 2002;277:44754-44759.
237. Ni CY, Murphy MP, Golde TE, Carpenter G. gamma -Secretase cleavage and nuclear localization of ErbB-4 receptor tyrosine kinase. Science. 2001;294:2179-2181.
238. Palomero T, Lim WK, Odom DT, et al. NOTCH1 directly regulates c-MYC and activates a feed-forward-loop transcriptional network promoting leukemic cell growth. Proc Natl Acad Sci U S A. 2006;103:18261-18266.
239. Li X, Gounari F, Protopopov A, Khazaie K, von Boehmer H. Oncogenesis of T-ALL and nonmalignant consequences of overexpressing intracellular NOTCH1. J Exp Med. 2008;205:2851-2861.
240. Barata JT, Cardoso AA, Nadler LM, Boussiotis VA. Interleukin-7 promotes survival and cell cycle progression of T-cell acute lymphoblastic leukemia cells by down-regulating the cyclin-dependent kinase inhibitor p27(kip1). Blood. 2001;98:1524-1531.
241. Travis A, Amsterdam A, Belanger C, Grosschedl R. LEF-1, a gene encoding a lymphoid-specific protein with an HMG domain, regulates T-cell receptor alpha enhancer function [corrected]. Genes Dev. 1991;5:880-894.
242. Waterman ML, Fischer WH, Jones KA. A thymus-specific member of the HMG protein family regulates the human T cell receptor C alpha enhancer. Genes Dev. 1991;5:656-669.
243. Hurlstone A, Clevers H. T-cell factors: turn-ons and turn-offs. EMBO J. 2002;21:2303-2311.

244. Kobielak A, Kobielak K, Trzeciak WH. A novel isoform of human lymphoid enhancer-binding factor-1 (LEF-1) gene transcript encodes a protein devoid of HMG domain and nuclear localization signal. Acta Biochim Pol. 2001;48:221-226.
245. Clevers H. Wnt/beta-catenin signaling in development and disease. Cell. 2006;127:469-480.
246. Cavallo RA, Cox RT, Moline MM, et al. Drosophila Tcf and Groucho interact to repress Wingless signalling activity. Nature. 1998;395:604-608.
247. Levanon D, Goldstein RE, Bernstein Y, et al. Transcriptional repression by AML1 and LEF-1 is mediated by the TLE/Groucho corepressors. Proc Natl Acad Sci U S A. 1998;95:11590-11595.
248. Staal FJ, Clevers HC. WNT signalling and haematopoiesis: a WNT-WNT situation. Nat Rev Immunol. 2005;5:21-30.
249. Giese K, Kingsley C, Kirshner JR, Grosschedl R. Assembly and function of a TCR alpha enhancer complex is dependent on LEF-1-induced DNA bending and multiple protein-protein interactions. Genes Dev. 1995;9:995-1008.
250. He TC, Sparks AB, Rago C, et al. Identification of c-MYC as a target of the APC pathway. Science. 1998;281:1509-1512.
251. Jung HC, Kim K. Identification of MYCBP as a beta-catenin/LEF-1 target using DNA microarray analysis. Life Sci. 2005;77:1249-1262.
252. Shtutman M, Zhurinsky J, Simcha I, et al. The cyclin D1 gene is a target of the beta-catenin/LEF-1 pathway. Proc Natl Acad Sci U S A. 1999;96:5522-5527.
253. Tapia JC, Torres VA, Rodriguez DA, Leyton L, Quest AF. Casein kinase 2 (CK2) increases survivin expression via enhanced beta-catenin-T cell factor/lymphoid enhancer binding factor-dependent transcription. Proc Natl Acad Sci U S A. 2006;103:15079-15084.
254. Reya T, O'Riordan M, Okamura R, et al. Wnt signaling regulates B lymphocyte proliferation through a LEF-1 dependent mechanism. Immunity. 2000;13:15-24.
255. van Genderen C, Okamura RM, Farinas I, et al. Development of several organs that require inductive epithelial-mesenchymal interactions is impaired in LEF-1-deficient mice. Genes Dev. 1994;8:2691-2703.
256. Zhou P, Byrne C, Jacobs J, Fuchs E. Lymphoid enhancer factor 1 directs hair follicle patterning and epithelial cell fate. Genes Dev. 1995;9:700-713.
257. Okamura RM, Sigvardsson M, Galceran J, Verbeek S, Clevers H, Grosschedl R. Redundant regulation of T cell differentiation and TCRalpha gene expression by the transcription factors LEF-1 and TCF-1. Immunity. 1998;8:11-20.
258. Petropoulos K, Arseni N, Schessl C, et al. A novel role for Lef-1, a central transcription mediator of Wnt signaling, in leukemogenesis. J Exp Med. 2008;205:515-522.
259. Wang W, Ji P, Steffen B, et al. Alterations of lymphoid enhancer factor-1 isoform expression in solid tumors and acute leukemias. Acta Biochim Biophys Sin (Shanghai). 2005;37:173-180.
260. Cantrell DA. Phosphoinositide 3-kinase signalling pathways. J Cell Sci. 2001;114:1439-1445.

261. Vanhaesebroeck B, Leevers SJ, Ahmadi K, et al. Synthesis and function of 3-phosphorylated inositol lipids. Annu Rev Biochem. 2001;70:535-602.
262. Damen JE, Liu L, Rosten P, et al. The 145-kDa protein induced to associate with Shc by multiple cytokines is an inositol tetraphosphate and phosphatidylinositol 3,4,5-triphosphate 5-phosphatase. Proc Natl Acad Sci U S A. 1996;93:1689-1693.
263. Lioubin MN, Algate PA, Tsai S, Carlberg K, Aebersold A, Rohrschneider LR. p150Ship, a signal transduction molecule with inositol polyphosphate-5-phosphatase activity. Genes Dev. 1996;10:1084-1095.
264. Alessi DR, Caudwell FB, Andjelkovic M, Hemmings BA, Cohen P. Molecular basis for the substrate specificity of protein kinase B; comparison with MAPKAP kinase-1 and p70 S6 kinase. FEBS Lett. 1996;399:333-338.
265. Klippel A, Kavanaugh WM, Pot D, Williams LT. A specific product of phosphatidylinositol 3-kinase directly activates the protein kinase Akt through its pleckstrin homology domain. Mol Cell Biol. 1997;17:338-344.
266. Stokoe D, Stephens LR, Copeland T, et al. Dual role of phosphatidylinositol-3,4,5-trisphosphate in the activation of protein kinase B. Science. 1997;277:567-570.
267. Toker A, Cantley LC. Signalling through the lipid products of phosphoinositide-3-OH kinase. Nature. 1997;387:673-676.
268. Toker A, Newton AC. Akt/protein kinase B is regulated by autophosphorylation at the hypothetical PDK-2 site. J Biol Chem. 2000;275:8271-8274.
269. Cross DA, Alessi DR, Cohen P, Andjelkovich M, Hemmings BA. Inhibition of glycogen synthase kinase-3 by insulin mediated by protein kinase B. Nature. 1995;378:785-789.
270. Brunet A, Bonni A, Zigmond MJ, et al. Akt promotes cell survival by phosphorylating and inhibiting a Forkhead transcription factor. Cell. 1999;96:857-868.
271. Rena G, Guo S, Cichy SC, Unterman TG, Cohen P. Phosphorylation of the transcription factor forkhead family member FKHR by protein kinase B. J Biol Chem. 1999;274:17179-17183.
272. Tang ED, Nunez G, Barr FG, Guan KL. Negative regulation of the forkhead transcription factor FKHR by Akt. J Biol Chem. 1999;274:16741-16746.
273. del Peso L, Gonzalez-Garcia M, Page C, Herrera R, Nunez G. Interleukin-3-induced phosphorylation of BAD through the protein kinase Akt. Science. 1997;278:687-689.
274. Heitman J, Movva NR, Hall MN. Targets for cell cycle arrest by the immunosuppressant rapamycin in yeast. Science. 1991;253:905-909.
275. Brown EJ, Albers MW, Shin TB, et al. A mammalian protein targeted by G1-arresting rapamycin-receptor complex. Nature. 1994;369:756-758.
276. Chiu MI, Katz H, Berlin V. RAPT1, a mammalian homolog of yeast Tor, interacts with the FKBP12/rapamycin complex. Proc Natl Acad Sci U S A. 1994;91:12574-12578.
277. Sabatini DM, Erdjument-Bromage H, Lui M, Tempst P, Snyder SH. RAFT1: a mammalian protein that binds to FKBP12 in a rapamycin-dependent fashion and is homologous to yeast TORs. Cell. 1994;78:35-43.
278. Sabers CJ, Martin MM, Brunn GJ, et al. Isolation of a protein target of the FKBP12-rapamycin complex in mammalian cells. J Biol Chem. 1995;270:815-822.

279. Guertin DA, Sabatini DM. Defining the role of mTOR in cancer. Cancer Cell. 2007;12:9-22.
280. Hara K, Yonezawa K, Weng QP, Kozlowski MT, Belham C, Avruch J. Amino acid sufficiency and mTOR regulate p70 S6 kinase and eIF-4E BP1 through a common effector mechanism. J Biol Chem. 1998;273:14484-14494.
281. Thomas G, Hall MN. TOR signalling and control of cell growth. Curr Opin Cell Biol. 1997;9:782-787.
282. Hresko RC, Mueckler M. mTOR.RICTOR is the Ser473 kinase for Akt/protein kinase B in 3T3-L1 adipocytes. J Biol Chem. 2005;280:40406-40416.
283. Sarbassov DD, Guertin DA, Ali SM, Sabatini DM. Phosphorylation and regulation of Akt/PKB by the rictor-mTOR complex. Science. 2005;307:1098-1101.
284. Crino PB, Nathanson KL, Henske EP. The tuberous sclerosis complex. N Engl J Med. 2006;355:1345-1356.
285. Brunn GJ, Hudson CC, Sekulic A, et al. Phosphorylation of the translational repressor PHAS-I by the mammalian target of rapamycin. Science. 1997;277:99-101.
286. Prevot D, Darlix JL, Ohlmann T. Conducting the initiation of protein synthesis: the role of eIF4G. Biol Cell. 2003;95:141-156.
287. Pullen N, Thomas G. The modular phosphorylation and activation of p70s6k. FEBS Lett. 1997;410:78-82.
288. Guertin DA, Sabatini DM. An expanding role for mTOR in cancer. Trends Mol Med. 2005;11:353-361.
289. Majumder PK, Febbo PG, Bikoff R, et al. mTOR inhibition reverses Akt-dependent prostate intraepithelial neoplasia through regulation of apoptotic and HIF-1-dependent pathways. Nat Med. 2004;10:594-601.
290. Neshat MS, Mellinghoff IK, Tran C, et al. Enhanced sensitivity of PTEN-deficient tumors to inhibition of FRAP/mTOR. Proc Natl Acad Sci U S A. 2001;98:10314-10319.
291. Bonnet D, Dick JE. Human acute myeloid leukemia is organized as a hierarchy that originates from a primitive hematopoietic cell. Nat Med. 1997;3:730-737.
292. Lapidot T, Sirard C, Vormoor J, et al. A cell initiating human acute myeloid leukaemia after transplantation into SCID mice. Nature. 1994;367:645-648.
293. Dean M, Fojo T, Bates S. Tumour stem cells and drug resistance. Nat Rev Cancer. 2005;5:275-284.
294. Konopleva M, Zhao S, Hu W, et al. The anti-apoptotic genes Bcl-X(L) and Bcl-2 are over-expressed and contribute to chemoresistance of non-proliferating leukaemic CD34+ cells. Br J Haematol. 2002;118:521-534.
295. Jamieson CH, Ailles LE, Dylla SJ, et al. Granulocyte-macrophage progenitors as candidate leukemic stem cells in blast-crisis CML. N Engl J Med. 2004;351:657-667.
296. Abrahamsson AE, Geron I, Gotlib J, et al. Glycogen synthase kinase 3beta missplicing contributes to leukemia stem cell generation. Proc Natl Acad Sci U S A. 2009;106:3925-3929.
297. Cozzio A, Passegue E, Ayton PM, Karsunky H, Cleary ML, Weissman IL. Similar MLL-associated leukemias arising from self-renewing stem cells and short-lived myeloid progenitors. Genes Dev. 2003;17:3029-3035.

298. Huntly BJ, Shigematsu H, Deguchi K, et al. MOZ-TIF2, but not BCR-ABL, confers properties of leukemic stem cells to committed murine hematopoietic progenitors. Cancer Cell. 2004;6:587-596.
299. Krivtsov AV, Twomey D, Feng Z, et al. Transformation from committed progenitor to leukaemia stem cell initiated by MLL-AF9. Nature. 2006;442:818-822.
300. Kuo YH, Landrette SF, Heilman SA, et al. Cbf beta-SMMHC induces distinct abnormal myeloid progenitors able to develop acute myeloid leukemia. Cancer Cell. 2006;9:57-68.
301. Somervaille TC, Cleary ML. Identification and characterization of leukemia stem cells in murine MLL-AF9 acute myeloid leukemia. Cancer Cell. 2006;10:257-268.
302. Armstrong F, Brunet de la Grange P, Gerby B, et al. NOTCH is a key regulator of human T-cell acute leukemia initiating cell activity. Blood. 2009;113:1730-1740.
303. Cox CV, Martin HM, Kearns PR, Virgo P, Evely RS, Blair A. Characterization of a progenitor cell population in childhood T-cell acute lymphoblastic leukemia. Blood. 2007;109:674-682.
304. Moss ML, Stoeck A, Yan W, Dempsey PJ. ADAM10 as a target for anti-cancer therapy. Curr Pharm Biotechnol. 2008;9:2-8.
305. Muraguchi T, Takegami Y, Ohtsuka T, et al. RECK modulates Notch signaling during cortical neurogenesis by regulating ADAM10 activity. Nat Neurosci. 2007;10:838-845.
306. Rizzo P, Osipo C, Foreman K, Golde T, Osborne B, Miele L. Rational targeting of Notch signaling in cancer. Oncogene. 2008;27:5124-5131.
307. Nam Y, Sliz P, Pear WS, Aster JC, Blacklow SC. Cooperative assembly of higher-order Notch complexes functions as a switch to induce transcription. Proc Natl Acad Sci U S A. 2007;104:2103-2108.
308. Nam Y, Sliz P, Song L, Aster JC, Blacklow SC. Structural basis for cooperativity in recruitment of MAML coactivators to Notch transcription complexes. Cell. 2006;124:973-983.
309. DeAngelo DJ, Stone RM, Silverman LB, et al. A phase 1 clincal trial of the Notch1 inhibitor MK-0752 in patients with T-cell acute lymphoblastic leukemia lymphoma (T-ALL) and other leukemias (abstract) J Clin Oncoll. 2006;24 (suppl):357s. Abstract 6585.
310. Wong GT, Manfra D, Poulet FM, et al. Chronic treatment with the gamma-secretase inhibitor LY-411,575 inhibits beta-amyloid peptide production and alters lymphopoiesis and intestinal cell differentiation. J Biol Chem. 2004;279:12876-12882.
311. Dominguez MG, Hughes VC, Pan L, et al. Vascular endothelial tyrosine phosphatase (VE-PTP)-null mice undergo vasculogenesis but die embryonically because of defects in angiogenesis. Proc Natl Acad Sci U S A. 2007;104:3243-3248.
312. Sharma VM, Draheim KM, Kelliher MA. The Notch1/c-Myc pathway in T cell leukemia. Cell Cycle. 2007;6:927-930.
313. Weerkamp F, van Dongen JJ, Staal FJ. Notch and Wnt signaling in T-lymphocyte development and acute lymphoblastic leukemia. Leukemia. 2006;20:1197-1205.

314. Aoyama K, Delaney C, Varnum-Finney B, Kohn AD, Moon RT, Bernstein ID. The interaction of the Wnt and Notch pathways modulates natural killer versus T cell differentiation. Stem Cells. 2007;25:2488-2497.
315. Duncan AW, Rattis FM, DiMascio LN, et al. Integration of Notch and Wnt signaling in hematopoietic stem cell maintenance. Nat Immunol. 2005;6:314-322.
316. Estrach S, Ambler CA, Lo Celso C, Hozumi K, Watt FM. Jagged 1 is a beta-catenin target gene required for ectopic hair follicle formation in adult epidermis. Development. 2006;133:4427-4438.
317. Fre S, Pallavi SK, Huyghe M, et al. Notch and Wnt signals cooperatively control cell proliferation and tumorigenesis in the intestine. Proc Natl Acad Sci U S A. 2009;106:6309-6314.
318. Pannequin J, Bonnans C, Delaunay N, et al. The Wnt Target Jagged-1 Mediates the Activation of Notch Signaling by Progastrin in Human Colorectal Cancer Cells. Cancer Res. 2009.
319. Phng LK, Potente M, Leslie JD, et al. Nrarp coordinates endothelial Notch and Wnt signaling to control vessel density in angiogenesis. Dev Cell. 2009;16:70-82.
320. Rodilla V, Villanueva A, Obrador-Hevia A, et al. Jagged1 is the pathological link between Wnt and Notch pathways in colorectal cancer. Proc Natl Acad Sci U S A. 2009;106:6315-6320.
321. Spaulding C, Reschly EJ, Zagort DE, et al. Notch1 co-opts lymphoid enhancer factor 1 for survival of murine T-cell lymphomas. Blood. 2007;110:2650-2658.
322. Ioannidis V, Beermann F, Clevers H, Held W. The beta-catenin--TCF-1 pathway ensures CD4(+)CD8(+) thymocyte survival. Nat Immunol. 2001;2:691-697.
323. Castrop J, van Wichen D, Koomans-Bitter M, et al. The human TCF-1 gene encodes a nuclear DNA-binding protein uniquely expressed in normal and neoplastic T-lineage lymphocytes. Blood. 1995;86:3050-3059.
324. Armitage P, Berry G. Statistical methods in medical research (ed 3rd). Oxford ; Boston: Blackwell Scientific Publications; 1994.
325. Milano J, McKay J, Dagenais C, et al. Modulation of notch processing by gamma-secretase inhibitors causes intestinal goblet cell metaplasia and induction of genes known to specify gut secretory lineage differentiation. Toxicol Sci. 2004;82:341-358.
326. Chan SM, Weng AP, Tibshirani R, Aster JC, Utz PJ. Notch signals positively regulate activity of the mTOR pathway in T-cell acute lymphoblastic leukemia. Blood. 2007;110:278-286.
327. Palomero T, Sulis ML, Cortina M, et al. Mutational loss of PTEN induces resistance to NOTCH1 inhibition in T-cell leukemia. Nat Med. 2007;13:1203-1210.
328. Williams RT, Roussel MF, Sherr CJ. Arf gene loss enhances oncogenicity and limits imatinib response in mouse models of Bcr-Abl-induced acute lymphoblastic leukemia. Proc Natl Acad Sci U S A. 2006;103:6688-6693.
329. Roy M, Pear WS, Aster JC. The multifaceted role of Notch in cancer. Curr Opin Genet Dev. 2007;17:52-59.

330. Feldman BJ, Hampton T, Cleary ML. A carboxy-terminal deletion mutant of Notch1 accelerates lymphoid oncogenesis in E2A-PBX1 transgenic mice. Blood. 2000;96:1906-1913.
331. Klinakis A, Szabolcs M, Politi K, Kiaris H, Artavanis-Tsakonas S, Efstratiadis A. Myc is a Notch1 transcriptional target and a requisite for Notch1-induced mammary tumorigenesis in mice. Proc Natl Acad Sci U S A. 2006;103:9262-9267.
332. Noguera-Troise I, Daly C, Papadopoulos NJ, et al. Blockade of Dll4 inhibits tumour growth by promoting non-productive angiogenesis. Novartis Found Symp. 2007;283:106-120; discussion 121-105, 238-141.
333. Ridgway J, Zhang G, Wu Y, et al. Inhibition of Dll4 signalling inhibits tumour growth by deregulating angiogenesis. Nature. 2006;444:1083-1087.
334. Scehnet JS, Jiang W, Kumar SR, et al. Inhibition of Dll4-mediated signaling induces proliferation of immature vessels and results in poor tissue perfusion. Blood. 2007;109:4753-4760.
335. Siekmann AF, Lawson ND. Notch signalling limits angiogenic cell behaviour in developing zebrafish arteries. Nature. 2007;445:781-784.
336. Diehn M, Clarke MF. Cancer stem cells and radiotherapy: new insights into tumor radioresistance. J Natl Cancer Inst. 2006;98:1755-1757.
337. Guzman ML, Jordan CT. Considerations for targeting malignant stem cells in leukemia. Cancer Control. 2004;11:97-104.
338. Ishikawa F, Yoshida S, Saito Y, et al. Chemotherapy-resistant human AML stem cells home to and engraft within the bone-marrow endosteal region. Nat Biotechnol. 2007;25:1315-1321.
339. Kelly PN, Dakic A, Adams JM, Nutt SL, Strasser A. Tumor growth need not be driven by rare cancer stem cells. Science. 2007;317:337.
340. Gothert JR, Brake RL, Smeets M, Duhrsen U, Begley CG, Izon DJ. NOTCH1 pathway activation is an early hallmark of SCL T leukemogenesis. Blood. 2007;110:3753-3762.
341. Mizutani K, Yoon K, Dang L, Tokunaga A, Gaiano N. Differential Notch signalling distinguishes neural stem cells from intermediate progenitors. Nature. 2007;449:351-355.
342. Hellstrom M, Phng LK, Hofmann JJ, et al. Dll4 signalling through Notch1 regulates formation of tip cells during angiogenesis. Nature. 2007;445:776-780.
343. Groves T, Parsons M, Miyamoto NG, Guidos CJ. TCR engagement of CD4+CD8+ thymocytes in vitro induces early aspects of positive selection, but not apoptosis. J Immunol. 1997;158:65-75.
344. Sell S. Stem cell origin of cancer and differentiation therapy. Crit Rev Oncol Hematol. 2004;51:1-28.
345. Engel I, Murre C. E2A proteins enforce a proliferation checkpoint in developing thymocytes. EMBO J. 2004;23:202-211.
346. Campese AF, Garbe AI, Zhang F, Grassi F, Screpanti I, von Boehmer H. Notch1-dependent lymphomagenesis is assisted by but does not essentially require pre-TCR signaling. Blood. 2006;108:305-310.

347. O'Neil J, Ventura JJ, Cusson N, Kelliher M. NF-kappaB activation in premalignant mouse tal-1/scl thymocytes and tumors. Blood. 2003;102:2593-2596.
348. Vilimas T, Mascarenhas J, Palomero T, et al. Targeting the NF-kappaB signaling pathway in Notch1-induced T-cell leukemia. Nat Med. 2007;13:70-77.
349. Cullion K, Draheim KM, Hermance N, et al. Targeting the Notch1 and mTOR pathways in a mouse T-ALL model. Blood. 2009;113:6172-6181.
350. Guzman ML, Swiderski CF, Howard DS, et al. Preferential induction of apoptosis for primary human leukemic stem cells. Proc Natl Acad Sci U S A. 2002;99:16220-16225.
351. Xu Q, Simpson SE, Scialla TJ, Bagg A, Carroll M. Survival of acute myeloid leukemia cells requires PI3 kinase activation. Blood. 2003;102:972-980.
352. Mullighan CG, Goorha S, Radtke I, et al. Genome-wide analysis of genetic alterations in acute lymphoblastic leukaemia. Nature. 2007;446:758-764.
353. Molofsky AV, He S, Bydon M, Morrison SJ, Pardal R. Bmi-1 promotes neural stem cell self-renewal and neural development but not mouse growth and survival by repressing the p16Ink4a and p19Arf senescence pathways. Genes Dev. 2005;19:1432-1437.
354. Lessard J, Sauvageau G. Polycomb group genes as epigenetic regulators of normal and leukemic hemopoiesis. Exp Hematol. 2003;31:567-585.
355. Lessard J, Sauvageau G. Bmi-1 determines the proliferative capacity of normal and leukaemic stem cells. Nature. 2003;423:255-260.
356. Guo W, Lasky JL, Chang CJ, et al. Multi-genetic events collaboratively contribute to Pten-null leukaemia stem-cell formation. Nature. 2008;453:529-533.
357. Hambardzumyan D, Becher OJ, Rosenblum MK, Pandolfi PP, Manova-Todorova K, Holland EC. PI3K pathway regulates survival of cancer stem cells residing in the perivascular niche following radiation in medulloblastoma in vivo. Genes Dev. 2008;22:436-448.
358. He XC, Yin T, Grindley JC, et al. PTEN-deficient intestinal stem cells initiate intestinal polyposis. Nat Genet. 2007;39:189-198.
359. Yilmaz OH, Valdez R, Theisen BK, et al. Pten dependence distinguishes haematopoietic stem cells from leukaemia-initiating cells. Nature. 2006;441:475-482.
360. Zhang J, Grindley JC, Yin T, et al. PTEN maintains haematopoietic stem cells and acts in lineage choice and leukaemia prevention. Nature. 2006;441:518-522.
361. Zhou J, Su P, Wang L, et al. mTOR supports long-term self-renewal and suppresses mesoderm and endoderm activities of human embryonic stem cells. Proc Natl Acad Sci U S A. 2009;106:7840-7845.
362. Cornberg M, Chen AT, Wilkinson LA, et al. Narrowed TCR repertoire and viral escape as a consequence of heterologous immunity. J Clin Invest. 2006;116:1443-1456.
363. Somervaille TC, Matheny CJ, Spencer GJ, et al. Hierarchical maintenance of MLL myeloid leukemia stem cells employs a transcriptional program shared with embryonic rather than adult stem cells. Cell Stem Cell. 2009;4:129-140.
364. Wong DJ, Liu H, Ridky TW, Cassarino D, Segal E, Chang HY. Module map of stem cell genes guides creation of epithelial cancer stem cells. Cell Stem Cell. 2008;2:333-344.

365. Sasaki T, Suzuki H, Yagi K, et al. Lymphoid enhancer factor 1 makes cells resistant to transforming growth factor beta-induced repression of c-myc. Cancer Res. 2003;63:801-806.
366. Ben-Porath I, Thomson MW, Carey VJ, et al. An embryonic stem cell-like gene expression signature in poorly differentiated aggressive human tumors. Nat Genet. 2008;40:499-507.
367. Gutierrez A, Sanda T, Grebliunaite R, et al. High frequency of PTEN, PI3K, and AKT abnormalities in T-cell acute lymphoblastic leukemia. Blood. 2009;114:647-650.
368. Lo TC, Barnhill LM, Kim Y, Nakae EA, Yu AL, Diccianni MB. Inactivation of SHIP1 in T-cell acute lymphoblastic leukemia due to mutation and extensive alternative splicing. Leuk Res. 2009;33:1562-1566.
369. Remke M, Pfister S, Kox C, et al. High-resolution genomic profiling of childhood T-ALL reveals frequent copy-number alterations affecting the TGF-beta and PI3K-AKT pathways and deletions at 6q15-16.1 as a genomic marker for unfavorable early treatment response. Blood. 2009;114:1053-1062.
370. Aouadi M, Tesz GJ, Nicoloro SM, et al. Orally delivered siRNA targeting macrophage Map4k4 suppresses systemic inflammation. Nature. 2009;458:1180-1184.
371. Kumar P, Ban HS, Kim SS, et al. T cell-specific siRNA delivery suppresses HIV-1 infection in humanized mice. Cell. 2008;134:577-586.
372. Cheng J, Haas M. Frequent mutations in the p53 tumor suppressor gene in human leukemia T-cell lines. Mol Cell Biol. 1990;10:5502-5509.
373. Shultz LD, Lyons BL, Burzenski LM, et al. Human lymphoid and myeloid cell development in NOD/LtSz-scid IL2R gamma null mice engrafted with mobilized human hemopoietic stem cells. J Immunol. 2005;174:6477-6489.
374. Pearson T, Shultz LD, Miller D, et al. Non-obese diabetic-recombination activating gene-1 (NOD-Rag1 null) interleukin (IL)-2 receptor common gamma chain (IL2r gamma null) null mice: a radioresistant model for human lymphohaematopoietic engraftment. Clin Exp Immunol. 2008;154:270-284.
375. Quintana E, Shackleton M, Sabel MS, Fullen DR, Johnson TM, Morrison SJ. Efficient tumour formation by single human melanoma cells. Nature. 2008;456:593-598.